2013

TERPENE AND TERPENOID EMISSIONS AND SECONDARY ORGANIC AEROSOL PRODUCTION

Rosa M. Flores
Michigan Technological University

Recommended Citation

Flores, Rosa M., "TERPENE AND TERPENOID EMISSIONS AND SECONDARY ORGANIC AEROSOL PRODUCTION", Dissertation, Michigan Technological University, 2013.
https://doi.org/10.37099/mtu.dc.etds/818

TERPENE AND TERPENOID EMISSIONS AND SECONDARY ORGANIC AEROSOL PRODUCTION

By

Rosa M. Flores

A DISSERTATION

Submitted in partial fulfillment of the requirements for the degree of

DOCTOR OF PHILOSOPHY

In Environmental Engineering

MICHIGAN TECHNOLOGICAL UNIVERSITY

2013

This dissertation has been approved in partial fulfillment of the requirements for the Degree of DOCTOR OF PHILOSOPHY in Environmental Engineering.

Department of Civil and Environmental Engineering

Dissertation Advisor: *Paul V. Doskey*

Committee Member :   *Chandrashekhar P. Joshi*

Committee Member :   *Claudio Mazzoleni*

Committee Member :   *Lynn Mazzoleni*

Committee Member :   *Judith Perlinger*

Department Chair: *David Hand*

To dad and mom

Table of Contents

Preface

Chapter 2, *Terpenoid Signatures of Conifer Essential Oils: New Measurements and a Review*, is a planned submission. The idea of using a literature review as the most appropriate type of manuscript to present measurements of 3 conifer essential oils was jointly discussed and implemented by Rosa Flores and Paul Doskey. Rosa was principal in gathering papers for the review and data collection and processing of the 3 essential oils. Rosa and Paul worked together to interpret the literature data. Rosa composed several drafts of the manuscript and Paul did the final editing in preparation for submission. David Perram is acknowledged for assistance with gas chromatography-mass spectrometry.

Chapter 3, *Estimating Terpene and Terpenoid Emission Signatures From Conifer Oleoresin Composition*, is a planned submission. Rosa Flores and Paul Doskey discussed approaches to use the extensive database gathered as part of the review (that is objective of Chapter 2) in a conceptual model to develop emission inventories for conifers. Paul developed the conceptual model and Rosa gathered and estimated physicochemical properties of terpenes and terpenoids. Paul and Rosa worked to interpret the data and Paul did the final editing of the manuscript in preparation for submission.

Chapter 4, *Comparison of Multistep Derivatization Methods for Identification and Quantification of Oxygenated Species in Organic Aerosol*, is a planned submission. Rosa Flores found a promising, 3-step derivatization method that was reported in the literature and discussed publishing implementation of the technique to analyze organic aerosol. Paul Doskey suggested comparing the 3-step method with other techniques as the basis of the manuscript. Rosa gathered data in the laboratory for the method comparison and interpreted the results. She prepared several drafts and Paul did the final editing of the manuscript in preparation for submission. David Perram is acknowledged for assistance with gas chromatography-mass spectrometry.

Chapter 5, *Using Multidimensional Gas Chromatography to Define a Carbon Number-Functionality Grid for Characterizing Oxidation of Organic Aerosol*, was accepted for publication in Atmospheric Environment on July 19, 2013. Rosa Flores and Judith Perlinger are first and second authors, respectively. Paul Doskey is third and corresponding author. David Perram is acknowledged for assistance with gas chromatography-mass spectrometry. The manuscript was removed from production on or about August 24, 2013 by coauthor Judith Perlinger.

Chapter 6, *Vapor- and Aerosol-Phase Atmospheric Organic Matter in the Midwestern United States: Methods and Measurements*, will potentially be divided into 2 planned submissions, one primarily on methods the other on measurements. Paul Doskey conceived the idea of making field measurements in St. Louis, MO. Paul and Rosa Flores collected samples and Rosa performed all analyses and interpretations of data. Rosa composed several drafts of the manuscript and Paul did the final editing in preparation for submission. David Perram is acknowledged for assistance with gas chromatography-mass spectrometry and Jay Turner for providing access to the St. Louis - Midwest Supersite.

Abstract

Approximately 90% of fine aerosol in the Midwestern United States has a regional component with a sizable fraction attributed to secondary production of organic aerosol (SOA). The Ozark Forest is an important source of biogenic SOA precursors like isoprene (> 150 mg m^{-2} d^{-1}), monoterpenes (10-40 mg m^{-2} d^{-1}), and sesquiterpenes (10-40 mg m^{-2}d^{-1}). Anthropogenic sources include secondary sulfate and nitrate and biomass burning (51-60%), vehicle emissions (17-26%), and industrial emissions (16-18%). Vehicle emissions are an important source of volatile and vapor-phase, semivolatile aliphatic and aromatic hydrocarbons that are important anthropogenic sources of SOA precursors. The short lifetime of SOA precursors and the complex mixture of functionalized oxidation products make rapid sampling, quantitative processing methods, and comprehensive organic molecular analysis essential elements of a comprehensive strategy to advance understanding of SOA formation pathways. Uncertainties in forecasting SOA production on regional scales are large and related to uncertainties in biogenic emission inventories and measurement of SOA yields under ambient conditions. This work presents a bottom-up approach to develop a conifer emission inventory based on foliar and cortical oleoresin composition, development of a model to estimate terpene and terpenoid signatures of foliar and bole emissions from conifers, development of processing and analytic techniques for comprehensive organic molecular characterization of SOA precursors and oxidation products, implementation of the high-volume sampling technique to measure OA and vapor-phase organic matter, and results from a 5 day field experiment conducted to evaluate temporal and diurnal trends in SOA precursors and oxidation products. A total of 98, 115, and 87 terpene and terpenoid species were identified and quantified in commercially available essential oils of *Pinus sylvestris*, *Picea mariana*, and *Thuja occidentalis*, respectively, by comprehensive, two-dimensional gas chromatography with time-of-flight mass spectrometric detection (GC × GC-ToF-MS). Analysis of the literature showed that

9

cortical oleoresin composition was similar to foliar composition of the oldest branches. Our proposed conceptual model for estimation of signatures of terpene and terpenoid emissions from foliar and cortical oleoresin showed that emission potentials of the foliar and bole release pathways are dissimilar and should be considered for conifer species that develop resin blisters or are infested with herbivores or pathogens.

Average derivatization efficiencies for Methods 1 and 2 were 87.9 and 114%, respectively. Despite the lower average derivatization efficiency of Method 1, distinct advantages included a greater certainty of derivatization yield for the entire suite of multi- and poly-functional species and fewer processing steps for sequential derivatization. Detection limits for Method 1 using GC × GC- ToF-MS were 0.09-1.89 ng μL^{-1}. A theoretical retention index diagram was developed for a hypothetical GC × 2GC analysis of the complex mixture of SOA precursors and derivatized oxidation products. In general, species eluted (relative to the alkyl diester reference compounds) from the primary column (DB-210) in bands according to n and from the secondary columns (BPX90, SolGel-WAX) according to functionality, essentially making the GC × 2GC retention diagram a Carbon number-functionality grid. The species clustered into 35 groups by functionality and species within each group exhibited good separation by n. Average recoveries of n-alkanes and polyaromatic hydrocarbons (PAHs) by Soxhlet extraction of XAD-2 resin with dichloromethane were 80.1 ± 16.1 and 76.1 ± 17.5%, respectively. Vehicle emissions were the common source for HSVOCs [i.e., resolved alkanes, the unresolved complex mixture (UCM), alkylbenzenes, and 2- and 3-ring PAHs]. An absence of monoterpenes at 0600-1000 and high concentrations of monoterpenoids during the same period was indicative of substantial losses of monoterpenes overnight and the early morning hours. Post-collection, comprehensive organic molecular characterization of SOA precursors and products by GC × GC-ToF-MS in ambient air collected with ~2 hr resolution is a promising method for determining biogenic and anthropogenic SOA yields that can be used to evaluate SOA formation models.

Chapter 1. Introduction

Approximately 90% of fine aerosol in major urban areas of the Upper Midwest has a regional component with a sizable fraction attributed to secondary organic aerosol (SOA). Precursors of SOA have anthropogenic and biogenic origins and are composed of a complex mixture of aliphatic and aromatic hydrocarbons. Vehicle emissions are an important source of volatile and semivolatile, vapor-phase aliphatic and aromatic hydrocarbons that are rapidly oxidized in the atmosphere and produce SOA. The Ozark Forest is an important source of biogenic SOA precursors like monoterpenes that represent as much as 20% of the total terpene (i.e., Σisoprene, monoterpenes, sesquiterpenes) emissions in the Midwest. Conifers are the principal source of monoterpenes and emissions are related to compound vapor pressure and increase exponentially with temperature. Emission inventories are based on top-down approaches that require measurement of emissions from conifer species under a variety of environmental conditions. Once emitted into the atmosphere, anthropogenic and biogenic SOA precursors react to form a complex mixture of OA species that are characteristic of the source. However, considerable uncertainty exists in predicting SOA formation on regional scales due to uncertainties in biogenic emission inventories, comprehensive organic molecular characterization of SOA, and quantification of SOA yields.

A complex mixture of terpenes and terpenoids (i.e., oxygen-containing terpenes) are found in oleoresins of conifers. The oleoresin is composed of oil, which is the source of terpenes and terpenoids, and the less volatile resin acids. Composition of conifer essential oil is related to taxonomy, phenology and age, biotic and abiotic stresses, and isolation and analytic techniques. An alternative strategy for developing conifer emission inventories might be a bottom-up approach based on comprehensive organic molecular characterization and quantification of oleoresin composition of conifer species. New measurements of terpenes and terpenoids in foliar oils of 3 species of

conifers by comprehensive, multidimensional gas chromatography (GC) with time-of-flight mass spectrometry (GC × GC-ToF-MS in the work described here) is presented and the accompanying review presents molecular signatures of numerous species of the *Pinaceae* and *Cupressaceae* families and discusses trends. Terpene and terpenoid oleoresin signatures could be used as input to emission modules that predict emissions through parameterizations of plant physiological processes and physicochemical properties of terpenes and terpenoids. Conifer emission pathways for terpenes and terpenoids include exhalation from foliar stomata and evaporation from resin blisters or traumatic resin ducts on the bole of the tree. A conceptual model is presented that considers physicochemical properties of terpenes and terpenoids and emissions from foliage and the bole of conifers to estimate emission signatures of terpenes and terpenoids from both pathways.

Measuring SOA yields to evaluate SOA formation models requires comprehensive organic molecular characterization of SOA precursors and oxidation products on short timescales for accurate observation of atmospheric dynamics. The reactive precursors and oxidation products are primarily present in the vapor and aerosol phases, which requires sampling techniques like the high-volume sampling method that separates the vapor the particle phases and is capable of collecting sufficient mass in a 2-hr sampling period to evaluate diurnal and temporal trends and determine SOA yields. Organic molecular characterization of SOA precursors and oxidation products is best achieved by GC × GC-ToF-MS, which is capable of separating the complex mixture of 1000's of SOA precursors and oxidation products and grouping the species according to molecular volume and functionality.

A 5 day field experiment was conducted in St. Louis, Missouri to measure diurnal and temporal trends in biogenic and anthropogenic SOA precursors and oxidation products. The metropolitan region is impacted by biogenic emissions that originate in the Ozark Forest. Samples were collected over 4- or 5-hr intervals during the day and in 11-hr intervals overnight over a 5-day period during August 2011 at the St. Louis – Midwest

Supersite (East St. Louis, MO). Post-collection analysis was by Soxhlet extraction with derivatization of functionalized species prior to comprehensive separation and identification by GC × GC-ToF-MS. Details of the sampling and analytic method are given and extraction efficiencies, reproducibilities, and method detection limits are presented. Temporal and diurnal trends in concentrations of SOA precursors and oxidation products are discussed.

Chapter 2. Terpenoid Signatures of Conifer Essential Oils: New Measurements and a Review

Rosa M. Flores[1] and Paul V. Doskey[1-3]

[1]Department of Civil and Environmental Engineering, [2]School of Forest Resources and Environmental Science, [3]Atmospheric Sciences Program.
Michigan Technological University. 1400 Townsend Dr. Houghton, MI. 49931.
rmflores@mtu.edu, pvdoskey@mtu.edu[◊]
[◊]corresponding author. Phone number: +1 906-487-2745

Abstract. A total of 98, 115, and 87 terpene and terpenoid species were identified and quantified in commercially available essential oils of *Pinus sylvestris*, *Picea mariana*, and *Thuja occidentalis*, respectively, by comprehensive, two-dimensional gas chromatography with time-of-flight mass spectrometric detection (GC × GC-ToF-MS). Compositions of foliar essential oils determined by GC-MS were generally in agreement; however, fewer chemical species were reported. A review of essential oil compositions of species of the *Pinaceae* and *Cupressaceae* families revealed distinctive features at the subfamily, genera, subgenera, and species levels. However, considerable variability in molecular signatures was also observed and related to phenology and age, biotic and abiotic stressors, and isolation and analytic techniques. Introgression and hybridization of species produced essential oils that were intemediate in composition to endmembers. Essential oil composition of new foliage exhibited significant seasonal variability and became invariant in older leaves. Monoterpene compositions of cortical oleoresins were variable in trees less than 25 years old and constant in more mature trees. Cortical oleoresin composition was similar to foliar composition of the oldest branches. Nutrient availability affected essential oil composition in some populations and exhibited no effects in others. Exposure to air pollutants like ozone and nitrogen and sulfur dioxide alters molecular signatures by affecting photosynthetic activity and production of terpene substrates that are required for terpene biosynthesis. Steam distillation with solvent

extraction is effective for isolating essential oils form foliage and the cortex; however, exhaustive extraction to determine oleoresin composition is best achieved by supercritical fluid extraction. Signatures of essential oils based on molar composition are more accurate than distributions based on the ratio of the area of the MS response of the identified species normalized to the total area of identified species due to the nonuniform MS response of terpenes and terpenoids.

2.1. Introduction

Oleoresins are viscous, odorous liquids that are synthesized by many conifer organs and stored in secretory cells, cavities, canals, epidermic cells, or glandular trichomes (Phillips & Croteau 1999; Langenheim 2003). Resin ducts or glands in foliage are distinct from the series of ducts in stems and the bole of the tree (Jeffrey 1925; Hanes 1927; Roller 1966; Suzuki 1979). The complex mixtures of volatile and semi-volatile organic compounds that compose conifer oleoresins include terpenes, terpenoids, and resin acids (Zulak & Bohlmann 2010). Distributions of the chemical species represent characteristic molecular signatures of oleoresins for various species of conifers (Mirov 1961, von Rudloff 1975b). Steam distillation is the standard method for isolating essential oils from oleoresins (Franklin & Keyzer, 1962); however, several other extraction methods have been used for quantitative analysis and identification of the individual species that compose essential oils (Simard *et al.* 1988; Maciag *et al* 2007).

Principal classes of organic compounds in essential oils are terpenes and terpenoids (i.e., oxygen-containing terpenes), and aromatic compounds. The species represent about 90% of the mass of identified organic compounds in conifer essential oils. Terpenes are composed of units of isoprene (2-Methyl-1, 3-Butadiene; C_5H_8), which is called a hemiterpene. Terpene and terpenoid distributions of essential oils are related to taxonomy (von Rudloff 1975b). The most abundant chemical species are typically monoterpenes ($C_{10}H_{16}$) and sesquiterpenes ($C_{15}H_{24}$), with diterpenes ($C_{20}H_{32}$), triterpenes ($C_{30}H_{48}$), and terpenoids present in lesser amounts. α-Pinene, and β-pinene account for about 90% of the monoterpenes in conifer essential oils and β-caryophyllene, longifolene, and farnesene are the primary sesquiterpenes (Bakkali *et al.* 2008). Typical terpenoids include linalool, camphor, and bornyl acetate.

Chemical species in essential oils are by-products of plant metabolic processes and possibly the result of excretory functions or pathological processes. Functions of the chemical species include the following: (1) to regulate transpiration, (2) to attract insects that disperse pollens and seeds, and (3) as anti-bacterial, -viral, -fungal, or – insecticidal agents (Bakkali *et al.* 2008). Biological activity (e.g., cytotoxicity, gene induction, anti-genetic effects, etc.) of essential oils is determined by chemical composition. Size of the oleoresin pool and composition is influenced by plant taxonomy; physiology, phenology and age; genetics and evolution; biotic stresses like herbivore and pathogen attacks; and abiotic stressors like nutrient availability and air quality (von Rudloff 1972b, 1975b; Lewinsohn *et al.* 1991; Martin *et al.* 2002, 2003; Hudgins *et al.* 2004; Kännaste *et al.* 2013; Judzentiene *et al.* 2007).

On a global scale, biogenic volatile organic compounds (BVOCs) account for 90% of reduced carbon emissions to the atmosphere (1000 ± 600 Tg a^{-1}) (Guenther *et al.* 1995; Kanakidou *et al.* 2005). The VOC emissions from vegetation in North America are composed of isoprene (51%), terpenes (31%), and terpenoids (16%) (Kesselmeier & Staudt 1999). Terpenes and terpenoids, which are abundant in foliar and cortical resins and resin blisters of conifers (Zavarin 1968), are emitted into the atmosphere and rapidly photooxidized forming secondary organic aerosol (SOA; Kulmala *et al.* 2004). The SOA are the most abundant fine particle in the global troposphere and are hydrophilic making the aerosol effective at scattering light and forming clouds, which increases albedo and cools the atmosphere. Coniferous forests are the principal source of monoterpenes and sesquiterpenes (Helmig *et al.* 2007). Average annual terpene emissions of *Pinus sylvestris* (Scots Pine) were composed of 3-carene (40%), α-pinene (30%), β-pinene (15%), camphene (5%), and other terpenes (<5%) like β-myrcene, sabinene, limonene, β-phellandrene, and γ-terpinene; however, considerable variability in emissions was observed for different branches of the same tree and different trees (Komenda & Koppmann 2002). Emission rates vary with leaf temperature, light

intensity, water and nutrient availability, herbivore grazing, humidity, and phenology (Hakola et al. 2006; Ninnemets *et al.* 2010a and 2010b). Monoterpene emissions from conifers are generally related to the pool size in plant tissues and increase exponentially with leaf temperature in a manner similar to compound vapor pressure (Guenther *et al.* 1991 and 1993).

Developing terpene and terpenoid emission inventories through analysis of ambient air and emission samples is complicated by rapid reaction with atmospheric oxidants, the complex relationship between emissions and environmental factors, enhancement of emissions with wounding and herbivore grazing, thermal instability during chemical analysis, and low levels of some chemical species in emissions (Lerdau *et al.* 1997; Litvak *et al.* 1999; Holzke *et al.* 2006; Ortega & Helmig 2008; Ortega *et al.* 2008). Emissions of some terpenes from *Pinus ponderosa* and *P. nigra*, which were not enhanced by wounding or herbivore grazing, were consistent with foliar extracts (Eav 2011). Thus, an alternative strategy for developing conifer emission inventories might include the following: (1) quantify molecular signatures of terpenes and terpenoids for various conifer species (see, e.g., Geron *et al.* 2000), (2) develop an emission module to simulates terpene emissions with parameterizations of plant physiological and physiochemical controls on foliar, stem, and bole emissions (see, e.g., Niinemets *et al.* 2004 and 2010), and (3) couple the conifer emission module with a phytogeography model that predicts growth patterns of various vegetation types in different environments (see, e.g., Prentice *et al.* 1992; Rizzo & Wiken 1992; Neilson 1995).

Here we present new measurements of the essential oil compositions of Scots pine, *Picea mariana* (black spruce), and *Thuja occidentalis* (Eastern white cedar) by comprehensive, two-dimensional gas chromatography with time-of-flight mass spectrometric detection (GC × GC-ToF-MS). Terpene and terpenoid signatures of the

essential oils are compared with reported compositions of foliar extracts. A review is presented of molecular signatures of various species of the families *Pinaceae* and *Cupressaceae*. Variations in foliar and cortical signatures of terpenes and terpenoids related to season, age, stresses, and isolation and analytic techniques are discussed.

2.2. Materials and Methods

2.2.1. Biological and chemical materials

Essential oils of Scots Pine, black spruce, and Eastern white cedar were purchased from Silky Scents (Corona, CA, USA). The manufacturer isolated the essential oils from conifer leaves of Scots pine and Eastern white cedar and leaves and twigs of black spruce using steam distillation. Authentic standards (>85.0% - >99.0% purity) of 8 monoterpenes (α- and β-pinene, camphene, myrcene, 3-carene, limonene, ocimene and terpinolene), 1 monoterpene alcohol (linalool), 5 sesquiterpenes (copaene, α-cedrene, β-caryophyllene, humulene, farnesene), and 3 sesquiterpene alcohols (*cis*-nerolidol, *trans*-nerolidol and cedrol)) were obtained from Sigma-Aldrich (St. Louis, MO, USA). Helium carrier gas (99.999%), liquid N_2, and industrial grade N_2, were obtained from Superior Water and Welding (Chassell, MI, USA).

2.2.2. Gas chromatographic-mass spectrometric methods

The GC × GC-ToF-MS system consisted of a modified Agilent 6890 GC (Agilent Technologies) and a Pegasus 4D ToF-MS (Leco, St. Joseph, MI, USA). Dimensions of the primary and secondary GC columns were 30 m × 0.25 mm I.D. with a 0.25-μm-

film-thickness of DB-5ms (Agilent Technologies, Santa Clara, CA) and a 1 m × 0.10 mm I.D. column with a 0.10-µm-film-thickness of 50% phenyl-methylpolysiloxane (DB-17; Agilent Technologies), respectively. A zero dead volume, stainless steel compression union (Sigma-Aldrich) was used to join the GC columns. The secondary column oven was located inside the main oven that houses the primary column for independent temperature control of the primary and secondary columns. A quad-jet, dual-stage thermal modulator, which consisted of 2 hot and 2 cold jets cooled by liquid N_2, was used to direct primary column effluent to the secondary column in 1-5 s pulses.

A similarity greater than 70 % was used to specify a high probability match of an unknown with compounds in the National Institute of Standards and Technology (NIST) mass spectral library. Amounts of chemical species in the essential oils are reported as a percentage and as a mole fraction of the total terpenes, terpenoids, and aromatic compounds identified in the essential oil. Peak area of the most abundant fragment ion of each species was divided by the total peak area of identified compounds to determine percent abundance of the species in the essential oil. Authentic standards were used to derive average MS response factors for classes of terpenes and terpenoids. Average ToF-MS response factors for monoterpenes, sesquiterpenes, and monoterpene and sesquiterpene alcohols were 28,600, 13,000, 8,600, and 4,500 area counts ng^{-1}, respectively. The response factors were used to quantify masses of the analytes in the essential oil. Mole fractions were determined by dividing the moles of the species by the total moles of identified species. The sum of the products of the mole fractions and the molecular weight of each species was operationally defined as the average molecular weight of the essential oil.

2.3. Results and discussion

Measurements of foliar and cortical oleoresin compositions isolated from a wide variety of conifer species using exhaustive extraction techniques and comprehensive separation and quantitation of the myriad of terpene and terpenoid species are required to develop a BVOC emission inventory from essential oil composition. Variations in the biosynthesis of terpenes and terenoids related to taxonomy; phenology, canopy architecture, and age; and exposure to biotic and abitoic stressors must also be considered. Many studies of essential oil composition report chemical species composition as a percent (based on peak area) of the total identified terpene and terpenoid species, and thus, variations in essential oil composition are discussed in the review in terms of percent composition. We also report new measurements of the molar composition of the essential oils of Scots pine, black spruce, and Eastern white cedar and compare results to foliar compositions of the species.

2.3.1. Essential oil composition of Pinus sylvestris (Scots Pine), Picea mariana (Black Spruce), and Thuja occidentalis (Eastern White Cedar).

Compositions of the essential oils of Scots pine, black spruce, and Eastern white cedar analyzed in the subject study are expressed as % area. Compositions expressed as % area are compared with values from the literature. Distributions derived from compositions based on % area and mole fraction are different. The MS responses for terpenes and terpenoids were not uniform, and thus, molar compositions rather than compositions expressed as % area more accurately reflect terpene and terpenoid distributions of essential oils. Various GC-MS techniques are routinely used in analysis of foliar and cortical oleoresins and about 70 chemical species are routinely reported. The GC × GC-MS methods have been used to determine enatiomeric terpene and

22

terpenoid compositions of foliar and cortical oleoresins (Valterová *et al.* 1995; Persson *et al.* 1996). In the subject study, 98, 115, and 87 terpenes and terpenoids of Scots pine, black spruce, and Eastern white cedar, respectively, were identified and quantified via analysis by GC × GC -ToF-MS, which demonstrates the ability of comprehensive, multidimensional gas chromatography to identify many more essential oil species than GC-MS methods. Total ion, comprehensive GC × GC chromatograms of the essential oils of Scots pine, black spruce, and Eastern white cedar are presented in Figs. S2.1-S2.3 Suppl. Terpenes and terpenoids identified in essential oils of Scots pine, black spruce, and Eastern white cedar accounted for 92, 31, and 52% of the total area, respectively. Thus, molar compositions might be skewed by unidentified species with molecular weights that are significantly different than those of the identified species.

Monoterpenes (89.4%) represented the most abundant compound class of the 98 chemical species identified in essential oil of Scots pine. α-Pinene (40.6%), β-pinene (18.1%), limonene (16.3%), and 3-carene (6. 9%) were found in highest concentration. Much smaller amounts of the monoterpene acetates, bornyl acetate (0.5%) and the monoterpene ketones, *D*-fenchone (4.9%) and *iso*-thujone (1.4%) were found. We found similar levels of monoterpenes, greater abundances of monoterpenoids, and a much lower content of sesquiterpenes than other studies (Fig. 1a). Levels of α- and β-pinene, sabinene, and limonene were much greater than the reported values. *D*-Fenchone and *iso*-thujone were observed in the essential oil analyzed here; however, these monoterpenoid ketones were not reported in other studies. Average β-carophyllene and δ-cadinene abundances reported by others were 3.1 and 6.0%, respectively; however, the combined concentration of the species in our essential oil was < 0.1%.

Monoterpene composition of essential oil of black spruce was 50.4% of the 115 chemical species in black spruce. Levels of α-pinene, β-pinene, 3-carene, limonene, and camphene in black spruce were 14.7, 16.8, 7.5, 5.2, and 5.0% respectively. Average camphene content reported by others was much greater and β-pinene levels were much less than the values reported here (Fig. 1b). Bornyl acetate (43.1%) was the most abundant chemical species and similar to the average of levels reported in other studies. The average of levels of δ-cadinene reported by others was 0.55%, which was much greater than the concentration reported here (0.01%). However, our essential oil sample included isolates from twigs in addition to leaves, which might have diluted leaf oil containing a much higher content of δ-cadinene than twig oil.

Monoterpene and monterpenoid contents of essential oil of Eastern white cedar were 23.4 and 70.3%, respectively, of the 87 chemical species identified. The most abundant monoterpenes in Eastern white cedar included α-pinene (4.3%), camphene (2.4%), β-pinene (2.5%), and sabinene (10.2%). The average levels of the same monoterpene species reported by others were lower (Fig. 1c). We also report α-terpinene and terpinolene in essential oil of Eastern white cedar, which were not reported by others. Our values for *D*-fenchone and bornyl acetate are higher and the content of *iso*-thujone and camphor lower than the average of values reported in other studies. Monoterpenoid ketones observed in essential oil of Eastern white cedar include α-thujone (30.4-61.5%), *iso*-thujone (6.5-9.0%), *D*-fenchone (0.27-14.5%), and camphor (0.3-3.3%). Fifteen diterpenes including beyerene have also been identified in essential oil of Eastern white cedar (von Rudloff 1961; Simard *et al.* 1988; Kamdem *et al.* 1993).

2.3.2. Variations related to taxonomy

The conifers are cone-bearing seed plants with vascular tissue that are part of division *Pinophyta*, one of 13 or 14 division-level taxa within the Kingdom Plantae. *Pinophyta* is classified into 3 orders including *Pinales*, which includes the *Pinacea* and *Cupressaceae* families. The *Pinaceae* family includes the *Pinoideae* (pine), *Piceoideae* (spruce), *Laricoideae* (larch), and *Abietoideae* (fir) subfamilies with about 250 species in total. The *Cupressaceae* (cypress) family includes the *Cuuninghamhiodeae*, *Taiwanioideae*, *Athrotaxidoideae*, *Sequoioideae*, *Taxodioideae*, *Callitroideae*, and *Cupressoideae* subfamilies with about 130-140 species in 27-30 genera.

Pinoideae - Pines are members of the subfamily *Pinoideae*, which is composed of 3 subgenera, *Pinus, Stobus*, and *Ducampopinus*. Signatures of the pines are distinguished from other *Pinaceae* subfamilies by the sesquiterpene content, particularly β-caryophyllene, δ-cadinene, germacrene D, bicyclo-germacrene, and longifolene (Fig. 2a). The *Pinus* subgenera are further divided into sections that include species growing in broad geographic regions. Data are sparse for *Parrya*; however, distributions of monoterpene alcohols (i.e., linalool, α-fenchol, *D*-borneol, terpinen-4-ol, and α-terpeneol) and monoterpene acetates (i.e., bornyl and α-terpinyl acetate) might be used to distinguish sections of the subfamily *Pinoideae* (Fig. 3). α- to β-Pinene ratios varied between and within subsections (Table 2). *Pinus, Strobi*, and *Cembrae* were the only sections without an occurrence of β-pinene being in greater abundance than α-pinene in the foliar essential oil of a species. In *Pinaster*, 2 of 5 species had an occurrence of a ratio <1. Average sesquiterpene contents of foliar essential oils varied within species of the *Pinus, Pinaster, Australes, Ponderosa, Strobi*, and *Cembrae* subsections and were 15.3, 27.6, 8.3, 6.9, 23.1, and 21.5%, respectively (Table 2). Germacrene D and Germacrene D-4-ol were the principal sesquiterpene and sesquiterpenoid observed in some species of the *Pinus* sugenera.

Differences in foliar oleoresin composition of subsection species can be used to identify introgressing populations and hybridization. Hybrids have been observed in overlapping populations of *Pinus banksiana* and *P. contorta* in central Alberta (Mirov 1956; Zavarin *et al.* 1969; Pauly & von Rudloff 1971). However, a chemical signature similar to hybrid populations in central Alberta has been observed in foliar oleoresins isolated from *P. contorta* populations growing in areas of Ontario (von Rudloff 1975b). The species are classified in subsection *Contortae*, which includes the North American pines of section *Trifoliae*. *Pinus clausa* of the *Australes* subsection might be related to *P. banksiana* and *P. contorta*; however, the foliar essential oil is intermediate between the 2 species and more similar to a hybrid (Joye et al. 1972). *Pinus flexilis* and *P. albicaulis*, which are species in subsection *Strobi* and *Cembrae*, respectively, have overlapping ranges throughout the Rocky Mountains of the upper United States and southern Canada (von Rudloff 1975b). However, high variability in essential oil composition of *P. albicaulis* precluded identification of hybrids (Mirov 1961).

Piceoideae – Essential oil composition of the *Piceoideae* (spruce) subfamily is characterized by high concentrations of the monoterpenoids, particularly piperitone, camphor, and bornyl acetate (Fig. 2b). The spruce subfamily is divided into 5 Clades. Data for essential oil compositions of Clade IV species, which are found in Eurasia, Asia, and Mexico, were not found. Monoterpenoid signatures of the Clades have distinguishing features (Fig. 4). Camphor and piperitone were absent in *Picea breweriana* (Brewer's spruce), which is the sole Clade I species. Levels of the 2 monoterpenoids were highest in *Picea sitchensis* (Sitka spruce), the only Clade II species, with lowest levels reported in Clade V species. Abundances of the camphor and piperitone in Clade III species were intermediate. Camphor to piperitone ratios in Clade II, III, and V were 0.7, 20.5 and 5.7, respectively. α-Fenchyl actetate was only found in Clade III and IV species and was highest in Clade III species.

26

Brewer's spruce is prevalent in the Klamath Mountains of North America. Bornyl acetate, 3-carene, and α-pinene are present in nearly equal concentration and dominate the distribution of terpenes and terpenoids in Brewer's spruce (von Rudloff 1975). The abundance of α-pinene is 4 times the level of β-pinene. Sitka spruce is found on the Pacific coast of North America. The distribution of substances in essential oil of the species is characterized by high levels of myrcene, camphor, and pipertone. α-Pinene levels are 20 times lower in concentration than myrcene and twice the abundance of β-pinene. *Picea engelmannii* (Engelmann spruce) and white spruce are found in western and northern North America, respectively, and are the only Clade III species. Camphor, bornyl acetate, and limonene dominate the distributions of the species; however, limonene is present at <1% in the essential oil of Engelmann spruce. α-Pinene levels are 10 times greater in White spruce and the ratio of β-pinene to α-pinene is 3 in Engelmann spruce and a factor of 10 lower in white spruce. Introgression between white and Engelmann spruce is extensive in central and southern British Columbia and the Rocky Mountains of Alberta (Wright 1955). White and Engelmann spruce are prevalent in the lower valleys and near the timberline, respectively, with hybrids being found at intermediate elevations. The group of substances, myrcene, 3-carene, and pipertone increased in abundance, limonene, camphor and bornyl acetate decreased in concentration, and α- and β-pinene levels remained the same in essential oils of spruce from the foothills to the treeline in the Rocky Mountains of Alberta where white and Engelmann spruce dominated at lower and higher elevation, respectively (Oglive & von Rudloff 1968). Hybrids with terpene and terpenoid distributions intermediate between the 2 species were identified at mid-Valley sites and similar to essential oil composition observed for hybrids in Montana (Habeck & Weaver 1969).

Picea abies (Norway spruce), black spruce, *Picea omorika* (Serbian spruce)*, Picea pungens* (blue spruce), and *Picea rubens* (red spruce) are 4 of the 16 species in Clade V. Distributions of substances in essential oils of Clade V species have similarities (Fig. 5);

however, there are major differences in levels of some terpenes and terpenoids (von Rudloff 1966, 1967, and 1975, Rottink & Hanover 1972, Wilkinson & Hanover 1972, Schönwitz *et al.* 1989 and 1990). Camphene and bornyl acetate dominate the distribution. Bornyl acetate levels are similar in black and red spruce, about half the abundance in Serbian spruce, and lowest in Norway spruce. Camphor levels are <1% in black and red spruce and about 5% in Norway spruce. Abundances of α-pinene are much greater than β-pinene levels and concentrations of the 2 species are similar in Norway, black, and blue spruce and much lower in red spruce. Ratios of α- and β-pinene in Serbian and red spruce are similar; however, the levels of α-pinene are similar to the levels in Norway, black, and blue spruce. Myrcene and limonene levels in Norway spruce are the highest of the Clade V species with myrcene levels being similar in black, Serbian, and red spruce.

Laricoideae – Monoterpene and monoterpenoid content of essential oils of the *Laricoideae* (larch) subfamily are more similar to levels in essential oils of the pine and spruce subfamilies, respectively; however, chemical signatures of the 3 subfamilies are distinct (Fig. 2c). Levels of α- and β-pinene in larch essential oil are similar and greater, respectively than abundances of the monoterpene species in pine. Of the monoterpenoids, 1:8 cineole and bornyl acetate levels in larch essential oil are similar in content to concentrations in spruce and pine, respectively. Abundances of terpinen-4-ol and α-terpineol in all 3 *Pinaceae* subfamilies are similar.

Signatures of the Larix and Pseudotsuga genera have distinct features (Fig. 6). Levels of α- and β-pinene in foliar essential oils of genus *Larix* species, particularly North American species, were greater and less, respectively, than the content of essential oils in *mensiesii* var. *menziessi* species of genus *Pseudotsuga* (Douglas fir). The coastal variety is var. menziesii and var. *glauca* is found inland and in the Rocky Mountains.

The inland variety is a hybrid with white spruce with a signature that is intermediate between white spruce and Douglas fir (von Rudloff 1972a, 1973a) and not characteristic of larch. The 2 varieties have characteristic signatures and separate ranges in the United States; however, ranges overlap in British Columbia and hybrids having intermediate essential oil compositions have been observed (von Rudloff 1973; Zavarin & Snajberk 1973). The Rocky mountain variety is distinctive with major abundances of santene, tricyclene, camphene, limonene, and bornyl acetate (von Rudloff 1972a). Distinctive signatures for northern and southern Rocky Mountain populations have been observed through analysis of cortical oleoresins (Zavarin & Snajberk 1973); however, the same trends were not observed in foliar oleoresins (von Rudloff 1975b). Northern, intermediate, and southern populations exhibit distinct distributions of foliar essential oils. γ-Terpinene, terpinolene, terpinen-4-ol, and α-terpineol abundances are also much greater in foliar essential oil of var. *menziessi* than the foliage oil of *Larix* species; however, δ-3-carene and myrcene levels are greater in *Larix* species.

Abietoideae – Signatures of the *Abietoideae* (fir) subfamily are characterized by similar levels of α- and β-pinene that are lower than other subfamilies of *Pinaceae*; however, abundances of δ-3-carene, limonene, and β-phellandrene are greater (Fig. 2d). Camphene and bornyl acetate contents of the oleoresin of the fir subfamily are similar to spruce. Ratios of α- to β-pinene in foliar essential oils of the *Abies*, *Cedrus*, and *Tsuga* subgenera were 0.9, 1.8, and 6.8, respectively (Fig. 7). Camphene content of *Balsamea* (14.6%) and *Tsuga* (14.7) and levels in *Cedrus* were much lower (1.6%). Very few of the studies report the level of sesquiterpenes; however, the content for *Cedrus atlantica* was particularly high (16.4%), and largely attributed to β-caryophyllene and muurolenes. Foliar extracts of species of the *Balsamea* and *Moni* sections of the genus *Abies* exhibited distinct signatures. Limonene and β-phellandrene content of foliar extracts of *Abies* species were high. In *Balsamea*, α- to β-pinene ratios in *A. balsamea* and *A. lasiocarpa* were 0.2 and 0.4, respectively, and in *A. sachalinesis*

29

and *A. veitchi* the ratios were 1.4 and 1.8. α-Pinene content of *A. firma* of *Moni* was 48.6% and the α- to β-pinene ratio was 32.4. Bornyl acetate levels in foliar essential oils of *Balsamea* and *Moni* were >15% and <5%, respectively. α- to β-Pinene ratios in *Cedrus atlantica* and *C. deodora* were 13.6 and 1.2, respectively; however, monoterpene levels in *C. deodora* and *C. atlantica* were 87.6 and 25.5%, respectively. Ratios of α- to β-pinene in *Tsuga Canadensis* and *T. sieboldii* were 6.1 and 7.1.

Ranges of fir species in North America stretch across Canada and upper regions of the United States and along the Pacific coast and Rocky Mountains from Canada to the United States/Mexico border (von Rudloff 1975b). Intermediate essential oil compositions related to hybridization and introgression of species have been observed (Zavarin *et al.* 1970, 1971, 1973; Zavarin & Snajberk 1972). Signatures of populations in central Alberta where ranges of *A. balsamea* and *A. lasiocarpa* overlap exhibited intermediate characteristics of the 2 species (45-55% *A. lasiocarpa*). Cortical oleoresin analysis indicated 3 distinctive *A. lasiocarpa* types in regions from northern British Columbia to Utah and Arizona (Zavarin *et al.* 1970); however, similar variations were not observed in foliar oleoresin extracts (von Rudloff 1975b). Analysis of foliar oleoresins of *A. grandis*, *A. amabilis*, *A. procera*, *A. concolor*, and *A. magnifica*, which populate areas along the Pacific coast and mountain ranges, have signatures characteristic of potential introgressions (von Rudloff 1975b). The species *A. grandis* and *A. concolor* are classified in section *Grandis*, *A. procera* and *A. magnifica* are *Noblis* section species, and *A. amabilis* one of 2 species in section *Amabalis*. Distinctive features of leaf oils of *A. amabilis*, *A. procera*, *A. concolor*, and *A. magnifica* included >20% each of δ-3-carene and β-phellandrene, >50% limonene, an α- to β-pinene ratio of 20, and ~50% β-phellandrene, which indicates species of the same section can have unique terpene and terpenoid distributions. However, signatures of *Balsamea* species, *A. balsamea*, *A. lasiocarpa* and *A. siberica* exhibit several

similarities as do *A. alba* and *A. siberica,* which are *Abies* and *Balsamea* species, respectively (Hunt & Rudloff 1974; von Rudloff, 1975b; Joye *et al.* 1972).

The genus *Tsuga* is classified into 2 subgenera, *Tsuga* and *Hesperopeuce. Tsuga* species of genus *Tsuga* in North America include *T. canadensis* (found in the upper Midwest and the Eastern seaboard) and *T. heterophylla* (found in the Pacific Northwest and Rocky Mountains along the U.S./Canadian border) of the subgenus *Tsuga* and *T. mertensiana* (found in Pacific coastal mountain ranges from Canada into Alaska) of the subgenus *Hesperopeuce*. Data for oleoresin composition of genus *Tsuga* species are scarce. *Tsuga canadensis* and *T. sieboldii* are both subgenus *Tsuga* species and are found in North America and Japan, respectively. α- to β-Pinene ratios of *T. canadensis* and *T. sieboldi* were 6.1 and 7.1, respectively. However, the distribution of other monoterpenes like camphene, myrcene, limonene, and α-phellandrene in *T. canadensis* was distinct from *T. sieboldi*. Foliar oils of *T. canadensis* contain camphene, *D*-borneol, and bornyl acetate and resemble oils of *Picea mariana* and *P. rubens*; however, santene is not found in the former (von Rudloff 1975b). Leaf essential oil of *T. heterophylla* does not contain terpenes and terpenoids characteristic of spruce and instead β-pinene, myrcene, α- and β-phellandrene, and *cis*-ocimene were the primary monoterpenes. The signature of *T. mertensiana* is intermediate between *T. canadensis* and *T. heterophylla* with the exception of >30% δ-3-carene in the foliar essential oil of the former, and thus, *T. mertensiana* cannot be considered a hybrid.

Cupressoideae – Genera of the subfamily *Cupressoideae* include *Thuja* and *Juniperus*, which are classified in the family *Cupressaceae*. Features of foliar essential oils that distinguish species of *Cupressoideae* from *Pinaceae* include low levels of monoterpenes with the exception of sabinene and monoterpenoids like α- and *iso*-thujone, camphor, terpinen-4-ol, citronellol, methyl eugenol, and safrole (Fig. 2e). High

levels of α- and *iso*-thujone in *Thuja* distinguish species of the genera from *Juniperus* species (Fig. 8). The *Thuja* species *T. occidentalis* and *T. Plicata* are found in eastern and western North America, respectively. Foliar essential oil composition of the 2 species is very similar with α- and *iso*-thujone, *D*-fenchone, and sabinene as principal chemical species. The diterpenes, kaurene, rimuene, and cupressene have also been observed in *Thuja* species (Aplin *et al.* 1963). Ranges of the 2 species in North America are far apart, and thus, introgression and hybridization and unlikely to occur. Analysis of foliar oils from a species of the *Chamaecyparis* genera of *Cupressaceae* that grows in Alaska, *C. nootkatensis*, indicates a distinctive signature with α-pinene, δ-3-carene, and limonene as principal components and sabinene being absent. Large amounts of sesquiterpenes, diterpenes, and esters of *iso*-valeric acid are also found in the species (Andersen & Syrdal 1970). The pattern appears to be characteristic of *Chamaecyparis* species and was observed in *C. lawsoniana* that grows in the Klamath Mountain valleys of Oregon, and *C. formosensis*, and *C. taiwanensis* from Taiwan.

Species of *Juniperus* section *Sabina* are classified into New and Old World species. Ranges of the New World species, *J. Virginiana*, *J. Scopulorum*, *J. Horizontalis*, and *J. Ashei* are the Eastern and Midwestern U.S., the Western U.S., across Canada and into the Upper Great Lakes, and south Texas, respectively. Overlapping ranges between the 4 species occur; and introgression and hybridization has been observed between *J. Virginiana* and *J. scopulorum* and possibly, *J. horizontalis* (Flake *et al.* 1969). Distinctive features of leaf essential oils of New World species include similar levels of monoterpenes and monoterpenoids, particularly sabinene and camphor, respectively. Distinguishing features of the foliar oils of *J. scopulorum* and *J. horizontalis* include larger amounts of *p*-cymene and terpinen-4-ol and smaller amounts of tricyclene, camphene, α-terpinene, and bornyl acetate. α-Terpinene, *p*-cymene, and camphor are also present in foliage oils of *J. osteosperma* and *J. californica*, which are found in the Western U.S. and similar to *J. ashei*. Essential oils of all 3 species are similar to foliar

oil of *Picea glauca*. Foliar essential oil of *J. communis*, which is classified in section *Juniperus* subsection *Juniperus*, contains >70% α-pinene and levels of myrtenal, myrtenol, myrtenyl acetate, citronellal, *iso*-citronellal and the sesquiterpenoids, nerolidol and farnesol that are distinct from section *Sabina* species.

2.3.3. Variations related to season and age

Essential oil composition is sensitive to plant phenology and photosynthetic activity that are driven by seasonal changes in irradiance. Branch orientation determines light exposure and canopy architecture alters transmission of light through the canopy. Seasonal dynamics of terpene and terpenoid biosynthesis in higher plants is driven by photosynthetic or photorespiratory production of precursors (Bäck et al. 2005). Substrates for terpene and terpenoid biosynthesis are generated by Calvin cycle activity, which can be kept operational by photosynthesis or photorespiration. The biosynthetic pathway occurs in 3 phases: (1) formation of C_5 units, (2) condensation of two or three C_5 units to form C_{10}, C_{15}, or C_{20} prenyl diphosphates, and (3) conversion of prenyl diphosphates to terpenes and terpenoids (Bohlmann *et al.* 1998). Carbon skeletons for the C_5 units are provided by glyceraldehyde-3-phosphate (GA-3-P), which is a Calvin cycle intermediate, and phosphoenolpyruvate (PEP) that is produced in glycolosis from sucrose. Metabolites formed from glucose can also serve as a substrate pool. Precursors for the terpenes and terpenoids are formed in a sequence of enzymatic reactions that converts PEP to pyruvate. The pyruvate reacts with GA-3-P to produce 1-deoxy-D-xylulose-5-phosphate (DOXP) and finally isopentyl pyrophosphate (IPP) that isomerizes to dimethylallyl pyrophosphate (DMAPP) (Lichtenthaler 1999). Prenyltransferase-catalyzed condensation of the two C_5 units generate geranyl diphosphate (GDP) and additions of IPP form farnesyl diphosphate (FDP) and

geranylgeranyldiphosphate (GGDP). Cyclization reactions involving GDP (C_{10}), FDP (C_{15}) and GGDP (C_{20}), which are catalyzed by a myriad of terpene and terpenoid synthases, produce monoterpenes, sesquiterpenes, and diterpenes, respectively. Common plant enzymes like oxidases, dehydrogenases, methyltransferases, carboxyltransferases, and acyltransferases add functionalities to terpene carbon skeletons and form terpenoids (Dudareva *et al.* 2004).

Terpene and terpenoid molecular signatures are sensitive to conifer phenology like bud formation and flushing, and maturation of foliage. Buds of *Pinaceae* of the Temperate Zone are in the resting and dormant phase during autumn and winter, respectively (Perry 1971). Buds of 50-yr-old White spruce in May contained mainly α-pinene, limonene, myrcene, and β-pinene; however, relative levels of α-pinene and β-pinene in young foliage decreased and reached a minimum in May (von Rudloff 1972b; Fig. 9). Relative abundances increased by mid-June to concentrations observed during fall and winter. Limonene and myrcene in foliage increased after bud flushing and steadily decreased to typical amounts observed by mid-June without going through a minimum. Bornyl acetate, camphene, sesquiterpenes (e.g., cadinene), and sesquiterpenoids (e.g., cadinol) were present in trace amounts in buds, rose in foliage in May, and decreased to minima in late May and June to levels typically of fall and winter. Camphene and camphor reached maxima at a later date than the other terpenes and terpenoids. Lower levels of activity were found in buds that formed in August. In contrast to the behavior of terpenes and terpenoids in foliage after bud flushing, small changes in relative amounts of α-pinene, camphene, camphor, bornyl acetate, and the sesquiterpenes were observed; however, large changes were found in relative abundances of β-pinene, limonene, and myrcene.

The sequence of terpene and terpenoid formation in buds and young foliage of black spruce is very different than white spruce (von Rudloff, 1975b). Camphene and borneol increased from trace levels in buds to maxima typical of mature foliage. Bornyl acetate was abundant in buds, decreased to a minimum in winter foliage, and increased to levels typical of spring buds. Temporal profiles for α- and β-pinene, myrcene, and 3-carene abundances in foliage were distinct. Myrcene reached a maximum immediately after bud flushing and the peak in concentration of 3-carene occurred during late winter. Unlike white spruce, 3-carene was a major component of foliage essential oil of *Picea pungens* (Blue spruce) throughout the year; however, the rate of decrease of 3-carene following bud flushing was not as prounounced (von Rudloff 1975b). Temporal profiles of foliage α- and β-pinene contents were also different than profiles of the chemical species for white and black spruce. Similar to white and black spruce, limonene and myrcene exhibit sharp maxima 2-3 wk after bud flushing. A fairly rapid increase in camphene, camphor, borneol, and bornyl acetate abundances in blue spruce following bud flushing was observed. However, unlike levels of borny acetate in fall buds of white and black spruce that diminished to trace levels, bornyl acetate levels in fall buds were 5%. Similar to white and black spruce, camphene and camphor reached maxima at a later date than the other terpenes and terpenoids. Myrcene was the most abundant chemical species in essential oil of new foliage of *Picea sitchensis* (Sitka spruce); however, monoterpenoids were not detected (Hrutfiord *et al.* 1974). Myrcene levels declined rapidly throughout the growing season as β-phellandrene, camphor, and pipertone concentrations increased. The 2-yr-old needles did not exhibit increases in myrcene content; however, pipertone reached a maximum and camphor levels decreased and then increased.

Variations in terpene and terpenoid distributions of Norway spruce foliage of different age on the same branch and from different branch elevations of clones have been reported (Merk *et al.* 1988). New needles of Norway spruce clones contained lower

levels of monoterpenoids, particularly camphor, than mature needles. However, levels of terpinyl acetate and α-terpineol were similar in new and mature needles and the bornyl acetate concentration was greater in new needles. Abundance of β-pinene in foliage collected near the top of trees was greater than levels in lower branches; however, tricyclene and camphene increased slightly and bornyl acetate increased in concentration by up to 100%. Two groups of terpenes in foliage of Norway spruce clones were distinguished according to seasonal variability of molecular signatures (Schönwitz et al. 1990). Levels of α- and β-pinene and to a lesser extent, myrcene and β-phellandrene were highest immediately after bud burst, exhibited a second peak during June/July, and diminished in concentration thereafter. Tricylene, camphene, sabinene, and terpenoids were not observed in the peak immediately after bud burst. Limonene content was very high in 3-wk-old needles, which has also been observed in other studies (von Rudloff 1975; Hall *et al.* 1986). Limonene might be an intermediate in the biosynthesis of terpenoids (Schütte 1984). Terpenes and terpenoids exhibited maxima in June/July. Variability in terpene composition was much lower in adult 1-yr-old needles. A second peak in terpene content was observed in adult 1-yr-old needles in February that was not found in the terpene concentration profile of juvenile needles. Temporal patterns of terpene molecular signatures for adult needles were nearly invariant with the exception of 1:8-cineole; however, terpene levels continued to vary seasonally in mature needles. Seasonal variability of molecular signatures with respect to needle age or branch elevation in wild populations are obscured due to wide variations in extractable terpene amounts, which is attributed to genetic diversity of the wild population (Zavarin *et al* 1971; Rudloff & Nyland 1979; Lapp & Rudloff 1982; Schönwitz *et al.* 1987).

Seasonal variations of terpene and terpenoid molecular signatures are less dramatic in *Abies balsamea* (Balsam fir) than in species of spruce (von Rudloff & Granat 1982). Prior to bud burst in May, levels of β-pinene, camphene, bornyl acetate, and piperitone

increased with concomitant decreases in limonene and myrcene abundances. Mature foliage exhibited very little variation in terpene and terpenoid content. Seasonal patterns of monoterpenes and sesquiterpenes in spruce species were distinct; however, β-caryophyllene and bisabolene in mature needles of Balsam fir were invariable. Levels of the sesquiterpenes were 3-4% in winter buds and diminished to about 1% in new foliage following bud burst. α- and β-Pinene and sabinene abundances in foliage of *Pseudotsuga menziesii* (Douglas fir) exhibited a seasonal increase in new growth and a decrease in mature needles (Maarse & Kepner 1970). Levels of 3-carene in new and mature growth diminished sharply at the end of July; however, myrcene and *cis*-ocimene increased in concentration from the beginning of May to the end of July. *cis*-Ocimene was absent in new growth and invariant in mature needles. Differences in new and mature foliage and seasonal variations were not observed for camphene, β-phellandrene, 1:8-cineole, limonene, γ-terpinene, or terpinolene. The monoterpenoids citronellal, citronellol, citronellyl acetate, geranyl acetate, and linalool were absent in emergent growth, increased in abundance with needle maturation, and did not exhibit seasonal variability in mature foliage. However, fenchyl alcolhol, bornyl acetate, terpinen-4-ol, and a-terpineol appear in new growth at levels similar to mature needles and do not exhibit seasonal variability in emergent or mature foliage.

Variations of terpene and terpenoid signatures of Pine species with season and age have also been reported (Zavarin *et al.* 1971). Levels of estragole decreased with needle maturation and were much lower than amounts in nearby mature foliage. The difference was observed beyond the age of needle maximum extension. Abundances of 3-carene were higher and levels of β-pinene were lower in developing needles during summer. Concentrations of α-pinene were invariable in young and mature needles. Myrcene, limonene, β-phellandrene, and terpinolene content of juvenile needles were greatest in summer. Abundances of monoterpenes in 1- and 3-yr old foliar oleoresins of *Abies magnifica, A. concolor, and A. lasiocarpa* were similar; however, distinct differences of

37

monoterpene levels in 1-yr foliar and cortical oleoresins were observed (Zavarin 1968). Seasonal variation in foliar essential oil of *Larix laricina* (Tamarack) has also been observed (Powell & Raffa 1999). α-Pinene, β-phellandrene, β-pinene, camphene, myrcene, and sabinene abundances in young shoots decreased from spring to autumn. A similar trend in essential oil composition with season was exhibited by mature shoots with the exception of β-phellandrene and camphene. Foliar monoterpenes and monoterpenoids in essential oil of *Juniperus pinchotii* exhibited greater variability in summer than winter (Adams 1970). The most abundant terpenes and terpenoids were sabinene and camphor, which increased from 16.6-22.9% and 29.6-36.5%, respectively, in summer and winter essential oils. Seasonal variations in monoterpene levels of cortical oleoresin of *Abies concolor* appear to be insignificant (Zavarin 1968).

Essential oil composition of conifer foliage can also vary with branch age, elevation and orientation (von Rudloff 1967). Limonene and α-pinene in foliage of white spruce increased (14.0-26.4% and 5.8-13.8%, respectively) and camphor decreased (52.0-25.4%) with branch elevation in a single tree of median age (25 yr) and height (11 m). However, essential oil compositions of leaves collected from branches located 1.5-6 m above ground level for most trees were fairly similar. Camphor in white spruce was 48.0-54.5%, 55.5%, and 41.9-41.9% in 3-5-yr-old, 12-18-yr-old, and over 50-yr-old trees, respectively. Levels of many terpenes and terpenoids in foliage on the North through West sides of 2 white spruce trees were consistent. Average differences with respect to the means were 0.35-0.75% and 0.31-0.69%. Largest variations were observed for camphor, which varied from 55.5-64.8% and 47.0-56.3% with orientation for 2 trees. 3-Carene and myrcene exhibited smaller variations that ranged from 4.05-9.42% and 59.9-50.8% with orientation for 2 trees, respectively. Levels of several monoterpenes in cortical oleoresins of *Abies magnifica*, with the exception of α-pinene, exhibited significant variation in trees that were less than about 25 years old (Fig. 10). Camphene, β-phellandrene, β-pinene, and limonene showed the most dramatic changes.

38

All the monoterpenes were lower in 1- and 3-yr old foliar oleoresin, with the exception of β-phellandrene content of cortical oleoresin, which was similar to foliar oleoresin amounts in the early years of growth and then rapidly diminished. Composition of foliar and cortical oleoresins were similar in the oldest branches of Sitka spruce (Hrutfiord et al. 1974)

2.3.4. Variations related to geographical location and stresses

Differences in abundances of several foliar terpenes and terpenoids in Scots pine have been observed across a southwest to southeast transect in Lithuania (Venskutonis *et al.* 2000) and in the northern region of the country (Judzentiene & Kupcinskiene 2008). Levels of α-pinene, δ-3-carene, β-caryophyllene, δ-cadinene, germacrene-*D*, germacrene-*D*-4-ol and α-cadinol across the south (and north) exhibited the largest differences and were 23.3 (13.2), 15.6 (11.7), 3.5 (4.5), 7.7 (4.2), 3.0 (1.6), 5.6 (2.3), and 4.4 (6.3)%, respectively. A much smaller suite of terpenes and terpenoids have been measured in Scots pine in Sweden, Bulgaria, and Turkey (Yazdani *et al.* 1985; Naydenov *et al.* 2005; Semiz *et al.* 2007). Ratios of α-pinene/β-pinene in southern Lithuania, northern Lithuania, Sweden, Bulgaria, and Turkey were 16, 11, 0.9, 5.7, and 31, respectively, and indicate a wide range of molecular signatures for Scots pine grown in different geographical locations. The ratio observed in Sweden was determined through direct analysis of cortical oleoresin isolated from emergent branch buds, which might indicate differences in cortical and foliar oleoresin composition. Levels terpenes and terpenoids have been measured in various species of spruce from regions across Canada, Minnesota USA, and Germany. Abundances of camphene, myrcene, β-pinene, limonene, δ-3-carene, camphor, and bornyl acetate in west (and east) Canada exhibited the largest differences and were 7.2 (10.0), 5.7 (4.5), 1.8 (6.8), 12.7 (8.2), 0.3 (0.6) 46.4

(26.8), and 11.0 (16.5), respectively (von Rudloff 1967). The same foliar terpene and terpenoid species in black spruce across Canada and Minnesota USA with the exception of β-pinene and limonene exhibited similar differences to those observed in white spruce; however, α-pinene showed larger variations in black spruce than white spruce. Foliar terpenes and terpenoids in Norway spruce growing in mountainous regions of southern Germany exhibited little variation in composition with elevation (Schönwitz et al. 1900). α-Pinene, camphene, myrcene, β-pinene, limonene, and bornyl acetate levels were 14.1, 25.0, 10.0, 1.6, 17.6, and 10.3%. Levels of α-pinene and limonene decreased and increased, respectively, and β-pinene was nearly invariant in cortical oleoresins isolated from populations of *Abies balsamea* from west to east across Canada and the upper United States (Fig. 11). Monoterpene compositions of cortical blister oleoresins from populations of *Abies lasiocarpa* in Washington, Montana, and Wyoming USA exhibited distinct trends (Zavarin *et al.* 1970). Levels of α-pinene, limonene and β-phellandrene (normalized to total monoterpene concentrations) were 22.4, 15.2, and 1.5, respectively, 4.0, 24.6, and 74.3, respectively, and 54.4, 31.3, and 2.7, respectively, in the Washington, Montana, and Wyoming populations.

Statistical analysis of terpene and terpenoid composition of essential oil of *Juniperus virginiana* across a transect from northeastern Texas to Washington, D.C. indicated that populations clustered clinally from northeast to southwest with the more homogeneous populations occurring in the Appalachian region. Signatures indicated hybridization with *J. ashei* was not the reason for the geographical variability (Flake *et al.* 1969). However, variations in terpene and terpenoid signatures of essential oils of other conifer species across geographical locations can be related to hybridization. Essential oil compositions of hybrids are characterized by distributions of chemical species that are intermediate between endmember species. Hybridization of white, Sitka, Engelmann, and blue spruces was reported to occur in the northwestern United States and southwestern Canada where ranges of the species overlap (Wright 1955). Introgression

between white and Engelmann spruce is prevalent in central and southern British Columbia and the Rocky Mountains of Alberta where hybrids are found at mid-elevation between the white and Engelmann spruces that grow in valleys and the treeline, respectively (Oglive & von Rudloff 1968, Habeck & Weaver 1969). The range of Engelmann spruce also overlaps with blue spruce in the Rocky Mountain region of the United States from Mexican to the Canadian border (Habeck & Weaver 1969). Ranges of white and black spruce overlap across Canada and the upper Great Lakes region; however, very few natural hybrids have been found. Essential oil composition of the Rosendahl spruce (a white × black spruce hybrid) is intermediate between the 2 spruce species (von Rudloff & Holst 1968).

Abiotic and biotic stressors might also be responsible for variations in terpene and terpenoid signatures of essential oils isolated from identical species of conifers across geographical locations. According to the Carbon-Nutrient Balance (CNB) hypothesis production of C-based secondary plant metabolites like the terpenes and terpenoids that are used as defense compounds increases as nutrient availability diminishes (Bryant *et al.* 1983; Herms & Mattson 1992; Peñuelas & Esiarte 1998). However, contrary to the CNB hypothesis increases in C availability did not increase the number of C atoms in terpenes (Hamilton *et al.* 2001) and N fertilization increased and decreased resin acid content in Norway spruce and Scots Pine, respectively (Kainulainen *et al.* 2000). However, terpene content of conifer foliage was unaffected by increased N availability. β-Pinene levels increased and α-pinene and myrcene abundance in essential oil of *Larix laricina* decreased with nutrient availability (Powell & Raffa 1999). Molecular signatures of terpenes and terpenoids in Estonian Scots pine populations were highly variable across a gradient in water availability and C/N ratio (Kännaste *et al.* 2013). Monoterpene and sesquiterpene content varied from 48-62% and 61-89%, respectively. Two unique pine chemotypes were identified by α-pinene and (+)-3-carene content; however, variability of molecular signatures was greatest at the dry site with the lowest

N availability, which is inconsistent with the CNB hypothesis. Levels of tricyclene, α-pinene, and camphene were higher in drought-stressed clones of Norway spruce; however, waterlogging did not have a significant effect (Kainulainen *et al.* 1992). Terpene and terpenoid biosynthesis is also induced to protect conifers against herbivores and pathogens (Zulak & Bohlmann 2010). Induction of biotic defensive responses in foliage of Norway spruce shifted molecular signature of terpene emission to greater proportions of oxygenated monoterpenes (e.g., linalool) and sesquiterpenes [e.g., (*E*)-β-farnesene] (Martin *et al.* 2003). Accumulation of monoterpenes and diterpenes in xylem of wood and bark of Norway spruce increased following induction of biotic defense responses and molecular signatures were different from foliage; however, sesquiterpene levels remained the same (Martin *et al.* 2002). The most abundant monoterpenes in order of decreasing amounts included the following: β-pinene, α-pinene, β-phellandrene, limonene, myrcene, Δ^3-carene, and camphene. Δ^3-Carene was not observed in unstressed Norway spruce. Levels of monoterpenoids (i.e., 1:8-cineole, α-fenchone, and bornyl acetate) and the diterpenoids (i.e., levopimaric acid, neoabietic acid, and pimaric acid) also increased upon induction of biotic defense responses. Relative amounts of (−)-α-pinene, (−)-camphene, (−)-β-pinene, and (+)-β-pinene increased in *Pinus caribaea* following insect attack (Fäldt *et al.* 2001); however, a decrease in the relative amount of (+)-α-pinene has also been observed (Valterová *et al.* 1995). Monoterpene signatures of *Pinus cubensis, P. contorta, P. ponderosa, and P. taeda* were unaffected by insect attack (Lewinsohn *et al.* 1991; Valterová *et al.* 1995; Phillips *et al.* 1999).

The ability of air pollutants like ozone (O_3), nitrogen dioxide (NO_2), sulfur dioxide (SO_2), ammonia (NH_3), and elevated carbon dioxide (CO_2) to induce biosynthesis of secondary plant metabolites in conifers has been investigated in fumigation experiments (Kainulainen *et al.* 1995 and 2000; Sallas *et al.* 2001; Manninen *et al.* 2002) and along transects downwind from pollution sources (Judzentiene *et al.* 2007). However, some

air pollutants can also inhibit biosynthesis by reducing photosynthetic capacity, which depletes substrates required for secondary metabolite production. Levels of monoterpenes like tricyclene, camphene, sabinene+β-pinene, and limonene+1,8-cineol increased in Scots pine foliage when fumigated with up to 1.7 times ambient levels of O_3 (~34-68 ppbv) (Kainulaninen *et al.* 2000). Myrcene and camphor increased in Norway spruce; however, resin acid content of both tree species was unchanged. Foliage levels of α-pinene, camphene, β-pinene, myrcene, and limonene in Scots pine decreased when exposed to 600 ppbv O_3 (Kainulainen *et al.* 1995). Monoterpene and resin acid content of cortical oleoresin from Scots pine and Norway spruce was unaffected by low-levels of O_3 exposure (~64 ppbv) (Manninen *et al.* 2002); however, Kainulainen et al. (1995) report increased concentrations of cortical resin acids in Scots pine exposed to 600 ppbv O_3 or 100 ppbv NO_2. Along transects of Scots pine exposed to SO_2 from pollution sources, diterpene content of foliage was lowest and monoterpene and sesquiterpene levels were highest near the source (Kupcinskiene *et al.* 2008). Sesquiterpene and sesquiterpenoid levels in foliage were highest and monoterpene content was lowest nearby an NH_3 pollution source (Kupcinskiene *et al.* 2008; Judzentiene *et al.* 2006), which is consistent with the CNB hypothesis. According to the CNB hypothesis, exposure of conifers to elevated levels of CO_2 is expected to increase C availability for synthesis of secondary plant metabolites like the terpenes and terpenoids (Bryant *et al.* 1983). Abundance of β-pinene increased in foliage of *Pinus taeda* exposed to CO_2 levels 150 and 300 ppmv above ambient (Williams *et al.* 1994). Levels of α-pinene in foliage of Scots pine increased by about 50% when exposed to 600-700 ppmv CO_2 (Heyworth *et al.* 1998; Sallas *et al.* 2001). Foliar levels of total monoterpenes and the molecular signature in Scots pine were unaffected when exposed to 645 ppmv CO_2 (Kainulainen *et al.* 1998), which is inconsistent with the CNB hypothesis.

2.3.5. Variations related to isolation and analytic methods

Molecular signatures of essential oils are sensitive to extraction and analytic methods. The traditional method of extracting essential oil from plant foliage is micro-hydrodistillation (HD; i.e., steam distillation), which is suitable for compounds with boiling points below about 200ºC (Franklin & Keyzer 1962; Simard *et al.* 1988; Kamdem *et al.* 1993). Other methods include simultaneous steam distillation-solvent extraction (SDE) (Godefroot *et al.* 1981; Orav *et al.* 1996), solvent extraction (Schönwitz *et al.* 1987; Muzika *et al.* 1990; 30), supercritical fluid extraction (SFE) (Hawthorne *et al.* 1993; Orav *et al.* 1998), headspace (HS) analysis (Vourela *et al.* 1989), and solid-phase microextraction (SPME) (Santos *et al.* 2006). Microcohobation (circulative steam) and vacuum distillation have been used to isolate essential oils (Franklin & Keyzer 1962). Micro-HD techniques are unsuitable for the hydrolysable contents (i.e, resin acids) of conifer oleoresin like pimaric, palustric, abietic, neobietic, dehydroabietic, and sandaracopimaric acids (Lewisohn *et al.* 1993) and is known to generate α-terpinene, γ-terpinene, linalool, and borneol (Koedam & Looman 1980). Linalool and α-terpineol were produced during steam distillation of *Pinus pinaster* foliage and absent in leaves extracted with pentane and methanol (Pauly *et al.* 1973). Yields of monoterpenes by HS are higher than yields by HD (Vourela *et al.* 1989) and similar to results by HS-SPME (Santos *et al.* 2006). Similar yields of volatile terpenes by HS analysis and direct analysis of the essential oil have been reported (Pohjola *et al.* 1989).

Marcusson- (Bicchi *et al.* 1990) and Clevenger-type (Judzentiene & Kupcinskiene 2008) micro apparatus are used for SDE. Compounds with low vapor pressures like the terpenoids are incompletely recovered by the SDE technique (Orav *et al.* 1998). Yields of many terpenes and terpenoids from spruce, fir, and cedar foliar oils via hexane

extraction of foliage ground in liquid nitrogen were lower than yields by the SDE method and yields by both techniques were highly variable (Muzika *et al.* 1990; 30). Hexane extraction was found to be more effective at isolating sesquiterpenes from *Juniperius communis* than HD and SFE (Damjanovic *et al.* 2003). Terpene and terpenoid yields are also sensitive to extraction time. Monoterpene ketone yields diminished with extraction time and monoterpene and monoterpene acetate yields increased (Simard *et al.* 1988). Several hours are required to extract monoterpenes from needles of blue spruce by SDE; however, isolation of monoterpenes from *Abies grandis* (Grand Fir) requires only 30 min (Muzika *et al.* 1990). Terpenes and terpenoids are stored in leaf resin ducts; however, volatile and sparingly water-soluble chemical species of the oleoresin are also located in cuticular waxes and plant mesophyll, respectively (Niinemets *et al.* 2004). Cuticular waxes of blue spruce are thicker than waxes of grand fir, and thus, longer times are required to obtain the highest yield. The SFE isolation method appears to be the most effective method to exhaustively extract the complex mixture of terpenes and terpenoids from plant foliage. The SDE and SFE techniques recovered similar amounts of monoterpenes; however, yields of terpenoids by SFE using CO_2 with polar modifiers were greater.

Terpene and terpenoid signatures are operationally defined by the GC analytic technique and quantitation method. The neat essential oil or oleoresin extract is vaporized in an injection port heated to about 200°C before entering the analytic column of the GC. Sesquiterpenes are thermally unstable and despite being recovered quantitatively by various extraction methods might decompose in the heated injection port (Helmig *et al.* 2003). Thus, actual levels of sesquiterpenes in conifer essential oils might be much higher than reported values. For new measurements of essential oil composition reported here, 98, 115, and 87 terpenes and terpenoids of Scots pine, black spruce, and Eastern white cedar, respectively, were identified and quantified via analysis by comprehensive GC × GC-ToF-MS. Other studies used various GC-MS

techniques and reported a maximum of about 70 terpenes and terpenoids in conifer essential oils. Superior separation compared to GC techniques is achieved in comprehensive GC × GC methods by diverting the entire, modulated effluent from a nonpolar primary column into a polar secondary column (Seeley & Seeley 2013). The GC × GC modulation process compresses peaks eluted from the primary column into pulses with much smaller temporal widths than peaks eluting from the column of a GC separation. As peaks become narrower analyte flux at the detector increases, which leads to a greater detector response and higher sensitivity compared to GC methods. Comprehensive GC × GC reduces analyte coelutions by connecting in series, a secondary column with different selectivity than the primary column and is ideal for separating enantiomers of terpenes and terpenoids in oleoresins (Persson *et al.* 1996; Sjödin *et al.* 2000; Fäldt *et al.* 2001). Compositions expressed as % area of identified terpenes and terpenoids are sensitive to the number of identified analytes, making it difficult to compare reported signatures. Also, MS response factors for terpenes and terpenoids are not uniform, and thus, comparability of reported compositions would be improved by expressing signatures as the molar compositions.

2.4. Conclusions

Considerable variability of essential oil composition is exhibited at the subfamily, genera, subgenera, and species levels of the *Pinaceae* and *Cupressaceae* families. Terpene and terpenoid signatures of the *Pinoideae*, *Piceoideae*, *Laricoideae*, and *Abietoideae* subfamilies of *Pinaceae* were characterized by high monoterpene and sesquiterpene content, high monoterpenoid abundance, levels of monoterpenes and monoterpenoids similar to the *Pinoideae* and *Piceoideae* subfamilies, and low concentrations of α- and β-pinene, respectively. Distributions of terpenes and

terpenoids in essential oils of the subfamily *Cupressoideae* of the *Cupressaceae* family were distinct and characterized by high concentrations of sabinene and α- and *iso*-thujone. Differences in terpene and terpenoid distributions of essential oils isolated from the same species growing in different geographical locations were significant. Species introgression and hybridization contributed to some of the differences; however, phenology and age, biotic and abiotic stressors, and isolation and analytic methods also influence chemical signatures. Composition of foliar essential oils is most variable during the first year of needle growth and becomes more constant in 2-yr and older foliage. Disributions of monoterpenes in cortical oleoresins exhibit changes during the first 25 years of growth and become similar to compositions of foliar oleoresins of similarly aged branches. According to the CNB hypothesis, terpene and terpenoid content of essential oils, which are secondary plant metabolites composed mainly of C, are expected to increase as N availiability diminishes; however, observations that agree with and contradict the hypothesis have been made. Foliar and cortical oleoresin composition also changes in response to biotic stressors like insect infestations. Exposure to air pollutants like O_3, NO_2, and SO_2 inhibits terpene and terpenoid biosynthesis and changes signatures by reducing photosynthetic capacity that depletes substrates required for production of secondary plant metabolites. The level of terpenes and terpenoids in bole and foliar emissions depend upon molar composition of cortical and foliar oleoresins, which requires measurement of essential oil yield. The SDE method effectively isolates essential oil; however, resin acids, which is an important component of oleoresins, are hydrolyzed and not recovered. The SFE technique is an exhaustive extraction method that appears to be most effective for measuring oleoresin compostion. The GC × GC-ToF-MS analysis of essential oil composition of Scots pine, black spruce, and Eastern white cedar reported here identified and quantified more species than GC-MS methods. There was general agreement with distributions reported in the literature. The MS response factors for terpenes and terpenoids are not uniform, and thus, signatures based on molar composition are more accurate than distributions determined from % area response.

Sensitvity of terpene and terpenoid signatures of conifers to phenology and age, biotic and abiotic stressors, and isolation and analytic methods complicates development of emission inventories that are based on essential oil composition. Current emission inventories, which are based on parameterizations developed from direct measurement of emissions, do not account for differences in foliar and cortical oleoresin composition and variations related to phenology, age, and biotic and abiotic stresses. Parameterizations that relate conifer terpinase activities to nutrient availability and insect infestations might be developed to estimate oleoresin compositions for populations affected by biotic and abiotic stressors. Comprehensive investigation of variations in oleoresin composition related to phenology and age and measurement of molar composition using exhaustive extraction techniques like SFE with quantitation by GC × GC-ToF-MS would greatly improve the accuracy of emssion inventories.

2.5. Acknowledgements

2.6. References

Adams RP (1970) Seasonal variation of terpenoid constituents in natural populations of *Juniperus pinchotii* Sudw. Phytochem 9:397-402

Andersen NH, Syrdal (1970) Terpenes and sesquiterpenes of *Chamaecyparis noot-katensis* leaf oil. Phytochem. 9:1325-1340

Aplin RT, Cambie RC, Rutledge PS (1963) The taxonomic distribution of some diterpene hydrocarbons. Phytochem. 2:205-214

Bäck J, Hari P, Hakola H, Juurola E, Kulmala M (2005) Dynamics of monoterpene emissions in *Pinus sylvestris* during early spring. Boreal Environ Res 10:409-424

Bakkali F, Averbeck S, Averbeck D, Idaomar M (2008) Biological effects of essential oils – A review. Food Chem Toxicol 46:446-475

Bicchi C, Amato D, Nano A, Frattini C (1990) Improved method for the analysis of small amounts of essential oils by microdistillation followed by capillary gas chromatography, J Chromatogr 279:409-416

Bohlmann J, Meyer-Gauden G, Croteau R (1998) Plant terpenoid synthases: Molecular biology and phylogenetic analysis. Proc Natl Acad Sci 95:4126-4133

Boudarene L, Rahim L, Baaliouamer A, Meklati BY (2004) Analysis of Algerian essential oils from twigs, needles and wood of *Cedrus atlantica* G.Manetti by GC/MS. J Essent Oil Res 16:531-534

Bryant JP, Chapin III FS, Klein DR (1983) Carbon/nutrient balance of boreal plants in relation to vertebrate herbivory. Oikos 40:357-368

Couchman FM, von Rudloff (1965) Gas-Liquid chromatography of terpenes Part XIII. The volatile oil of the leaves of Juiperus horizontalis Moench. Can J Chem 43: 1017-1021

Damjanovic BM, Skala, D, Petrovic-Djakov D, Baras J (2003) A comparison between the oil, hexane extract and supercritical carbon dioxide extract of *Juniperus communis* L. J Essent Oil Res 15:90-92

Dudareva N, Pichersky E, Gershenzon J, (2004) Biochemistry of plant volatiles. Plant Physiol 135:1893-1902

Eav J (2011) Comparison of monoterpene oil composition and volatile emissions from ponderosa and Austrian pine.

url:http://nldr.library.ucar.edu/respository/assets/soars/SOARS-000-000-000-226.pdf

Fäldt J, Sjödin K, Persson M, Valterová I, Borg-Karlson A-K (2001) Correlations between selected monoterpene hydrocarbons in the xylem of six Pinus (Pinaceae) species. Chemoecol 11:97-106

Flake RH, von Rudloff E, Turner BL (1969) Quantitative study of clinal variation in *Juniperus virginiana* using terpenoid data. Proc Nat Acad Sci 64:487-494

Franklin WJ, Keyzer H (1962) Semimicro and micro steam distillation. The estimation of the essential oil content of small plant samples. Anal Chem 34:1650-1653

Geron C, Rasmussen R, Arnts RR, Guenther A (2000) A review and synthesis of monoterpene speciation from forests in the United States. Atmos. Environ. 34:1761-1781

Godefroot M, Sandra P, Verzele M (1981) New method for quantitative essential oil analysis. J Chromatogr 203: 325-335

Guenther A, Hewitt CN, Erickson D, Fall R, Geron C, Graedel T, Harley P, Klinger L, Lerdau M, McKay WA, Pierce T, Scholes B, Steinbrecher R, Tallamraju R, Taylor J, Zimmerman P (1995) A global model of natural volatile organic compound emissions. J Geophys Res 100:8873-8892

Guenther AB, Monson RK, Fall R (1991) Isoprene and monoterpene emission rate variability: observations with *Eucalyptus* and emission rate algorithm development. J Geophys Res 96:10,799-10,808

Guenther AB, Zimmerman PR, Harley PC, Monson RK, Fall R (1993) Isoprene and monoterpene emission rate variability: model evaluations and sensitivity analyses. J Geophys Res 98:12,609-12,617

Habeck JR, Weaver TW (1969) A chemosystematic analysis of some hybrid spruce (*Picea*) populations in Montana. Can J Bot 47:1565-1570

Hakola H, Tarvainen V, Bäck J, Ranta H, Bonn B, Rinne J and Kulmala M (2006) Seasonal variation of mono- and sesquiterpene emission rates of Scots pine. Biogeosci 3:93-101

Hall GD, Langenheim JH (1986) Temporal changes in the leaf monoterpenes of *Sequoia sempervirens*. Biochem Syst Ecol 14:61-69

Hamilton JG, Zangerl AR, DeLucia EH, Berenbaum MR (2001) The carbon-nutrient balance hypothesis: its rise and fall. Ecol Lett 4:86-95

Hanes CS (1927) Resin canals in seedling conifers. J Linn Soc London, Bot 47:613-636

Hawthorne SB, Riekkola M-L, Serenius K, Holm Y, Hiltunen R, Hartonen K (1993) Comparison of hydrodistillation and supercritical fluid extraction for the determination of essential oils in aromatic plants. J Chromatogr 634:297-308

Helmig D, Ortega J, Duhl T, Tanner D, Guenther A, Harley P, Wiedinmyer C, Milford J, Sakulyanontvittaya T (2007) Sesquiterpene emissions from pine trees – identifications, emission rates and flux estimates for the contiguous United States. Environ Sci Technol 41:1545-1553

Helmig D, Revermann T, Pollmann J, Kaltschmidt O, Jimenez Hernandez A, Bocquet F, David D (2003) Calibration system and analytical considerations for quantitative sesquiterpene measurements in air. J Chrom A 1002:193-211

Herms DA, Mattson WJ (1992) The dilemma of plants: to grow or defend. Q Rev Biol 67:283-335

Heyworth CJ, Iason GR, Temperton V, Jarvis PG, Duncan AJ (1998) The effect of elevated CO_2 concentration and nutrient supply on carbon-based plant secondary metabolites in *Pinus sylvestris* L., Oecologia 115:344-350

Holzke C, Hoffman T, Jaeger L, Koppmann R, Zimmer W (2006) Diurnal and seasonal variation of monoterpene and sesquiterpene emissions from Scots pine (*Pinus sylvestris* L.). Atmos Environ 40:3174-3185

Hrutfiord BF, Hopley SM, Gara RI (1974) Monoterpenes in Sitka Spruce: Within tree and seasonal variation. Phytochem 13:2167-2170

Hudgins JW, Christiansen E, Franceschi VR (2004) Induction of anatomically based defense responses in stems of diverse conifers by methyl hasmonate: a phylogenetic response. Tree Physiol 24:251-264

Hunt RS, von Rudloff E (1974) Chemosystematic studies in the genus Abies. I. Leaf and twig oil analysis of alpine and balsam firs. Can J bot 52:477-487

bin Jantan I, Said Ahmad A, Rashih Ahmad A (2002) A comparitive study of the oleoresins of three *Pinus* species from Malaysian Pine Plantations, J Essent Oil Res 14:327-332

Jeffrey EC (1925) Resin canals in the evolution of the conifers. Proc Natl Acad Sci 11:101-105

Joye Jr. NM, Proveaux AT, Lawrence RV (1972) Composition of pine needle oil. J Chrom Sci 10:590-592

Judzentiene A, Kupcinskiene E (2008) Chemical composition of essential oils from needles of *Pinus sylvestris* L. grown in northern Lithuania. J Essent Oil Res 20:26-29

Judzentiene A, Slizyte J, Stikliene A, Kupcinskiene E (2006) Characteristics of essential oil composition in the needles of young stand of Scots pine (*Pinus sylvestris* L.) growing along aerial ammonia gradient. Chemija 17:67-73.

Judzentiene A, Stikliene A, Kupcinskiene E (2007) Changes in the essential oil composition in the needles of Scots pine (*Pinus sylvestris* L.) under anthropogenic stress. TheSci.WorldJ 7:141-150

Kainulainen P, Holopainen JK, Holopainen T (1998) The influence of elevated CO2 and O3 concentrations on Scots pine needles: Changes in starch and secondary metabolites over three exposure years. Oecologia 114:455-460

Kainulainen P, Holopainen JK, Oksanen J (1995) Effects of gaseous air pollutants on secondary chemistry of Scots pine and Norway spruce seedlings. Water Air Soil Pollut 85:13931398.

Kainulainen P, Oksanen J, Palomäki V, Holopainen JK, Holopainen T (1992) Effect of drought and waterlogging stress on needle monoterpenes of *Picea abies*. Can J Bot 70:1613-1616

Kainulainen P, Utriainen J, Holopainen JK, Oksanen J, Holopainen T (2000) Influence of elevated ozone and limited nitrogen availability on conifer seedlings in an open-air

fumigation system: effects on growth, nutrient content, mycorrhiza, needle ultrastructure, starch and secondary compounds. Global Change Biol 6:345-355.

Kamdem PD, Hanover JW, Gage DA (1993) Contribution to the study of the essential oil of Thuja occidentalis L. J Essent Oil Res. 5:117-122

Kanakidou M, Seinfeld JH Pandis SN, Barnes I, Dentener FJ, Facchini MC, van Dingenen R, Ervens B, Nenes A, Nielsen CJ, Swietlicki E, Putaud JP, Balkanski Y, Fuzzi S, Horth J, Moortgat GK, Winterhalter R, Myhre CEL, Tsifaridis K, Vignati E, Stephanou EG, Wilson J (2005) Organic aerosol and global climate modeling: a review. Atmos Chem Phys 5: 1053-1123

Kännaste A, Copolivici L, Pazouki L, Suhhorutsenko M, Niinemets Ü (2013) Highly variable chemical signatures over short spatial distances among Scots pine (*Pinus sylvestris*) populations. Tree Physiol 00:1-14

Kesselmeier J, Staudt M (1999) Biogenic volatile organic compounds (VOC): An overview on emission, physiology and ecology. J Atmos Chem 33:23-88

Koedam A, Looman A (1980) Effect of pH during distillation on the composition of the volatile oil from Juniperus Sabina. Planta Med Suppl:22-28

Kolesnikova RD, Latysh VG, Krasnoboyarova LV, Deryuzhkin RI, Chernodubov AI (1976) The chemical composition of the essential oil of the Larch. Chem Nat Cmpds 12:402-407

Komenda M, Koppmann R (2002) Monoterpene emissions from Scots pine (Pinus sylvestris): Field studies of emission rate variabilities. J Geophys Res 107: doi:10.1029/2001JD000691

Kulmala M, Suni T, Lehtinen KEJ, Dal Masso M, Boy M, Reissell A, Rannik Ü, Aalto P, Keronen P, Hakola H, Bäck J, Hoffmann T, Vesala T, Hari P (2004) A new feedback mechanism linking forests, aerosols, and climate. Atmos Chem Phys 4:557-562

Kupcinskiene E, Stikliene A, Judzentiene A (2008) The essential oil qualitative and quantitative composition in the needles of Pinus sylvestris L. growing along industrial transects. Environ Pollut 155: 481-491.

Kurose K, Okamura D, Yatagi M (2007) Composition of the essential oils from the leaves of nine Pinus species and the cones of three of Pinus species. Flav Fragr J 22:10-20

Langenheim JH (2003) *Plant Resins: Chemistry, Evolution, Ecology, and Ethnobotany.* Timber Press Inc., Cambridge, U.K.

Lapp MS, von Rudloff E (1982) Chemosystematic studies in the genus *Pinus*. IV. Leaf oil composition and geographic variation in jack-pine of eastern North America. Can J Bot 60:2762-2769

Lerdau M, Litvak M, Palmer P, Monson R (1997) Controls over monoterpene emissions from boreal forest conifers. Tree Physiol 17:563-569

Lewinsohn E, Gijzen M, Savage TJ, Croteau R (1991) Defense mechanisms of conifers. Relationship of monoterpene cyclase activity to anatomical specialization and oleoresin monoterpene content. Plant Physiol 96:38-43.

Lewisohn E, Savage TJ, Gijzen M, Croteau R (1993) Simultaneous analysis of monoterpenes and diterpenoids of conifer oleoresin. Phytochem Anal 4:220-225

Lewisohn E, Savage TJ, Gijzen M, Croteau R (1993) Defense mechanisms of conifers. Differences in constitutive and wound-induced monoterpene biosynthesis among species. Plant Physiol 96:38-43

Lichtenthaler HK (1999) The 1-deoxy-D-xylulose-5-phosphate pathway of isoprenoid biosynthesis in plants. Annu Rev Plant Physiol 50:47-65

Litvak ME, Madronich S, Monson RK (1999) Herbivore-Induced monoterpene emissions from coniferous forests: Potential impact on local tropospheric chemistry. Ecol Appl 9:1147-1159

Maarse H, Kepner RE (1970) Changes in composition of volatile terpenes in Douglas fir needles during maturation. J Agr Food Chem 18:1095-1101

Maciag A, Milakovic D, Christensen HH, Antolovic V, Kalemba D (2007) Essential oil composition and plant-insect relations in Scots pine (*Pinus sylvestris* L.), Food Chem Biotechnol 71:71-95

Manninen A-M, Utriainen J, Holopainen JT, Kainulainen P (2002) Terpenoids in the wood of Scots pine and Norway spruce seedlings exposed to ozone at different nitrogen availability. Can J For Res 32:2140-2145

Martin DM, Gershenzon J, Bohlmann J (2003) Induction of volatile terpene biosynthesis and diurnal emission by methyl jasmonate in foliage of Norway spruce. Plant Physiol 132:1586-1599

Martin D, Tholl D, Gershenzon J, Bohlmann J (2002) Methyl jasmonate induces traumatic resin ducts, terpenoid resin biosynthesis, and terpenoid accumulation in developing xylem of Norway spruce stems. Plant Physiol 129:1003-1018

Mirov NT (1961) Composition of Gum Turpentines of Pines. Pacific Southwest Forest and Range Experiment Station, U.S. Department of Agriculture, Forest Service, Technical Bulletin No. 1239

Muzika R-M, Campbell CL, Hanover JW, Smith AL (1990) Comparison of techniques for extracting volatile compounds from conifer needles. J Chem Ecol 16:2713-2722.

Naydenov K, Tremblay FM, Alexandrov A, Fenton NJ (2005) Structure of *Pinus sylvestris* L. populations in Bulgaria revealed by chloroplast microsatellites and terpenes analysis: Provenance tests. Biochem Syst Ecol 33:1226-1245

Neilson RP (1995) A model for predicting continental-scale vegetation distribution and water balance. Ecol Appl 5:362-385

Niinemets Ü, Loreto F, Reichstein M (2004) Physiological and physicochemical controls on foliar volatile organic compound emissions. Trends Plant Sci. 9:180-186

Niinemets Ü, Arneth A, Kuhn U, Monson RK, Peñuelas J, Staudt M (2010a) The emission factor of volatile isoprenoids: stress, acclimation, and development responses. Biogeosci 7:2203-2223

Niinemets Ü, Monson RK, Arneth A, Ciccioli P, Kesselmeier J, Kuhn U, Noe SM, Peñuelas J, Staudt M (2010b) The leaf-level emission factor of volatile isoprenoids: caveats, model algorithms, response shapes and scaling. Biogeosci. 7:1809-1832

Oglive RT, von Rudloff E (1968) Chemosystematic studies in the genus *Picea* (Pinaceae). IV. The introgression of white and Engelmann spruce as found along the Bow River. Can J Bot 46:901-908

Orav A, Kailas K, Koel M (1998) Simultaneous distillation, extraction and supercritical fluid extraction for isolating volatiles and other materials from conifer needles. J Essent Oil Res 10:387-393

Orav A, Kailas T, Liiv M (1996) Analysis of terpenoic composition of conifer needle oils by steam distillation/extraction, gas chromatography and gas chromatography-mass spectrometry. Chromatographia 43:215-219.

Ortega J, Helmig D (2008) Approaches for quantifying reactive and low-volatility biogenic organic compound emissions by vegetation enclosure techniques – Part A. Chemosphere 72:343-364

Ortega J, Helmig D, Daly RW, Tanner DM, Guenther AB, Herrick JD (2008) Approaches for quantifying reactive and low-volatility biogenic organic compound emissions by vegetation enclosure techniques – Part B: Applications. Chemosphere 72:365-380

Pauly G, Gleizes M, Bernard-Dagan C (1973) Identification des constituants de l'essence des aiguilles de *Pinus pinaster*. Phytochem 12:1395-1398

Pauly G, von Rudloff E (1971) Chemosystematic studies in the genus *Pinus*: the leaf oil of *Pinus contorta* var. *latifolia*. Can J Bot 49: 1201-1210

Peñuelas J, Esiarte M (1998) Can elevated CO_2 affect secondary metabolism and ecosystem functioning? Trends Ecol Evol 13: 20-24

Perry TO (1971) Dormancy of trees in winter. Science 171:29-36

Persson M, Sjödin K, Borg-Karlson A-K, Norin T, Ekberg I (1996) Relative amounts and enantiomeric compositions of monoterpene hydrocarbons in xylem and needles of *Picea abies*. Phytochem 42:1289-1297

Phillips MA, Croteau RB (1999) Resin-based defenses in conifers. Trends Plant Sci. 4:184190

Phillips MA, Savage TJ, Croteau R (1999) Monoterpene synthases of Loblolly pine (*Pinus taeda*) produce pinene isomers and enantiomers. Arch Biochem Biophys 372:197-204.

Pohjola J, Hiltunen R, Shantz MV (1989) Variation and inheritance of terpenes in Scots pine. Flavour Fragr J 4:121-124

Powell JS, Raffa KF (1999) Sources of variation in concentration and composition of foliar monoterpenes in Tamarack (*Larix laricina*) seedlings: Roles of nutrient availability, time of season, and plant architecture. J Chem Ecol 25:1771-1797

Prentice IC, Cramer W, HarrisonSP, Leemans R, Monserud RA, Solomon AM (1992) A global biome model based on plant physiology and cominance, soil properties and climate. J. Biogeogr 19:117-134

Radwan MA, Crouch GL, Harrington CA, Ellis WD (1982) Terpenes of ponderosa pine and feeding preferences by pocket gophers. J Chem Ecol 8:241-253

Rizzo B, Wiken E (1992) Assessing the sensitivity of Canada's ecosystems to climatic change. Clim Change 20:81-95

Roller KJ (1966) Resin canal position in the needles of Balsam, Alpine and Fraser firs. For Sci 12: 348-355

Rottink BA, Hanover JW (1972) Identification of Blue spruce cultivars by analysis of cortical oleoresin monoterpenes. Phytochem 11:3255-3257

Roussis V, Petrakis PV, Ortiz A, Mazomeno BE (1995) Volatile constituents of needles of five Pinus species grown in Greece 39:357-361

von Rudloff E (1961) Gas-Liquid chromatography of terpenes Part IV. The analysis of the volatile oil of the leaves of Eastern white cedar. Can J Chem 39:1200-1206

von Rudloff E (1962a) Gas-Liquid chromatogarphy of terpenes Part V. The volatile oils of the leaves of Black, White, and Colorado spruce. Tappi J 45:181-184

von Rudloff E (1962b) Gas-Liquid chromatography of terpenes VI. The volatile oil of Thuja plicata Donn. Phytochem 1:195-202

von Rudloff E (1963) Gas-Liquid chromatography of terpenes Part IX. The volatile oil of the leaves of Juniperus Sabina L. Can J Chem 41:2876-2881

von Rudloff E (1964) Gas-Liquid chromatography of terpenes Part X. The volatile oils of the leaves of Sitka and Engelmann spruce. Can J Chem 42:1057-1062

von Rudloff E (1966) Gas-Liquid chromatography of terpenes—XIV. The chemical composition of the volatile oil of the leaves of *Picea rubens* Sarg. And chemotaxonomic correlations with other North American spruce species. Phytochem 5:331-341

von Rudloff E (1967a) Chemosystematic studies in the genus Picea (Pinaceae) I. Introduction. Can J Bot 45:891-901

von Rudloff E (1967b) Chemosystematic studies in the genus Picea (Pinaceae) II. The leaf oil of Picea glauca and P. mariana. Can J Bot 45:1703-1714

von Rudloff E (1972a) Chemosystematic studies in the genus *Pseudotsuga*. I. Leaf oil analysis of the coastal and Rocky Mountain varieties of the Douglas fir. Can J Bot 50:1025-1040

von Rudloff E (1972b) Seasonal variation in the composition of the volatile oil of the leaves, buds, and twigs of white spruce (*Picea glauca*). Can J Bot 50:1595-1603

von Rudloff E (1973a) Chemosystematic studies in the genus *Pseudotsuga*. III. Population differences in British Columbia as determined by volatile leaf oil analysis. Can J For Res 3:433-452

von Rudloff E (1973b) Geographical variation in the terpene composition of the leaf oil of Douglas fir. Pure Appl. Chem. 34:401-410

von Rudloff E (1975a) Seasonal variation of the terpenes of the leaves, buds, and twigs of blue spruce (*Picea pungens*). Can J Bot 53:2978-2982

von Rudloff E (1975b) Volatile leaf oil analysis in chemosystematic studies of North American conifers. Biochem Syst Ecol 2:131-167

von Rudloff E (1987) The volatile twig and leaf oil terpene compositions of three Western North American Larches, Larix laricina, Larix occidentalis, and Larix lyalli J Nat Prod 50:317-321

von Rudloff E, Couchman FM (1964) Gas-Liquid chromatography of terpenes Part XI. The volatile oil of the leaves of Juniperus scopulorum Sarg. Can J Chem 42:1890-1895

von Rudloff E, Granat M (1982) Seasonal variation of the terpenes of the leaves, buds, and twigs of balsam fir (Abies balsamea). Can J Bot 60:2682-2685

von Rudloff E, Holst MJ (1968) Chemosystematic studies in the genus *Picea* (Pinaceae). III. The leaf oil of a *Picea glauca × mariana* hybrid (Rosendahl spruce). Can J Bot 46:1-4

von Rudloff E, Nyland E (1979) Chemosystematic studies in the genus Pinus. III. The leaf oil terpene composition of lodgepole pine from Yukon territory. Can J Bot 57: 1367-1370

Sallas L, Kainulainen P, Utriainen J, Holopainen T, Holopainen JK (2001) The influence of elevated O3 and CO2 concentrations on secondary metabolites of Scots pine (*Pinus sylvestris* L.) seedlings. Global Change Biol 7:303-311.

Santos AM, Vasconcelos T, Mateus E, Farrall MH, Gomes Da Silva MDR, Paiva MR, Branco M (2006) Characterization of the volatile fraction emitted by phloems of four pinus species by solid-phase microextraction and gas chromatography-mass spectrometry. J Chrom A 1105:191-198

Schantz VM, Juvonen S (1966) Über die zusammensetzung der atherischen öle bei verschiedenen *Picea*-arten. Acta Botan Fenn 73:1

Schönwitz R, Kloos M, Merk L, Ziegler H (1990a) Patterns of monoterpenes stored in the needles of Picea abies (L.) Karst. from several locations in mountainous regions of southern Germany. Trees 4:27-33

Schönwitz R, Lohwasser K, Kloos M, Ziegler H (1990b) Seasonal variation in the monoterpenes in needles of *Picea abies* (L.) Karst. Trees 4: 34-40

Schönwitz R, Merk L, Ziegler H, Trees 1 (1987) Naturally occurring monoterpenoids in needles of *Picea abies* (L.) Karst. Trees 1:88-93

Schönwitz R, Merk L, Ziegler H (1989) Variability in the monoterpenes of needles of *Picea abies* (L.) Karst. Flav Fragr J 4:149-153

Schutte H-R (1984) Secondary Substances. Monoterpenes. Prog Bot 119-139

Seeley JV, Seeley SK (2013) Multidimensional gas chromatography: Fundamental advances and new applications. 85:557-578

Semiz G, Heijari J, Isik K, Holopainen JK (2007) Variation in needle terpenoids among *Pinus sylvestris* L. (Pinaceae) provenances from Turkey. Biochem Syst Ecol 35:652-661

Shaw AC (1950) The essential oil of *Picea mariana* (MILL) B.S.P. Can J Res 28B:268-276

Shaw AC (1953) The essential oil of Thuja occidentalis L. Can J Chem 31:277-283.

Simard S, Hachey J-M, Collin GJ (1988) The variation of the essential oil composition with the extraction process, the case of *Thuja occicentalis* L. and *Abies balsamea* (L) Mill. J Wood Chem Technol 8:561-573

Sjödin K, Persson M, Fäldt J, Ekberg I, Borg-Karlson A-K (2000) Occurrence and correlations of monoterpene hydrocarbon enantiomers in Pinus sylvestris and Picea abies. J Chem Ecology 26:1701-1720

Smith B, Prentice I, Sykes M (2001) Representation of vegetation dynamics in the modeling of terrestrial ecosystems: comparing two contrasting approaches within European climate space. Global Ecol Biogeogr 10:621-637

Suzuki M (1979) The course of resin canals in the shoots of conifers III. Pinaceae and summary analysis. Bot Mag Tokyo 92:333-353

Svajdlenka E, Mártonfi P, Tomasko I, Grancai D, Nagy M (1999) Essential oil composition of *Thuja occidentalis* L. Samples from Slovakia. J Essent Oil Res 11:532-536

Tatro VE, Scora RW, Vasek FC, Kumamoto J (1973) Variations in the leaf oils of three species of Junipers. 60:236-241

Toma S, Bertman S (2012) The atmospheric potential of biogenic volatile organic compounds from needles of white pin (Pinus strobus) in Northern Michigan. Atmos Chem Phys 12:2245-2252

Tsitsimpikou C, Petrakis PV, Ortiz A, Harvala C, Roussis V (2001) Volatile needle terpenoids of six *Pinus* species. J Essent Oil Res 13:174-178

Valterová I, Sjödin K, Vrkoc J, Norin T (1995) Contents and enantiomeric compositions of monoterpene hydrocarbons in xylem oleoresins from four *Pinus* species growing in Cuba. Comparison of trees unattacked and attacked by *Dioryctria Horneana*. Biochem System Ecol 23:1-15

Vasek FC, Scora RW (1967) Analysis of the oils of Western North American Junipers by gas-liquid chromatography. Amer J Bot 54:781-789

Venskutonis PR, Vyskupaiyte K, Plausinaitis R (2000) Composition of essential oils of *Pinus syslvestris* L. from different locations of Lithuania. J Essent Oil Res 12:559-565

Vinutha AR, von Rudloff (1968) Gas-liquid chromatography of terpenes. Part XVII. The volatile oil of the leaves of *Juniperus virginiana* L. Can J Chem 46:3743-3750

Vourela H, Pohjola J, Krause C, Hiltunen R (1989) Application of headspace gas chromatography in essential oil analysis. Part IX. Selective loss terpene compounds during hydrodistillation. Flavour Fragr J 4:117-120

Wilkinson RC, Hanover JW (1972) Geographic variation in the monoterpene composition of Red spruce. Phytochem 11:2007-2010

Wilkinson RC, Hanover JW, Wright JW, Flake RH (1971) Genetic variation in the monoterpene composition of White spruce 17:83-90

Williams RS, Lincoln DE, Thomas RB (1994) Loblolly pine grown under elevated CO2 affects early instar pine sawfly performance. Oecologia 98:64-71.

Wright JW (1955) Species crossability in Spruce in relation to distribution of taxonomy. Forest Sci 1:319-349

Yatagai M, Sato T (1986) Terpenes of leaf oils of conifers. Biochem Syst Ecol 14:469-478

Yazdani R, Nilsson JE, Ericsson T (1985) Geographical variation in the relative proportion of monoterpenes in cortical oleoresin of Pinus sylvestris in Sweden. Silvea Genet 34:201-208

Zavarin E (1968) Chemotaxonomy of the genus *Abies*—II. Within tree variation of the terpenes in cortical oleoresin. Phytochem 7:92-107

Zavarin E, Cobb FW, Bergot J, Barber HW (1971) Variation of the *Pinus ponderosa* needle oil with season and needle age. Phytochem 10:3107-3114

Zavarin E, Snajberk K (1972) Geographical variability of monoterpenes from *Abies balsamea* and *A. fraseri*. Phytochem 11:1407-1421

Zavarin E, Snajberk K (1973) Geographic variability of monoterpenes from cortex of *Pseudotsuga menziessii*. Pure Appl Chem 34:411-434

Zavarin E, Snajberk K, Critchfield WB (1973) Monoterpene variability of Abies amabilis cortical oleoresin. Biochem. Syst. 1:87-93

Zavarin E, Snajberk K, Reichert T, Tsien E (1970) On the geographic variability of the monoterpenes from the cortical blister oleoresin of Abies lasiocarpa. *Phytochem* 9:377-395

Zulak KG, Bohlmann J (2010) Terpenoid biosynthesis and specialized vascular cells of conifer defense. J Integr Plant Biol 52:86-97

Table 2.1. List of terpenes and terpenoids in Figures 2.1-2.8.

Terpene or Terpenoid	Bar Number	Terpene or Terpenoid	Bar Number
Santene	1	1:8-Cineole	28
p-Cymene	2	Linalool	29
Tricyclene	3	α-Fenchol	30
α-Fenchene	4	*D*-Borneol	31
α-Thujene	5	Terpinen-4-ol	32
α-Pinene	6	α-Terpineol	33
Camphene	7	Citronellol	34
β-Pinene	8	Eugenol	35
Sabinene	9	Methyl Eugenol	36
Myrcene	10	Estragole	37
δ-3-Carene	11	Safrole	38
Phellandrene	12	Methyl citronellate	39
α-Terpinene	13	α-Fenchyl acetate	40

Terpene or Terpenoid	Bar Number	Terpene or Terpenoid	Bar Number
Limonene	14	Bornyl acetate	41
β-Phellandrene	15	Myrtenyl acetate	42
cis-Ocimene	16	α-Terpinyl acetate	43
trans-Ocimene	17	Citronellyl acetate	44
γ-Terpinene	18	Geranyl acetate	45
Terpinolene	19	β-Caryophyllene	46
Carvone	20	δ-Cadinene	47
D-Fenchone	21	α-Cyperone	48
α-Thujone	22	Elemol	49
iso-Thujone	23	Elemyl acetate	50
Piperitone	24	Σ Monoterpenes[a]	51
Camphor	25	Σ Monoterpenoids[a]	52
Thymol	26	Σ Sesquiterpenes[a]	53
Methyl Thymol	27	Σ Sesquiterpenoids[a]	54

[a]Includes sum of all terpenes or terpenoids reported in the literature.

Table 2.2. Signature characteristics of foliar oils of subsections of the *Pinus* and *Strobus* subgenera of *Pinaceae*.

Pinus Species	α-Pinene/β-Pinene	Σ Sesquiterpenes (%)	Germacrene D (%)
Pinus			
densiflora	2.0	14.8	10.7
mugo	100	0.1	nr[a]
nigra	11.9	17.6	nr[a]
sylvestris	26.1	22.7	14.3
	15.0	21.1	2.3
Pinaster			
brutia	0.4	13.9	7.6
canariensis	7.4	56.4	50.6
halepensis	12.2	24.1	0.5
merkusii	30.7	8.5	nr[a]
pinaster	0.6	35.3	11.5

Pinus Species	α-Pinene/β-Pinene	Σ Sesquiterpenes (%)	Germacrene D (%)
Australes			
caribaea	16.9	0.3	nr[a]
clausa	0.9	<0.01	nr[a]
ellioti	0.7	9.0	nr[a]
palustris	0.4	14.9	14.9
Rigida	0.7	3.3	nr[a]
serotina	0.4	11.2	nr[a]
taeda	1.6	11.0	nr[a]
Contorta			
banksiana	2.1	nr[a]	nr[a]
contorta	0.3	nr[a]	nr[a]
Ponderosae			
hartweggi	0.5	12.0	nr[a]
ponderosa	0.4	1.8	nr[a]

Pinus Species	α-Pinene/β-Pinene	Σ Sesquiterpenes (%)	Germacrene D (%)
Strobi			
parviflora	8.8	27.1	6.7
strobus	3.3	18.9	8.0
Cembrae			
koraiensis	4.5	26.1	nr[a]
pumila	9.1	17.0	5.3

[a]Not reported.

Table 2.3. Locations for *Abies balsamea* populations sampled by Zavarin and Snajberk (1972).

Population	Location	Latitude		Longitude		Elevation
		°	Min	°	Min.	m
1	Great Lake, Saskatchewan	54	18	107	49	2000
2	Sled Lake, Saskatchewan	54	24.4	107	19.8	1666
3	Candle Lake, Saskatchewan	53	50	105	18	2000
4	Armit River, Saskatchewan	52	50	101	51	2000
5	Duck Mountain, Mannitoba	51	35	101	00	2400
6	Riding Mountain, Mannitoba	50	37	99	37	2300
7	Warroad Highway, Minnesota	48	53	95	28	1400
8	Rainy River, Minnesota	48	30	93	48	1200
9	Aitkin Lake, Minnesota	46	30	93	43	1800
10	Laurentia Divide, Minnesota	47	39	92	32	2000
11	Land O'Lakes, Wisconsin	46	10	89	11	2000
12	Kinross, Michigan	46	07	84	31	1500
13	Espanola, Ontario	46	15	81	46	1200
14	Petawawa Forest, Ontario	46	00	77	27	1500

| Population	Location	Latitude		Longitude		Elevation
15	Saranac Lake, New York	44	20	74	10	2000
16	Quebec, Quebec	46	57	71	30	690
17	Orono, Maine	44	57	68	38	150
18	Fredericton, New Brunswick	45	55	66	40	350
19	Truro, Nova Scotia	45	14-36	63	01-32	100-1000
20	Corner Brook, Newfoundland	48	55	57	54	450
21	Gander, Newfoundland	48	56	54	31	450
22	St. John, Newfoundland	47	37	52	47	450
23	Promised Land Lake, Pennsylvania	41	19.5	75	13.3	1720
24	Bear Meadows, Pennsylvania	40	44	77	45.4	1820
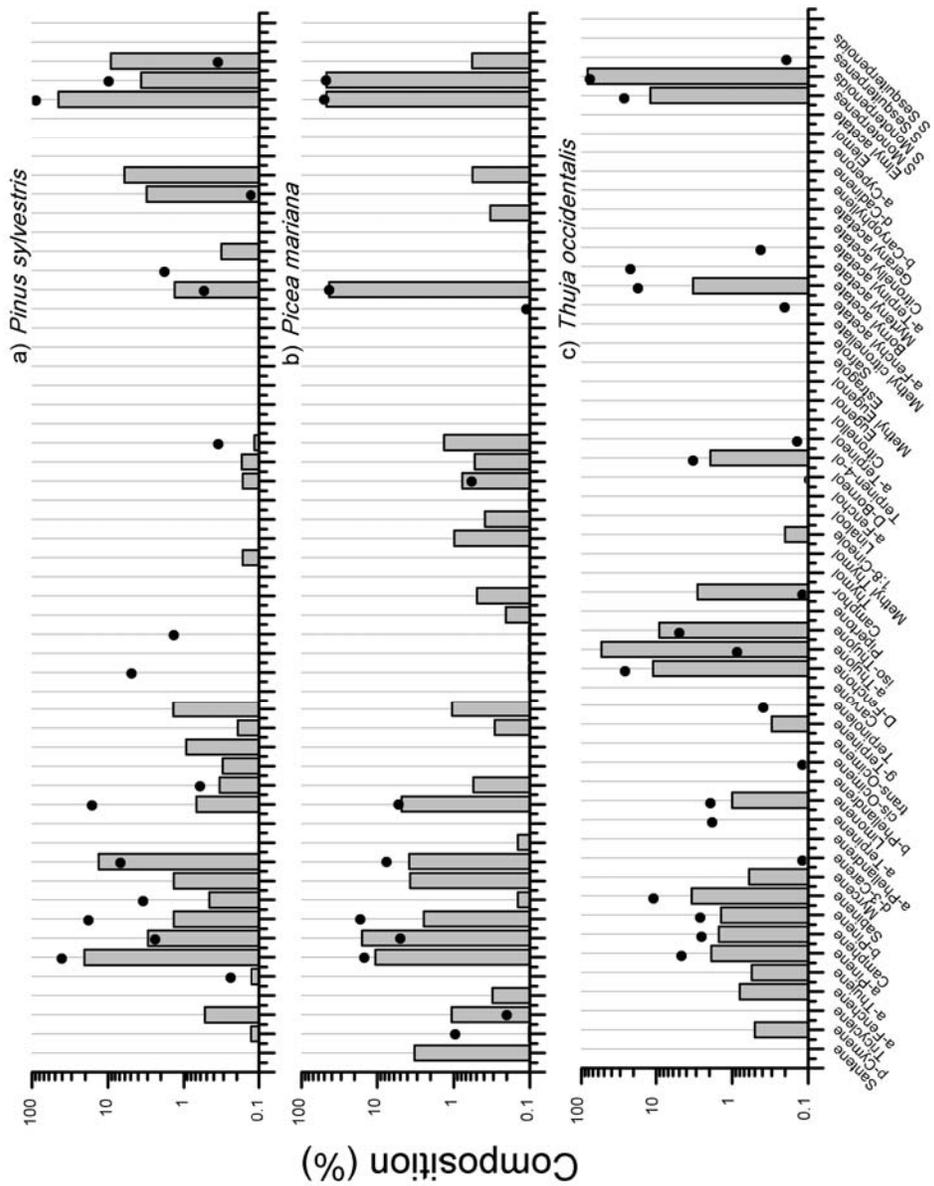
Figure 2.1. Comparison of essential oil of (a) *Pinus sylvestris*, (b) *Picea mariana*, and (c) *Thuja occidentalis* analyzed in this study (black dots) with average compositions reported in the literature (bars).
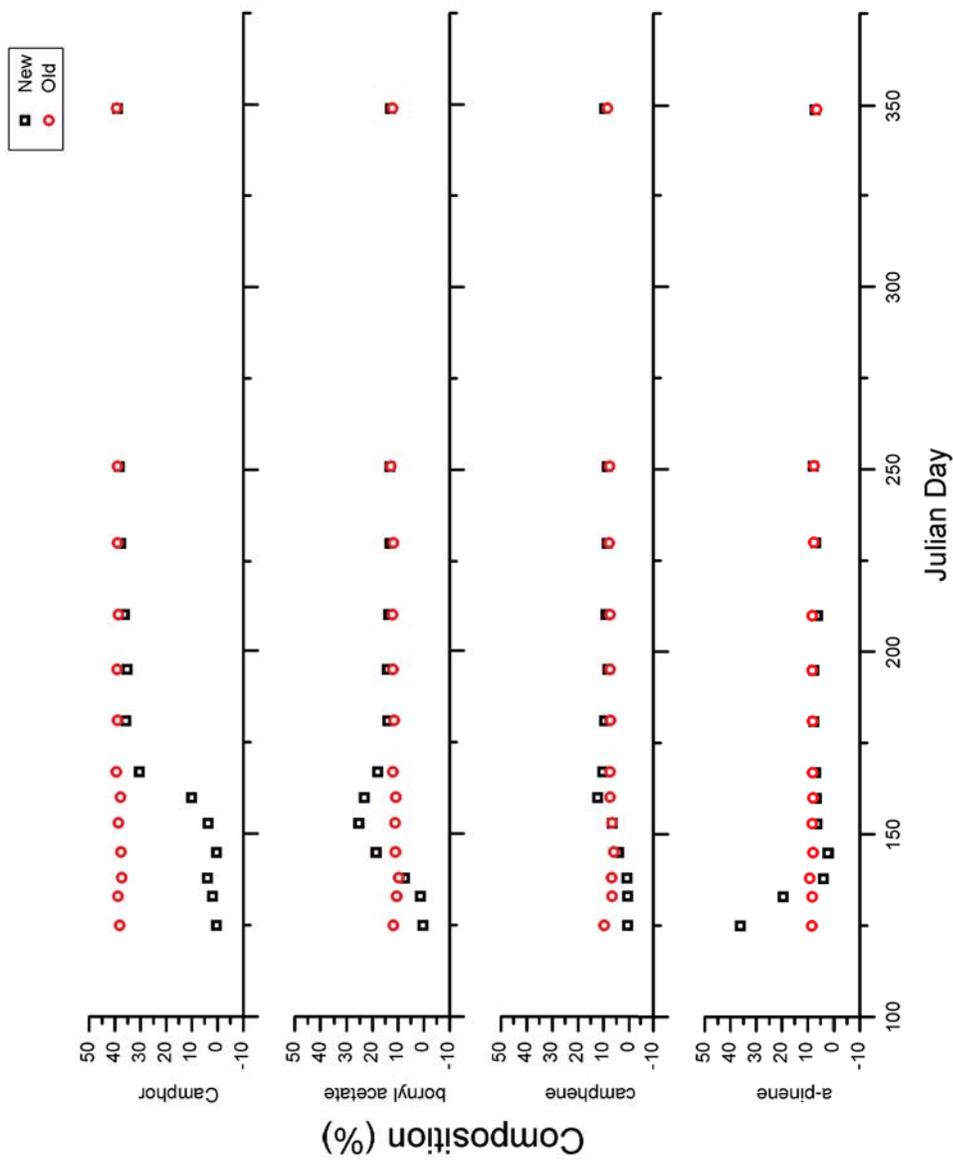
Figure 2.2. Variation of essential oil composition for the (a) *Pinoideae*, (b) *Piceoideae*, (c) *Laricoideae*, and (d) *Abietoideae* subfamilies of the family *Pinaceae* and the (e) *Cupressoideae* subfamily of the family *Cupressaceae* reported in the literature.

Figure 2.3. Essential oil composition of the (a) *Pinus*, (b) *Pineae*, (c) *Trifloiae*, (d) *Quinquefoliae*, and (e) *Parrya* sections of the subfamiliy *Pinoideae* reported in the literature.

Figure 2.4. Essential oil composition of (a) Clade I, (b) Clade II, (c) Clade III, and (d) Clade V of the subfamily *Piceoideae* reported in the literature.

Figure 2.5. Essential oil composition the (a) *abies*, (b) *mariana*, (c) *pungens*, and (d) *rubens* species of Clade V of the subfamily *Piceoideae* reported in the literature.

Figure 2.6. Essential oil composition of the (a) *Larix* and (b) *Pseudotsuga* genera of the subfamily *Laricoideae* reported in the literature.

Figure 2.7. Essential oil composition of the (a) *Abies*, (b) *Cedrus*, and (c) *Tsuga* genera of the subfamily *Abietoideae* reported in the literature.

Figure 2.8. Essential oil composition of the (a) *Juniperus* and (b) *Thuja* genera of the subfamily *Cupressoideae* family *Cupressaceae* reported in the literature.

Figure 2.9. Seasonal variation in foliar composition of (a) camphor, (b) bornyl acetate, (c) camphene, and (d) α-pinene of *Picea glauca* reported by von Rudloff 1972b.
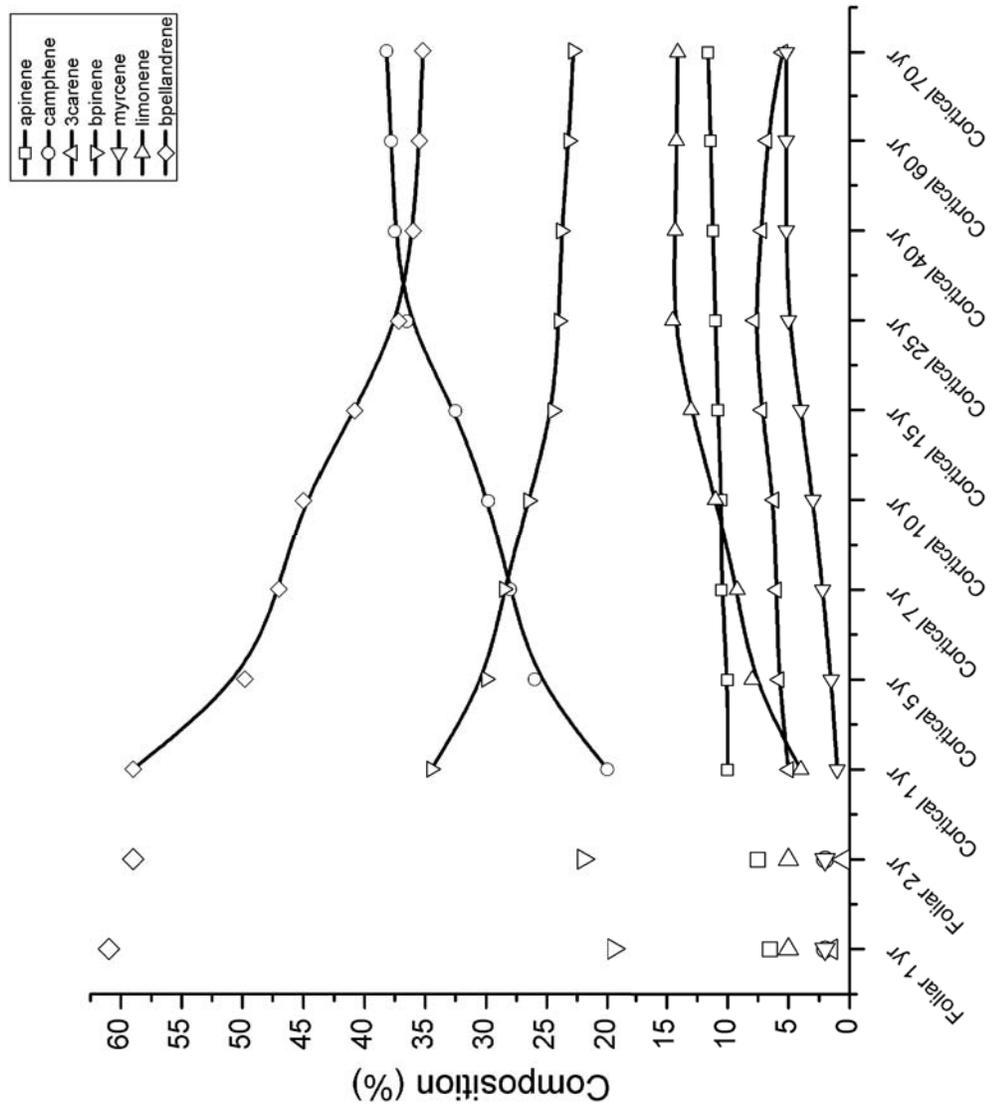
Figure 2.10. Variation in foliar and cortical oleoresin monoterpene composition with age in *Abies magnifica* (Zavarin 1968). (The sum of the levels of individual monoterpenes was set equal to 100%.)
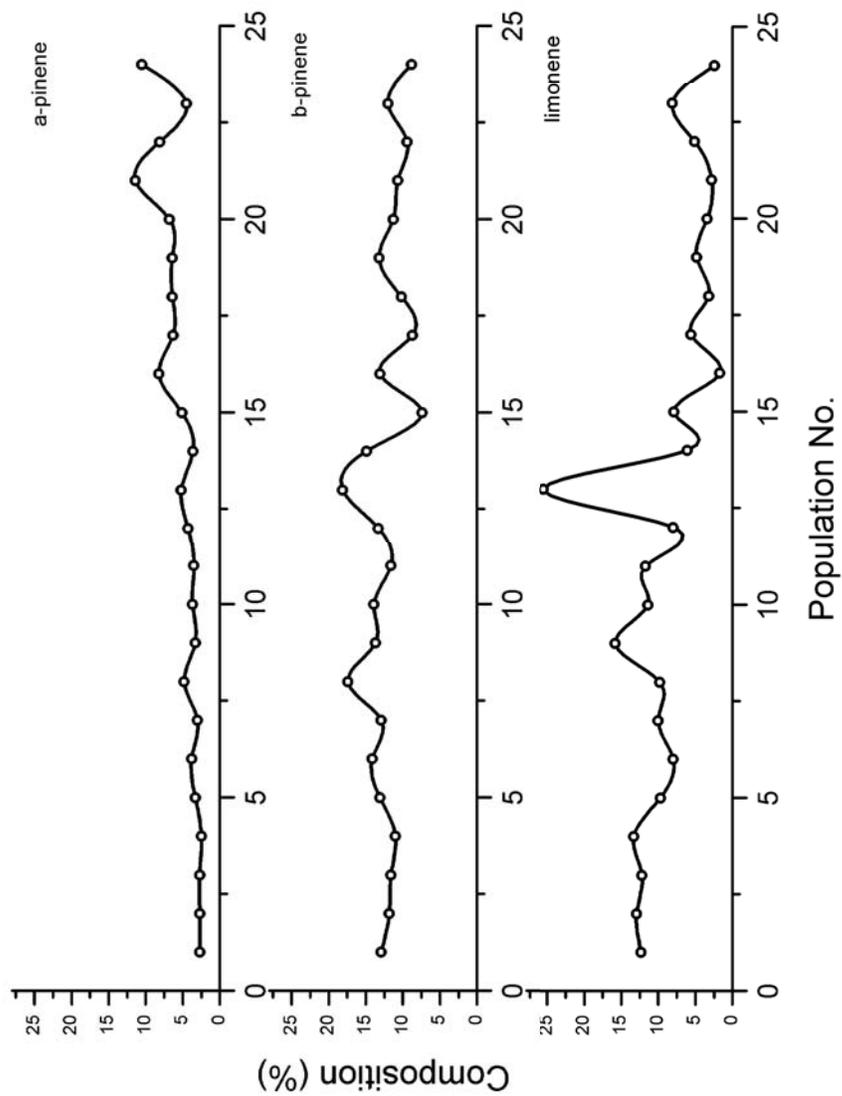
Figure 2.11. Geographical variation in α- and β-pinene and limonene levels in cortical oleoresins of *Abies balsamea* across Canada (Zavarin & Snajberk 1972). (Locations of populations are given in Table 3.)

Supplementary Material

The supplementary material includes total ion chromatograms of commercially available (Silky Scents, Corona, CA, USA) essential oils of *Pinus sylvestris*, *Picea mariana*, and *Thuja occidentalis* analyzed in the subject study (Figs.2S.1-3). Essential oil compositions of the 3 species are presented in Table 2.1 and compared with essential oil compositions of *Pinaceae* and *Cupressaceae* species in Table 2.2.
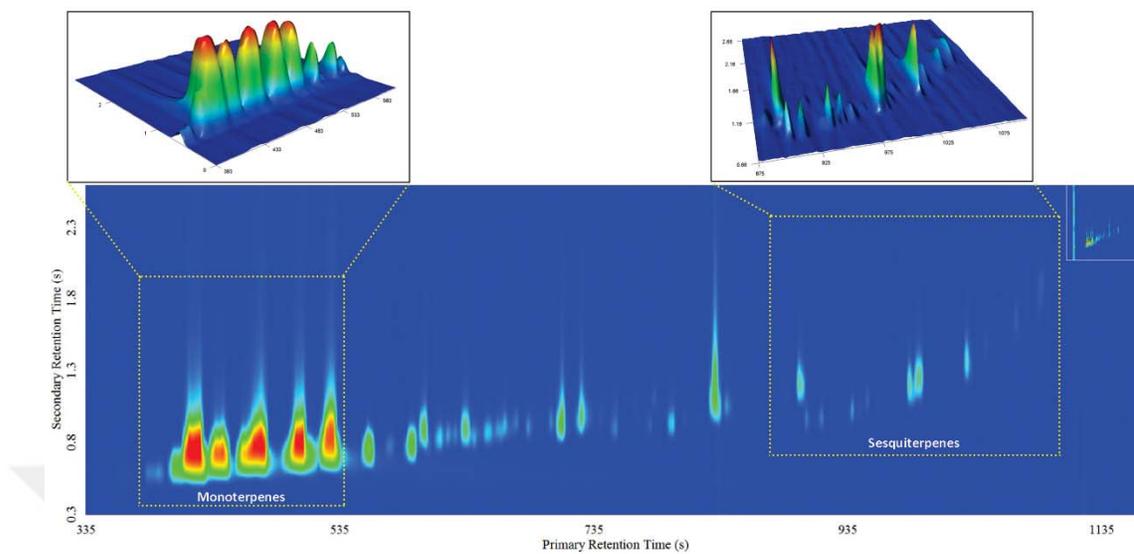
Figure S2.1. Total ion chromatogram from GC × GC-ToF-MS analysis of essential oil of *Pinus sylvestris* analyzed in this work.
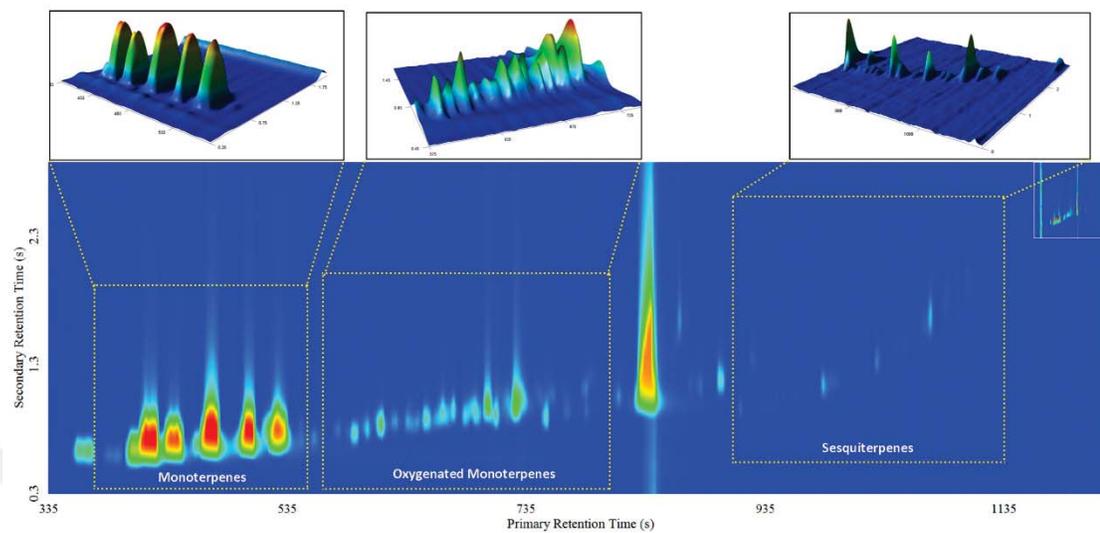
Figure S2.2. Total ion chromatogram from GC × GC-ToF-MS analysis of essential oil of *Picea mariana* analyzed in this work.
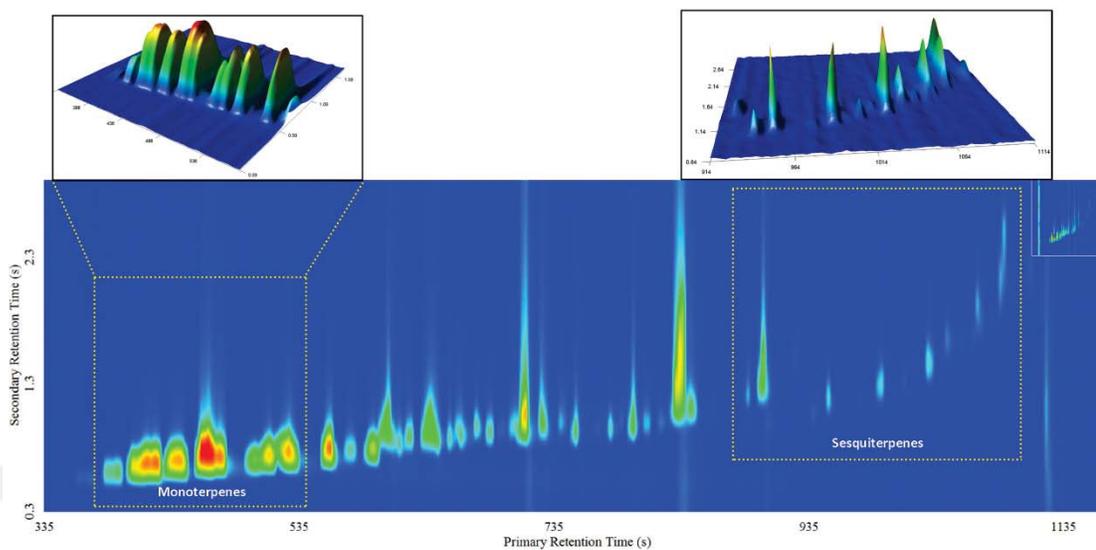
Figure S2.3. Total ion chromatogram from GC × GC-ToF-MS analysis of essential oil of *Thuja occidentalis* analyzed in this work.

Chapter 3. Estimating Terpene and Terpenoid Emission Signatures from Conifer Oleoresin Composition

Rosa M. Flores[1] and Paul V. Doskey[1-3]

[1]Department of Civil and Environmental Engineering, [2]School of Forest Resources and Environmental Science, [3]Atmospheric Sciences Program.

Michigan Technological University. 1400 Townsend Dr. Houghton, MI. 49931.

rmflores@mtu.edu, pvdoskey@mtu.edu[◊]

[◊]corresponding author. Phone number: +1 906-487-2745

ABSTRACT

A conceptual model was developed to estimate signatures of terpene and terpenoid emissions form oleoresins stored in specific locations in foliage, stems, and the bole of conifers. The emission pathways included (1) exhalation from foliar stomata and (2) evaporation from resin blisters or traumatic resin ducts induced by herbivore and pathogen infestation. Estimated activity coefficients of α-pinene, α-terpineol, germacrene D, and germacrene D-4-ol were approximately 1 in leaf apoplastic fluids with electrolyte and sugar levels of 34.3 and 4.3 mM, respectively, and > 1 in oleoresin rich in monoterpenes and resin acids. Differences in activity coefficients for the chemical species were responsible for lower partial pressures in the substomatal cavity than above exudations of cortical oleoresin on the bole. Terpene alcohols had greater affinities for apoplastic fluids and oleoresin with high resin content (52%) due to hydrogen bonding with the matrix, which reduced partial pressures of the chemical species in the substomatal cavity and above cortical oleoresin rich in diterpenoic acids. Affinities of terpenes for oleoresin with high monoterpene content (91%) through van der Waals interactions were greater than terpene alcohols and generated higher partial pressures of terpene alcohols above cortical oleoresin rich in monoterpenes. Trends in estimated emission signatures were correlated with the air/octanol partition coefficient (K_{AO}). A comparison of foliar oleoresin composition of *Pinus strobus* with the signature of measured emissions revealed that β-phellandrene, terpinolene, myrcene, and α-terpineol did not follow the same trend with K_{AO}. The trend for myrcene has been observed by others and attributed to transient biosynthesis of myrcene in nonspecific storage sites and differences in the kinetics of release from hydrophobic and hydrophillic, nonspecific storage locations.

Keywords: Terpenes, Terpenoids, Partition coefficients, conifer oleoresin, Biogenic volatile organic compound (BVOC) emissions

3.1. Introduction

About 90% of reduced carbon emissions to the global troposphere (1000 ± 600 Tg C a^{-1}) are attributed to biogenic volatile organic compounds (BVOCs; Guenther et al. 1995; Kanakidou et al. 2005). The BVOC are rapidly photooxidized and form secondary organic aerosol (SOA; Kulmala et al., 2004). The SOA are the most abundant fine particle in the global troposphere and are hydrophilic making the aerosol effective at scattering light and forming clouds, which increases albedo and cools the atmosphere. Emissions of terpenes and terpenoids (i.e., oxygen-containing terpenes) from coniferous forests are one of the principal sources of BVOCs (Helmig et al., 2007); however, considerable uncertainty exists in developing emission inventories. Emission factors for vegetation like conifers that accumulate terpenes and terpenoids in specialized storage tissues within leaves have been developed for many species through measurement of emission rates under various environmental conditions (Ortega et al., 2008). The emission factors are used in models to derive plant-specific emission inventories (Geron et al., 2000). The monoterpene emission algorithm for specific storage tissues is based on evaporation and diffusion from the storage site (Tingey et al., 1980; Guenther et al., 1991, 1993). Emission rates are predicted to increase exponentially with temperature in a manner similar to monoterpene vapor pressure; however, monoterpene emission rates are greater than rates predicted by changes in monoterpene vapor pressure with temperature (Tingey et al., 1991).

Conifer oleoresins, which are synthesized by many plant organs and stored in secretory cells, cavities, canals, or glands, are composed of a volatile mixture of monoterpenes, monoterpenoids, sesquiterpenes, sesquiterpenoids and the less volatile diterpenes and diterpenoic acids (Langeheim, 2003; Zulak and Bohlmann 2010). Composition of conifer oleoresins varies with taxonomy, phenology and age, and biotic and abiotic stresses (see, e.g., Chapter 2). Terpenes and terpenoids are emitted from foliage and the stems and bole of conifers via resin blisters and induction of traumatic resin ducts by

herbivores and pathogens (Martin et al., 2002). Resin ducts or glands in foliage are distinct from the series of ducts in stems and the bole of the tree (Jeffrey, 1925; Hanes, 1927; Roller, 1966; Suzuki, 1979). Thus, terpenes and terpenoids are emitted from conifers (1) by exhalation from foliage stomata and (2) through evaporation from resin blisters and traumatic resin ducts.

Resin canals in conifer foliage are embedded in the mesophyll tissue that is immersed in the apoplastic fluid, which contains a complex mixture of organic and inorganic electrolytes (i.e., amino acids and salts, respectively) and neutral organic compounds (i.e, sugars) (Canny, 1995; Lohaus et al., 2001). Terpenes and terpenoids diffuse from specific storage sites containing foliar oleoresin through the mesophyll into intercellular airspaces and through the substomatal cavity that is located proximal to the stoma. Release of terpenes and terpenoids from the stoma can be delayed through nonspecific storage in plant tissues within the leaf (Niinemets and Reichstein, 2002; Niinemets et al., 2004). Cortical oleoresins rise to the surface of conifer stems and the bole and evaporate directly into the atmosphere from blisters or traumatic resin ducts. Compositions of foliar and cortical oleoresins are distinct during the first 25 years of growth and become similar in the oldest branches of conifers (Zavarin, 1968; Hrutford et al., 1974). Signatures of foliar oleoresins vary dramatically with phenology during the first year of growth and are invariant in mature foliage (von Rudloff, 1972).

Here we propose a conceptual model for estimating terpene and terpenoid emission signatures from physicochemical properties and conifer oleoresin composition. Kinetic controls on emissions are not considered. Signatures of emissions from specific storage sites in foliage, stems, and the bole are derived for an oleoresin with high monoterpene and resin acid contents. We use the average terpene and terpenoid composition of foliar extracts of *Pinus strobus* reported by Toma and Bertman (2012) as the measured signature of foliar oils, estimate signatures of foliar and bole emissions from the

oleoresin composition, and compare with measurements of foliar emissions from *Pinus stobus* (Ortega et al., 2008).

3.2. Methods

Emission signatures are estimated for α-pinene, germacrene D, and germacrene D-4-ol, which were 3 of the most abundant terpenes and terpenoids isolated from foliar oils of *Pinus strobus* in Northern Michigan over a 3-yr period (Toma and Bertman, 2012). α-Terpineol was not reported; however, the chemical species was one of the more abundant monoterpene alcohols reported by Yatagai and Sato (1986) in foliar oils of *Pinus strobus* and is the value used in the subject study. The foliar oil composition was converted to oleoresin composition (Fig. 1) by multiplying the species composition in mole fraction by the average yield of foliar oil from oleoresin of *Pinus strobus* (Mirov, 1961). Molar composition of cortical oleoresin of *Pinus strobus* has not been reported, and thus, foliar and cortical oleoresin compositions were assumed equal for the subject study.

Vapor pressures, aqueous solubilities, Henry's law constants, and octanol/water partition coefficients were estimated using the SPARC Performs Automated Reasoning in Chemistry (SPARC) chemical property estimator (SPARC, 2013) and are presented in Table 1. There was some disagreement with SPARC-estimated values for aqueous solubilities, Henry's law constants, and octanol/water partition coefficients of α-pinene and α-terpineol and values reported in the compilation by Copolovici and Niinemets (2005). However, values for vapor pressures and physicochemical properties of germacrene and germacrene D-4-ol were not part of the compilation, and thus for consistency, we used SPARC-estimated values for the 4 chemical species. Cortical oleoresin compositions of *Pinus contorta* and *Abies grandis* from the detailed analysis by Lewinsohn et al. (1993) represent the high resin and monoterpene content oleoresin, respectively, in Table 1.

99

3.2.1. Modeling Approach

Terpenes and terpenoids evaporate from resin blisters and traumatic resin ducts directly into the atmosphere and are estimated from the composition of the oleoresin and species vapor pressure as follows:

$$p_{A1}^* = x_{A3}\gamma_{A3}p_A^\circ \qquad (1)$$

where: x_{A1} (Pa) is the mole fraction of the species in air (i.e., partial pressure) above the mixture, γ_{A3} is the activity coefficient of the substance in the oleoresin mixture, and p_A° (Pa) is the vapor pressure of the substance in the liquid state. Model substances used in the subject study are liquids at 25°C, and thus, a melting point correction is unnecessary in estimating p_A°. The magnitude of γ_{A3} is sensitive to molecular structure and functionality of the chemical species and the other species in the oleoresin mixture. Values of γ_{A3} can be estimated by several techniques that are based on group contribution methods provided the composition of the oleoresin mixture is known (Wilson, 1964; Hansen, 1969; Gmehling et al., 1982; Fredenslund and Sorensen, 1994). Compositions of foliar and cortical oils, which are largely composed of terpenes and terpenoids, have been reported for many conifer species (see, e.g., Chapter 2); however, measurements of conifer resin composition are few. We used trends in activity coefficients for polyaromatic hydrocarbons and phenols in wood combustion aerosol and diesel soot estimated by the Hansen Group Contribution Method as reported by Jang et al. (1997) to estimate γ_{A3} for terpenes and terpenoids in conifer oleoresin with high resin and high monoterpene contents, respectively (Table 1). Wood combustion aerosol contains polyphenols and mono-, di-, and polycarboxylic acids (Mayol-Bracero et al., 2002) and is expected to have polar character like oleoresin with a high diterpenoic acid content. Diesel soot is a complex mixture of aromatic hydrocarbons and likely similar in nature to oleoresin with abundant monoterpenes.

Resin ducts in foliage are located in the mesophyll that is immersed in apoplastic fluid containing a mixture of electrolytes and sugars. Intercellular airspaces connect the mesophyll to the substomatal cavity. Thus, terpenes and terpenoids are in a dynamic equilibrium between oleoresin, apoplastic fluid, the mesophyll, and air in the substomatal cavity. Concentration of substance in the apoplastic fluid are estimated as follows:

$$c_{A2} = x_{A3} \gamma_{A2} c_{A2}^*$$ (2)

where: c_{A2} and γ_{A2} are the concentration (mol m^{-3}) and activity coefficient of the substance in the apoplastic fluid, respectively, and c^*_{A2} is the aqueous solubility of the substance in the liquid state. Values of γ_{A2} are sensitive to composition of the apoplastic fluid. Copolovici and Niinemets (2007) evaluated salting-in and salting-out effects of apoplastic electrolytes and sugars on limonene and linalool partitioning from water into air and octanol as expressed by the Henry's law constant (H) and octanol/partition coefficient K_{OW}, respectively. Salting-out (Setschnow) coefficients for limonene and linalool in aqueous solutions of potassium chloride at 30ºC were 0.0231 and 0.167, respectively, and average salting-in (Setschnow) coefficients for limonene and linalool in aqueous solutions of glucose and sucrose were -1.0159 and -0.0173, respectively. Here we apply salting-in and salting-out coefficients for limonene to both α-pinene and germacrene D and for linalool to both α-terpineol and germacrene D-4-ol (Table 1) to estimate effects on partitioning to air as follows:

$$\log\left(\frac{H_{AF}}{H}\right) = k_H C_{AF}$$ (3)

where: H and H_{AF} are the Henry's law constant in pure water and the apoplastic fluid (Pa m^3 mol^{-1}), respectively, k_H (M^{-1}) is the salting-in or salting-out coefficient, and C_{AF}

(M) is the concentration of electrolytes or sugars in the apoplastic fluid. The same relationship is applied to estimate effects on partitioning to octanol as follows:

$$\log\left(\frac{K_{OW,AF}}{K_{OW}}\right) = k_H C_{AF} \tag{4}$$

where: K_{OW} and $K_{OW,AF}$ are the dimensionless octanol/water partition coefficients (vol water vol^{-1} octanol) for pure water and the apoplastic fluid, respectively, and other properties are the same as in eqn. (3). Lohaus et al. (2001) reported average levels of 32.3 and 4.3 mM of inorganic electrolytes and sugars in apoplastic fluids of several agricultural crops. Copolovici and Ninemets (2007) report significant effects on partitioning from water into air and octanol for simulated apoplastic fluid concentrations of electrolytes and sugars that were about an order of magnitude higher than the levels reported by Lohaus (2001). Differences in values of H and K_{OW} in pure water and apoplastic fluid with 32.3 mM inorganic electrolytes and 4.3 mM sugars were at most 2%. Values of γ_{A2} in apoplastic fluids are estimated from the following equation that is derived from eqns. (3) and (4),

$$\log \gamma_{A2} = k_H C_{AF} \tag{5}$$

Values of γ_{A2} for the terpenes and terpenoids in apoplastic fluids considered here are approximately 1, and thus, the solution can be considered ideal.

Terpenes and terpenoids that dissolve in apoplastic fluids will partition to the mesophyll. Assuming dissolution in octanol and the meosphyll are similar, the concentration of the chemical species in octanol is calculated as follows:

$$c_{AO} = c_{A2} K_{OW} \tag{6}$$

where: c_{AO} is the concentration of the substance in octanol. The aqueous environment of the mesophyll is in contact with intercellular airspaces. If the substance were partitioning directly from the apoplastic fluids to the intercellular airspace, the concentration of the substance in the intercellular airspace would be calculated as follows:

$$c_{A1} = c_{A2} K_{AW} \qquad (7)$$

where: c_{A1} is the concentration in air (mol m^{-3}) and K_{AW} is the dimensionless Henry's law constant (vol water vol^{-1} air). Dividing eqn. (6) by eqn. (5) results in the following expression that is used to calculate the partial pressure of the substance above the mesophyll:

$$c_{A1} = c_{AO} K_{AO} \qquad (7)$$

where $K_{AO} = K_{AW} K_{OW}^{-1}$ and is defined as the air/octanol partition coefficient.

3.3. Results and discussion

Emission signatures for the foliar and bole pathways are shown in Fig. 2. Values of H and K_{OW} for the terpenes and terpenoids were similar in apoplastic fluids with electrolyte and sugar contents of 32.3 and 4.3 mM, respectively. The solution can be considered ideal and values of γ_{A2} for the terpenes and terpenoids are approximately 1 under the conditions. If the apoplastic fluids and oleoresin are ideal solutions, $\gamma_{A3} \approx \gamma_{A2} \approx 1$, partial pressure of the substances in the substomatal cavity can be calculated by dividing eqn. (1) by eqn. (2). At infinite dilution, the partitioning is governed by Henry's law, which is the ratio of p°_{A} to c^{*}_{A2} when the aqueous solubility of the chemical species is $< 1 \times 10^{4}$ M (Mackay and Shiu, 1981). Thus, if the apoplastic fluids and oleoresin were ideal solutions, emission signatures for both pathways would be

identical. However, values of γ_{A3} are greater than 1 (Table 1), the oleoresin is considered a nonideal solution, and partial pressures of the terpenes and terpenoids are predicted to be greater than levels of the species in the substomatal cavity (Fig. 2). Trends in partial pressures of the non-functionalized terpenes, α-pinene and germacrene D, above oleoresin with a high resin acid content (52%) and in the substomatal cavity in contact with the aqueous environment of the mesophyll are different than the trends of the terpene alcohols under the same conditions. The K_{AO} values for α-terpineol and germacrene D-4-ol are 3.3 and 2.3 orders of magnitude less than the values for α-pinene and germacrene D, which indicates terpene alcohols have greater affinities for polar organic phases through hydrogen bonding with resin acids and water (Goss and Schwarzenbach, 2003), which is consistent with trends in Fig. 2. The converse is true for terpenes and terpene alcohols above the oleoresin with a high monoterpene content (91%). Terpene alcohols exert higher partial pressures and the terpenes have greater affinity for the nonpolar, monoterpene-rich oleoresin through van der Waals interactions (Goss and Schwarzenbach, 2003). Solute molecular size also influences partitioning. The larger germacrene D and germacrene D-4-ol, which have K_{AO} values 2.5 and 1.5 orders of magnitude less than the values for α-pinene and α-terpineol, have greater affinity for organic phases.

Signatures of terpenes and terpenoids in foliar oleoresin of *Pinus strobus* (Toma and Bertman, 2012) and basal emission rates (Ortega et al., 2008) are compared in Fig. 1. If terpenes and terpenoids of the foliar oleoresin in specific storage sites partition into apoplastic fluid that can be considered an ideal solution, signatures of foliar oleoresin and emissions from conifers might correlate with log K_{AO}. The correlation appears to hold for some terpene and terpenoid species in foliar oleoresin of *Pinus strobus*. α- and β-Phellandrene had abundances of 0.52 and 0.718, respectively, and similar K_{OA} values; however, the mole fraction of β-phellandrene in the emissions was a factor of 3 higher than α-phellandrene. Camphene, limonene, and terpinolene have the same values of log K_{OA}; however, ratios of the mole fraction in emissions to foliar oleoresin are 7.1, 7.8,

and 9.0, respectively. α-Terpineol has a log K_{AO} value of -7.02 and a ratio of 3.3 that appears abnormally high compared to terpenes with much higher K_{AO} values. Ratios are 2.5 and 7.8 for β-pinene and myrcene, respectively, which have similar values of log K_{OA}. Light-dependent monoterpene emissions have been observed in deciduous trees that lacked specific storage sites for oleoresins (Loreto et al., 1996; Staudt and Seufert, 1995). Eav (2011) observed emissions of myrcene from *Pinus nigra* foliage during light and dark periods; however, myrcene was not found in foliar oils. Absence of myrcene in foliar oleoresin might indicate terpene biosynthesis occurs in leaf sites other than specific storage locations. Non-specific storage of terpenes and terpenoids in hydrophobic leaf tissues other than the mesophyll like internal surfaces of the waxy cuticle can cause lags in emission of monoterpenes and sesquiterpenes that affect emission signatures (Niinemets and Reichstein, 2002). Terpenes and terpenoids emission signatures are likely altered by the distribution and relative abundance of hydrophillic and hydrophobic leaf tissues. Myrcene was observed in foliar oils of *Pinus strobus*; however, light-induced biosynthesis might contribute some of the emissions and non-specific storage in hydrophobic leaf tissue might contribute to emission during dark periods.

3.4. Conclusions

A conceptual model was developed to estimate emission signatures of terpenes and terpenoids from conifer oleoresin composition. The model considers emissions through leaf stomata and from resin blisters and traumatic resin ducts induced by herbivore and pathogen infestations. Signatures of emissions from resin blisters and traumatic resin ducts were determined using the species liquid vapor pressure and the molar composition of the cortical oleoresin, which was assumed to be similar in composition to foliar oils in the subject study. Signatures of exhalations from leaf stomata were regulated by partitioning of terpenes and terpenoids from specific storage sites in the mesophyll immersed in apoplastic fluid to intercellular airspaces. Partial pressure of the terpenes and terpenoids in the substomatal cavity was regulated by molar composition

of the foliar oleoresin, solubility in apoplastic fluids, K_{OW}, and K_{AO}. The apoplastic fluid was estimated to be an ideal solution at levels of 34.3 and 4.3 mM for electrolytes and sugars, respectively. Cortical oleoresin was treated as a nonideal mixture and activity coefficients for oleoresin high in resin acid and monoterpene content were derived from estimates of activity coefficients reported for wood combustion aerosol and diesel soot, respectively.

Activity coefficients for the apoplastic fluid and cortical oleoresin were 1 and >1, respectively, and thus, estimates of partial pressures of terpenes and terpenoids above the cortical oleoresin were greater than partial pressures in the substomatal cavity. Terpene alcohols had greater affinities for mesophyll immersed in apoplastic fluid and cortical oleoresin with a high resin acid content, which led to lower partial pressures than the terpenes. However, terpenes exerted lower partial pressures above cortical oleoresin rich in monoterpenes than the terpene alcohols. Molar composition of foliar oleoresin was similar to the signature of emissions from *Pinus strobus*; however, β-phellandrene, terpinolene, myrcene, and α-terpineol did not follow the same trends as species with similar values of K_{AO}. Light-induced terpene and terpenoid emissions and biosynthesis and storage in non-specific locations like hydrophobic and hydrophillic leaf tissues other than the mesophyll might be responsible for delays in emissions.

Developing conifer-specific emission inventories from oleoresin composition might be a promising approach for reducing uncertainties in predictions of BVOC emissions. Emission potentials of the foliar and bole release pathways are dissimilar and should be considered for conifer species that develop resin blisters or are infested with herbivores or pathogens. Foliar and cortical oleoresin compositions are distinct and vary with taxonomy, phenology and age, and abiotic and biotic stresses (see, e.g., Chapter 2), which need to be addressed when developing emission inventories from oleoresin signatures. The conceptual model presented here is based on thermodynamics and is adequate for evaluating trends in emission signatures for the foliar and bole release

pathways. However, algorithms for the kinetics of release from non-specific storage and light-induced biosynthesis, which act in concert with mesophyll and stomatal conductances to regulate terpene and terpenoid emissions, need to be incorporated to forecast conifer emission rates.

3.5. Acknowledgements

3.6. References

Canny, M.J., 1995. Apoplastic water and solute movement: New rules for an old space. Annual Review of Plant Physiology and Plant Molecular Biology 46, 215-236.

Copolovici L., Niinemets, Ü., 2005. Temperature dependencies of Henry's law constants and octanol/water partition coefficients for key plant volatile monoterpenoids. Chemosphere 61, 1390-1400.

Copolovici L., Niinemets, Ü., 2007. Salting-in and salting-out effects of ionic and neutral osmotica on limonene and linalool Henry's law constants and octanol/water partition coefficients. Chemosphere 69, 621-629.

Eav, J., 2011. Comparison of monoterpene oil composition and volatile emissions from ponderosa and Austrian pine. url: http://nldr.library.ucar.edu/respository/assets/soars/SOARS-000-000-000-226.pdf.

Flores, R.M., 2013. Terpene and terpenoid signatures of conifer essential oils: New measurements and a review. In *Vapor- and Aerosol-Phase Organic Matter in the Midwestern United States: Methods and Measurements*, Ph.D. Dissertation, Michigan Technological University, Houghton, MI.

Fredenslund, A., Sorensen, J.M., 1994. Group contribution estimation methods. In *Models for Thermodynamic and Phase Equilibria Calculations*, Heinemann, H. Ed., Marcel Dekker, New York.

Geron, C., Rasmussen, R., Arnts, R.R., Guenther, A., 2000. A review and synthesis of monoterpene speciation from forests in the United States. Atmospheric Environment 34, 1761-1781.

Gmehling, J., Rasmussen, P., Fredenslund, 1982. Vapor-Liquid equilibria by UNIFAC group contribution. Revision and extension. 2. Industrial and Engineering Chemistry Process Design and Development 21, 118-127.

Goss, K.-U., Schwarzenbach, R.P., 2003. Rules of thumb for assessing equilibrium partitioning of organic compounds: Successes and pitfalls. Journal of Chemical Education 80, 450-455.

Guenther, A., Hewitt, C.N., Erickson, D., Fall, R., Geron, C., Graedel, T., Harley, P., Klinger, L., Lerdau, M., McKay, W.A., Pierce, T., Scholes, B., Steinbrecher, R., Tallamraju, R., Taylor, J., Zimmerman, P., 1995. A global model of natural volatile organic compound emissions. Journal of Geophysical Research 100, 8873-8892.

Guenther, A.B., Monson, R.K., Fall, R., 1991. Isoprene and monoterpene emission rate variability: Observations with Eucalyptus and emission rate algorithm development, Journal of Geophysical Research 96, 10,799-10,808.

Guenther, A.B., Zimmerman, P.R., Harley, P.C., Monson, R.K., Fall, R., 1993. Isoprene and monoterpene emission rate variability: model evaluations and sensitivity analyses. Journal of Geophysical Research 98, 12,609-12,617.

Hanes, C.S., 1927. Resin canals in seedling conifers. Botanical Journal of the Linnean Society 47, 613-636.

Hansen, C.M., 1967. The three dimensional solubility parameter – key to paint component affinities I. – Solvents, plasticizers, polymers and resins, Journal of Paint Technology 39, 104-117.

Helmig, D., Ortega, J., Duhl, T., Tanner, D., Guenther, A., Harley, P., Wiedinmyer, C., Milford, J., Sakulyanontvittaya, T., 2007. Sesquiterpene emissions from pine trees – identifications, emission rates and flux estimates for the contiguous United States. Environmental Science & Technology 41, 1545-1553.

Hrutfiord, B.F., Hopley, S.M., Gara, R.I., 1974. Monoterpenes in Sitka Spruce: Within tree and seasonal variation. Phytochemistry 13, 2167-2170.

Jang, M., Kamens, R.M., Leach, K.B., Strommen, M.R., 1997. A thermodynamic approach using group contribution methods to model the partitioning of semivolatile organic compounds on atmospheric particulate matter. Environmental Science & Technology 31, 2805-2811.

Jeffrey, E.C., 1925. Resin canals in the evolution of the conifers. Proceedings of the National Academy of Science of the United States of America 11, 101-105.

Kanakidou, M., Seinfeld, J.H., Pandis, S.N., Barnes, I., Dentener, F.J., Facchini, M.C., van Dingenen, R., Ervens, B., Nenes, A., Nielsen, C.J., Swietlicki, E., Putaud, J.P., Balkanski, Y., Fuzzi, S., Horth, J., Moortgat, G.K., Winterhalter, R., Myhre, C.E.L., Tsifaridis, K., Vignati, E., Stephanou, E.G., Wilson, J., 2005. Organic aerosol and global climate modeling: a review. Atmospheric Chemistry and Physics 5, 1053-1123.

Kulmala, M., Suni, T., Lehtinen, K.E.J., Dal Masso, M., Boy, M., Reissell, A., Rannik, Ü., Aalto, P., Keronen, P., Hakola, H., Bäck, J., Hoffmann, T., Vesala, T., Hari, P., 2004. A new feedback mechanism linking forests, aerosols, and climate. Atmospheric Chemistry and Physics 4, 557-562.

Langenheim, J.H., 2003. *Plant Resins: Chemistry, Evolution, Ecology, and Ethnobotany*. Timber Press Inc., Cambridge, U.K.

Lewinsohn, E., Savage, T.J., Gijzen, M., Croteau, R., 1993. Simultaneous analysis of monoterpenes and diterpenoids of conifer oleoresin. Phytochemical Analysis 4, 220-225.

Lohaus, G., Pennewiss, K., Sattelmacher, B., Hussman, M., Muehling, K.H., 2001. Is the infiltration-centrifugation technique appropriate for the isolation of apoplastic fluid? A critical evaluation with different plant species. Physiologia Plantarum 111, 457-465.

Loreto, F., Ciccioli, P., Cecinato, A., Brancaleoni, E., Frattoni, M., Tricoli, D., 1996. Influence of environmental factors and air composition on the emission of α-pinene from *Quercus ilex* leaves. Plant Physiology 110, 267-275.

Mackay, D., Shiu, W.Y., 1981. A critical review of Henry's law constants for chemicals of environmental interest. Journal of Physical and Chemical Reference Data 10, 1175-1199.

Martin, D., Tholl, D., Gershenzon, J., Bohlmann, J., 2002. Methyl jasmonate induces traumatic resin ducts, terpenoid resin biosynthesis, and terpenoid accumulation in developing xylem of Norway spruce stems. Plant Physiology 129, 1003-1018.

Mayol-Bracero, O.L., Guyon, P., Graham, B., Roberts, G., Andreae, M.O., Decessari, S., Facchini, M.C., Fuzzi, S., Artaxo, P., 2002. Water-soluble organic compounds in biomass burning aerosls over Amazonia. 2. Apportionment of the chemical composition and importance of the polyacidic fraction. Journal of Geophysical Research 107, D20, 8091, doi:10.1029/2001JD000522.

Mirov, N.T., 1961. *Composition of Gum Turpentines of Pines*. Pacific Southwest Forest and Range Experiment Station, U.S. Department of Agriculture, Forest Service, Technical Bulletin No. 1239

Niinemets, Ü., Loreto, F., Reichstein, M., 2004. Physiological and physicochemical controls on foliar volatile organic compound emissions. Trends in Plant Science 9, 180-186.

Niinemets, Ü., Reichstein, M., 2002. Effects of nonspecific monoterpenoid storage in leaf tissues on emission kinetics and composition in Mediterranean scerophyllous *Quercus* species: a model analysis. Global Biogeochemical Cycles 16, 1110 DOI: 10.1029/2002GB001927.

Ortega, J., Helmig, D., Daly, R.W., Tanner, D.M., Guenther, A.B., Herrick, J.D., 2008. Approaches for quantifying reactive and low-volatility biogenic organic compound emissions by vegetation enclosure techniques – Part B: Applications. Chemosphere 72, 365-380.

Roller, K.J., 1966. Resin canal position in the needles of Balsam, Alpine and Fraser firs. Forest Science 12, 348-355.

von Rudloff, E., 1972. Seasonal variation in the composition of the volatile oil of the leaves, buds, and twigs of white spruce (*Picea glauca*). Canadian Journal of Botany 50, 1595-1603.

SPARC, 2013. url, http://ibmlc2.chem.uga.edu/sparc/test/login.cfm?CFID=37220&CFTOKEN=56882687.

Staudt, M., Seufert, G., 1995. Light-dependent emissions of monoterpenes by holm oak (*Quercus ilex* L.). Naturwissenschaften 82, 89-92.

Suzuki, M., 1979. The course of resin canals in the shoots of conifers III. *Pinaceae* and summary analysis. The Botanical Magazine Tokyo 92, 333-353.

Tingey, D.T., Manning, M., Grothaus, L.C., Burns, W.F., 1980. Influence of light and temperature on monoterpene emission rates from slash pine. Plant Physiology 65, 797-801.

Tingey, D.T., Turner, D.P., Weber, J.A. 1991. Factors controlling the emissions of monoterpenes and other volatile organic compounds. In *Trace Gas Emissions by Plants*, Sharkey, T.D., Holland, E.A., Mooney, H.A., eds. pp. 93-119, Academic Press, San Diego, CA.

Toma, S., Bertman, S., 2012. The atmospheric potential of biogenic volatile organic compounds from needles of white pine (*Pinus strobus*) in Northern Michigan. Atmospheric Chemistry and Physics 12, 2245-2252.

Wilson, G.M., 1964. Vapor-Liquid equilibrium. XI. A new expression for the excess free energy of mixing. Journal of the American Chemical Society 86, 127-130.

Yatagai, M., Sato, T., 1986. Terpenes of leaf oils from conifers. Biochemical Systematics and Ecology 14, 469-478.

Zavarin, E., 1968. Chemotaxonomy of the genus *Abies*—II. Within tree variation of the terpenes in cortical oleoresin. Phytochemistry 7, 92-107.

Zulak, K.G., Bohlmann, J., 2010. Terpenoid biosynthesis and specialized vascular cells of conifer defense. Journal of Integrative Plant Biology 52, 86-97.

Table 3.1. Vapor pressures (p°), aqueous solubilities ($c_2{}^*$), Henry's law constants (H), air/ and octanol/water partition coefficients (K_{AW} and K_{OW}, respectively), air/octanol partition coefficients K_{AO} estimated using SPARC (2013). Activity coefficients for species in oleoresin (γ_{A3}) estimated from the compilation of activity coefficients by Jang et al. (1997), which were derived by the Hansen group contribution method (Hansen, 1967) for chemical species in wood combustion aerosol and diesel soot.

Species	log p° (Pa)	log $c_2{}^*$ (mol m^{-3})	log H (Pa m^3 mol^{-1})	[a]log K_{AW}	[a]log K_{OW}	[a]log K_{AO}	γ_{A3}	
							MT[b]	RA[c]
α-Pinene	2.93	-1.65	4.57	1.18	4.72	-3.54	1.3	3.0
α-Terpineol	0.535	1.41	-0.873	-4.27	2.58	-6.85	2.5	1.2
Germacrene D	0.215	-4.17	4.39	0.991	7.00	-6.01	1.7	3.4
Germacrene D-4-ol	-1.40	-1.09	-0.312	-3.71	4.62	-8.33	2.9	1.6

[a]Dimensionless partition coefficients (vol vol^{-1}).

[b]Monoterpene mole fraction in *Abies grandis* cortical oleoresin = 0.91 (Lewinsohn et al., 1993).

[c]Resin acid mole fraction in *Pinus contorta* cortical oleoresin = 0.52 (Lewinsohn et al., 1993).
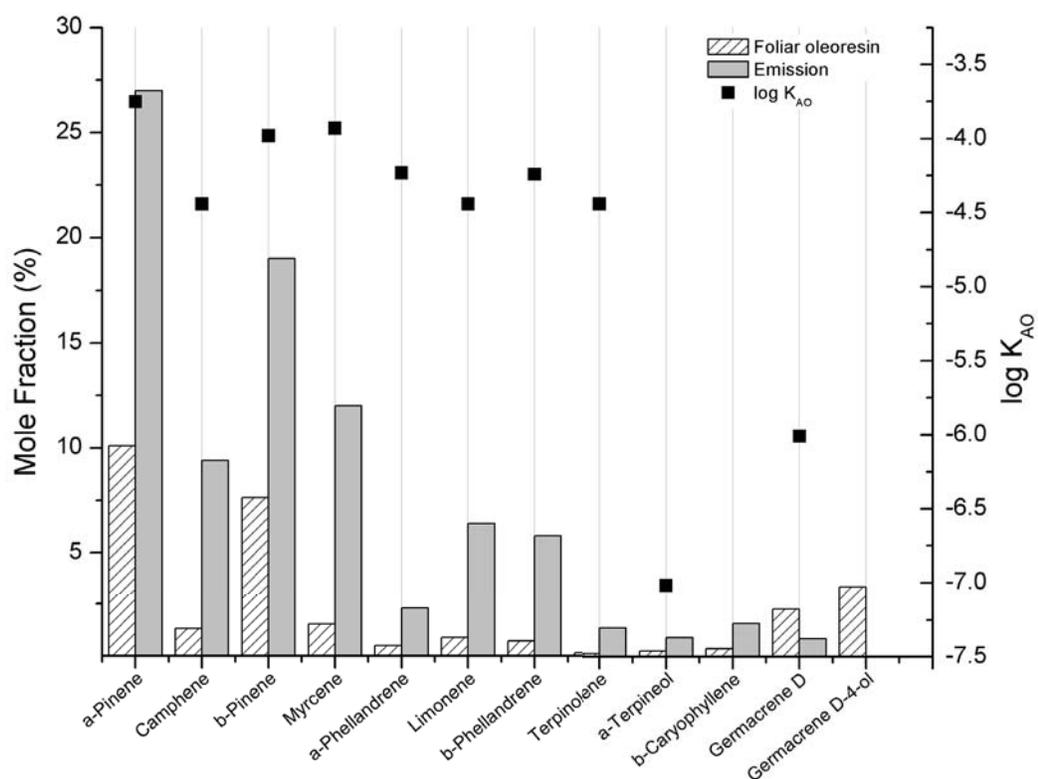
Figure 3.1. Comparison of the molar composition of foliar oleoresin and emissions from *Pinus strobus*. Average molar composition of foliar oleoresin was estimated from measurements of foliar oils by Toma and Bertman (2012) and foliar oil yields by Mirov (1961). The emission signature is derived from the average of values reported by Ortega et al. (2008). Values of K_{AO} were estimated from the compilation of terpene and terpenoid physicochemical properties by Copolovici and Niinemets (2005).
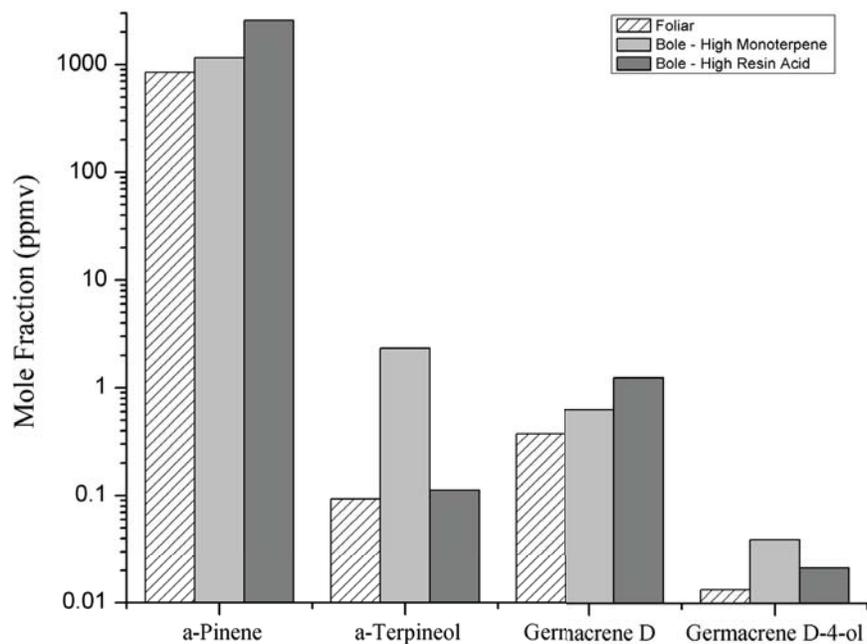
Figure 3.2. Estimated terpene and terpenoid signatures for emissions from the foliar and bole release pathways. The average molar composition of foliar oils of Pinus strobus reported by Toma and Bertman (2012) and corrected for yield of foliar oils (Mirov, 1961) was used to derive the foliar oleoresin emission signature. Cortical oleoresin compositions of *Pinus contorta* and *Abies grandis* from the detailed analysis by Lewinsohn et al. (1993) represent the high resin and monoterpene content oleoresin, respectively.

Chapter 4. Comparison of Multistep Derivatization Methods for Identification and Quantification of Oxygenated Species in Organic Aerosol

Rosa M. Flores[†] and Paul V. Doskey[*,†,‡,§]

[†]Department of Civil and Environmental Engineering, Michigan Technological University, Houghton, Michigan 49931, United States
[‡]School of Forest Resources and Environmental Science, Michigan Technological University, Houghton, Michigan 49931, United States
[§]Atmospheric Sciences Program, Michigan Technological University, Houghton, Michigan 49931, United States

ABSTRACT

Secondary organic aerosol (SOA) is a complex mixture of compounds with various oxygen-containing functional groups. Quantification of SOA by comprehensive multidimensional gas chromatography (GC) with mass spectrometric (MS) detection [GC × GC-time-of-flight (ToF)-MS in the work presented here] requires derivatization to minimize ambiguities in identifications. We compared two, 3-step derivatization methods that differed in the reaction to derivatize carboxylic acids. Method 1 sequentially converts multi- and poly-functional species with C=O, –COOH, and –OH moieties (1) to methyloximes with O-methylhydroxylamine hydrochloride (MHA), (2) to methyl esters with (Trimethylsilyl)diazomethane in methanol (TMSD/MeOH), and (3) to trimethylsilyl ethers with N,O-bis(trimethylsilyl)-trifluoroacetamide (BSTFA), respectively. In Step 2 of Methods 1 and 2 derivatization of –COOH moieties is accomplished with TMSD/MeOH and 10% (v/v) boron trifluoride (BF_3) in MeOH or *n*-butanol (*n*-BuOH), respectively. The BF_3/(MeOH or *n*-BuOH) was ineffective at converting species with more than 2 –OH moieties. Average standard deviations for derivatization of 36 model compounds by the 3-step methods using TMSD/MeOH and BF_3/(MeOH) were 7.42 and 14.75%, respectively. Average derivatization efficiencies for Methods 1 and 2 were 87.9 and 114%, respectively. Despite the lower average derivatization efficiency of Method 1, distinct advantages included a greater certainty of derivatization yield for the entire suite of multi- and poly-functional species and fewer processing steps for sequential derivatization. Detection limits for Method 1 using GC × GC- ToF-MS were 0.09-1.89 ng μL^{-1}.

KEYWORDS

4.1. Introduction

Aerosols play an important role in tropospheric chemistry, climate, and human and environmental health. Primary organic aerosol (POA) is directly emitted by natural and anthropogenic sources and is distributed in the fine and coarse aerosol modes.[1] Secondary organic aerosol (SOA) is the most abundant fine aerosol in the global troposphere and is formed through a series of gas-phase reactions followed by homogeneous nucleation and heterogeneous reactions in the organic and aqueous films of preexisting aerosol.[2] The SOA is composed of thousands of species that represent a continuum of polarity attributed to the types and numbers of oxygen (O)-containing functional groups [e.g., alcohol (–OH), carbonyl (C=O), carboxylic acid (–COOH)] of SOA species. Forecasting SOA production on regional to global scales is problematic due to uncertainties in emission inventories of SOA precursors and quantification of precursor oxidation products.[3] Multidimensional gas chromatography with time-of-flight mass spectrometric detection (GC × GC-ToF-MS) has proven useful in identifying and quantifying the myriad of species that compose SOA.[4-6] However, O-containing functional groups of SOA species limit transfer through GC systems due to interactions with active surface sites and are poorly resolved by some GC stationary phases. Chemical derivatization, which reduces species polarity, is included in OA processing techniques to facilitate transfer through GC systems and improve resolution.

One- and two-step derivatization methods have been used to identify and quantify O-containing aerosol species isolated in chamber experiments[7-10] and from ambient[10-15] and indoor air.[16] One-step methods have been used to derivatize species with –COOH,[17-20] C=O,[21-25] and –OH moieties[9,26-28] or for simultaneous quantitation of species with –OH and –COOH functionalities.[12,29-31] Bi- and multi-functional compounds are typically derivatized with two-step methods.[7,32-35] Aliquots of filters containing sampled aerosol have been processed individually by several derivatization methods for comprehensive identification and quantitation of multifunctional species.[34,36,37] Three-step derivatization methods that allow unambiguous determination

of -COOH and -OH species have been reported[37-39] and applied to identify and quantify mono- and multi-functional species in aerosol.[34,39-41]

The C=O functionalities are derivatized in the first step and –OH and –COOH moieties are derivatized in the second step. Carbonyls are converted to oxime derivatives with *O*-(2,3,4,5,6-pentafluorobenzyl)hydroxylamine hydrochloride (PFBHA)[22] or *O*-methylhydroxylamine hydrochloride (MHA).[36,38] Prior to derivatization with PFBHA, which takes up to 24 hr for completion, the aerosol extract is reduced to dryness, and thus, volatile species might be lost, which is not the case with MHA that can be added to the aerosol extract to effect derivatization in about 1 hr. Carboxylic acids are typically alkylated, acylated, or silylated with methanol (MeOH) or *n*-butanol (*n*-BuOH) in the presence of a strong Lewis acid like boron trifluoride (BF$_3$), [14,42-45] diazomethane,[36,46-48] and *N,O*-bis(trimethylsilyl)-trifluoroacetamide (BSTFA) or *N*-methyl-*N*-(trimethylsilyl) trifluoroacetamide (MSTFA).[17] The BF$_3$/butanol technique has the lowest detection limits; however, the procedure is the most time-consuming of the derivatization methods.[20] Diazomethane reacts instantaneously and forms few byproducts; however, toxicity of diazomethane is a concern.[20] (Trimethylsilyl)diazomethane (TMSD) in methanol, which is a less toxic and more stable derivatizing agent than diazomethane, has also been used to methylate carboxylic acids.[38,49,50] Silylation of alcohols with BSTFA or MSTFA is efficient, fast, reproducible, and quantitative.[7,17,20,32,37] However, reaction artifacts have been observed[51] and derivatives are prone to decomposition during storage of processed extracts through infiltration of trace amounts of water.[20]

Here we compare two, 3-step derivatization methods developed from modifications of 3 techniques[37,38,42]. The first method consists of the following sequential derivatization steps: (1) conversion of carbonyls to methyloximes with MHA, (2) reaction of carboxylic acids with TMSD in MeOH to form methyl esters, and (3) transformation of alcohols to trimethylsilyl ethers with a solution containing 1% trimethylchlorosilane (TMCS) in BSTFA (v/v). Steps 1 and 3 of second procedure are identical to Method 1;

however, carboxylic acids are converted to methyl or butyl esters with 10% BF_3 in MeOH or *n*-BuOH in the second step. Mass spectral libraries for derivatives, detection limits, and yields are reported for 3-step derivatizations of oxygenated species characteristic of SOA.

4.2. Experimental Method

Chemicals and Solvents. All chemicals, standards, and derivatization reagents with the exception of dihydroxyacetone (MP Biomedicals, Santa Ana, CA) and pyruvic acid and hydroxybenzaldehyde (Wako Chemicals, Richmond, VA) were purchased from Sigma-Aldrich Chemical Co. (St. Louis, MO) in the highest purity available and were used with no further purification. All solvents were GC grade and purchased from Burdick and Jackson (Muskegon, MI). The derivatization agents included 1% TMCS in BSTFA (v/v), 10% BF_3 in MeOH, 10% BF_3 in *n*-BuOH (v/v), 98% MHA, and TMSD.

Model Compounds. A total of 34 compounds were selected for the method comparison (Table 1). The target analytes were grouped according to the following functionalities and bi-functionalities: -OH, -COOH, C=O and –COOH, -COOH and –OH, and C=O and –OH. The substances were derivatized, identified, and quantified using procedures described below.

Sample Preparation. Stock standards of model compounds were prepared according to functionality in either MeOH or 1:1 (v/v) DCM in ACN at a level of 600 µg L^{-1}. Derivatizing reagents and stock solutions were stored at 4°C. Two, 3-step derivatization methods based on modifications of 3 techniques were evaluated. [37,38,42]. The methods differ in derivatization reagents for carboxylic acids and the order of derivatization of carbonyls and carboxylic acids. Acetals and ketals, which are in equilibrium with hemi-

acetals and –ketals, are formed when carbonyls react with an alcohol in the presence of an acid catalyst.[42] Thus, in the procedure using BF_3 in n-BuOH, carbonyls are converted to methyloximes in the first step with MHA to avoid enolation of ketones and aldehydes with BSTFA (used to derivatize alcohols in the third step), and carboxylic acids are converted to butyl esters in the second step.[37] Samples were analyzed within 24 hours of derivatization.

Reactions occurring in Method 1 and 2 are shown in Fig. 1. In step 1, carbonyls were converted to methyloximes with 20 µL of MHA in acetonitrile (ACN), which is dried over activated Alumina to remove all traces of water and is heated to 75°C immediately before derivatization to facilitate dissolution of MHA. Carboxylic acids were converted to methyl esters in step 2 by ultrasonication of the working standard mixture with 1-12 µL TMSD and 1-8 µL methanol for 20 min. In step 3, alcohols were converted to trimethylsilyl ethers by reacting with 100-245 µL TMCS/BSTFA at 70°C for 60 min. In step 2 of Method 2, carboxylic acids were converted to methyl or butyl esters with 50-150 µL of BF_3/(MeOH or n-BuOH at 65°C for 20 min. Following derivatization of carboxylic acids, the acid was neutralized with 0.5 ml of a saturated aqueous solution of sodium chloride (NaCl). The aqueous solution was extracted 3 times with 1 mL of 1:1 (v/v) hexane (Hex):dichloromethane (DCM) and the extracts combined. The organic extract was dried by eluting through a Pasteur pipette containing 500 mg of anhydrous sodium sulfate (Na_2SO_4) and reduced to 100 µL with a gentle stream of nitrogen (N_2). Alcohols were converted to trimethylsilyl esters in step 3 with 180 µL TMCS/BSTFA at 70°C for 60 min.

GC/MS analysis. Analyses were performed on a GC×GC-ToF-MS (Pegasus IV, Leco, St Joseph, MI) equipped with a programmable temperature vaporizer inlet (PTV; Gerstel, Linthicum, MD). Dimensions of the primary and secondary GC columns were 30 m × 0.25 mm I.D. with a 0.25-µm-film-thickness of (50%-Trifluoropropyl)-methylpolysiloxane (DB-210; Agilent Technologies, Santa Clara, CA) and a 1 m × 0.10

mm I.D. column with a 0.10-µm-film-thickness of 90% Cyanopropyl Polysilphenylene-siloxane (BPX90; Agilent Technologies), respectively.[52] A zero dead volume, stainless steel compression union (Sigma-Aldrich) was used to join the GC columns. The secondary column oven was contained inside the main oven that houses the primary column for independent temperature control of the primary and secondary columns. A quad-jet, dual-stage thermal modulator, which consisted of 2 hot and 2 cold jets cooled by liquid N_2, was used to direct primary column effluent to the secondary column in 3-5 s pulses.

Derivatized samples were injected in the solvent vent mode into the PTV, which was packed with silanized glass wool. The PTV was held at 60°C for 0.2 min and then increased to 240°C at 12°C min^{-1}. Solvent vent and purge flows were 50 and 80 mL of helium min^{-1}, respectively. The GC oven was held at 60 °C for 1 min and incrementally increased to 180, 200, and 240°C at 20, 11, and 8 °C min^{-1}, respectively. Temperatures of the secondary column oven and modulator were offset at 5 and 8°C, respectively, with respect to the temperature of the primary oven, and secondary oven, respectively. The flow of ultra-high purity helium through the primary and secondary columns was held constant at 1 mL min^{-1}.

The ToF-MS was operated at -70 eV in positive electron ionization (EI) mode. Ion source and transfer line temperatures were 250 and 260°C, respectively. Mass spectra were acquired from 50 to 500 m/z at 200 Hz. Unique fragment ions were selected from the most abundant fragment ions (Table 1) to quantify the target analytes (Quant Ion; Table 2). Mass spectral and retention time libraries of model compounds were created with derivatives of authentic standards. Derivatized working standards were analyzed following the second and third steps of each method to simplify identifications and create the libraries. Mass spectra of the derivatized model compounds were compared with spectra in NIST libraries and the literature.

Data Processing. Serial dilutions of the stock standard were prepared to develop a calibration curve. A 5-point calibration curve over the range of 0.2-12 ng of derivatized target analyte was determined as the average of 6 replicate injections of the working standards. Unique fragment ions were used for quantification (Table 1). Limits of detection (LODs) that were determined using quant ions (Table 2) were calculated from calibration curves as LOD = 3 × (*SD*/*m*) where *SD* is the standard deviation of 6 replicate injections of the lowest mass (0.2 ng) of the calibration curve and *m* is the slope.[43] The LODs for the model compounds ranged from 0.09-1.89 ng μL^{-1} (Table 2).

4.3. Results and Discussion

Solvent Selection for Preparation of Standards and Derivatizing Agents. Solvents were selected to effectively dissolve the various groups of model compounds that spanned a wide range of polarities. Mono-functional species with –OH and -COOH moieties were dissolved in methanol (MeOH), and multi- and poly-functional species with C=O, -OH, and -COOH moieties were dissolved in a 1:1 (v/v) mixture of ACN and DCM. The selected solvents also facilitated performing a 2-step derivatization method prior to a 3-step derivatization method. Maintaining MHA in solution in ACN at 25°C was problematic. The solution was heated at 75°C overnight to facilitate dissolution of MHA; however, crystallization occurred immediately upon cooling to 25°C. The MHA solution was heated to 75°C immediately before use to avoid crystallization. Interferences of the derivatization reactions by water were avoided by careful drying of solvents and reagents. Eliminating water from alcohols is necessary to avoid formation of acetals and ketals from aldehydes and ketones when using BF$_3$/alcohol or BSTFA as derivatizing agents. The ACN was dried with activated Alumina and stored overnight over activated Molecular Sieve 3A. Alumina and Molecular Sieve 3A were activated at 360°C for 5 h and 300-320°C for 15 h and used immediately or stored in a desiccator for a maximum of 3-4 months.

Sequential Derivatization Order. Aldehydes and ketones are derivatized in the first step of both methods, followed by conversion of carboxylic acids and then alcohols. Carboxylic acids require derivatization prior to conversion of –OH moieties. Reaction of the C=O functionality of ketones and aldehydes with MeOH in the presence of an acid catalyst,[37,38] initially forms –OH containing hemi-acetals and -ketals. If the mixture was subsequently derivatized with BSTFA, the –OH moieties would be silylated and ketones and aldehydes might mistakenly be identified as alcohols. Also, BSTFA abstracts hydrogen (H) from -OH functionalities of alcohols and carboxylic acids and forms trimethylsilyl ethers, which might make identification of the -OH moiety in alcohols and carboxylic acids ambiguous.

Molar amounts of derivatizing agents to accomplish reactions in Fig. 1 that were tested in the study are presented in Table 3. Derivatization of carboxylic acids to form alkyl esters in Methods 1 and 2 was accomplished through reaction with TMSD/MeOH and BF_3/(MeOH or n-BA), respectively. In step 3 of Methods 1 and 2, alcohols were converted to trimethylsilyl ethers by reacting with BSTFA. In Method 1, MeOH reacts with carboxylic acids in the presence of TMSD in Step 2 to form methyl esters. The MeOH that is not consumed in Step 2 reacts with BSTFA in Step 3, and thus, MeOH amounts must be adjusted according to reaction stoichiometry of Step 1 and minimized so as not to consume the BSTFA required to accomplish Step 3. For Method 1, we followed recommendations of Kowalewski and Gierczak[38] who optimized amounts of derivatizing agents and reaction time for each step and reported minimum and maximum amounts required for each reaction. However, experiments to determine derivatization efficiency of Step 1 indicated reaction of carbonyls with MHA at 70°C was complete in 1 h rather than the recommended 2 h. Also, pyridine (PYR) was replaced by ACN as the solvent for MHA. Dissolution of MHA in PYR was instantaneous; however, PYR created an elevated baseline in total ion chromatograms (TICs) that negatively affected LODs. For Method 1, we replaced PFBHA with MHA

as the derivatizing agent for aldehydes and ketones in Step 1 to avoid additional processing steps, which involved purification, neutralization, and extraction of the derivatives[22] that might contribute to compound analytic errors. In Step 2 of Methods 1 and 2 carboxylic acids are esterified with TMSD/MeOH and BF$_3$/(MeOH or n-BuOH), respectively. Step 2 of Method 2,[37] which might contribute to additional analytic errors, are avoided and includes the following processes: (1) neutralization with a saturated aqueous solution of NaCl, (2) extraction of the derivative with Hex/DCM, (3) drying over Na$_2$SO$_4$, and (4) reduction of the extract volume with a slow stream of N$_2$. Esterification with TMSD avoids additional processing steps and minimizes analytical errors.

Identification of Derivatives. The most abundant fragment ions of model compound derivatives are presented in Table 1. A characteristic fragment ion was not observed for methyloxime derivatives of model carbonyl compounds. A fragment ion with m/z 43 (tentatively loss of two hydrogen atoms from [N–O–CH$_3$]$^{•−}$) was observed for derivatives of cis-pinonic, S-S-2-hydroxy-3-pinanone, and keto-pinic acid. Many of the methyl esters formed through reaction of n-alkadioic acids with either TMSD in the presence of MeOH or BF$_3$/MeOH have the characteristic fragment ion [C$_2$H$_3$O$_2^{•}$ = 59]; however, mono- and multi-functional aromatic acids did not. Fragment ions in highest abundance for the trimethylsilyl (TMS) derivatives were [Si(CH$_3$)$_3$ = 73] and [OSi(CH$_3$)$_3$ = 90]. Fragment ion [Si(CH$_3$)$_3$ = 73] is also characteristic of bleed from silanized GC columns and can create misidentifications when used alone to make compound assignments. However, TMS derivatives can be identified with confidence by using the 2 characteristic fragment ions, molecular ions, and molecular ions that have lost methyl groups. Fragment ions unique to each species were identified and used to quantify the model compounds (i.e., Quant Ions) and are listed in Table 2.

Derivatization Efficiency. The MS responses of model compounds derivatized by Methods 1 and 2 using molar amounts of derivatizing agents presented in Table 3 are shown in Figs. 2 and 3, respectively. The largest instrumental responses with the lowest standard deviations were obtained when analytes were derivatized with the maximum molar amounts in Method 1. Average standard deviations for experimental molar amounts used by Kowalewski and Gierczak,[38] and the recommended minimum and maximum molar amounts were 17.84, 10.61, and 7.42%, respectively (Table 2). The average derivatization yield for all model compounds considering minimum moles and maximum molar amounts of derivatizing agent was 87.9%.

Method 2, which accomplishes conversion of carboxylic acids to methyl esters by reacting with BF_3/MeOH, exhibited slightly higher derivatization efficiencies than Method 1, which used TMSD/MeOH for the conversion. Average standard deviations for all model compounds were 5.55, 14.75, and 14.79% when 50, 100, and 150 μL of BF_3/MeOH were used to accomplish the derivatization (Table 2). Average derivatization efficiencies when 100 and 150 μL of BF_3/MeOH were used was 160%. Derivatizations of malic and tartaric acid and *n*-hexadecanol exhibited the highest standard deviations. Eliminating the outliers reduced the average derivatization efficiency to 114%, is within the acceptable standard error for 100 and 150 μL of BF_3/MeOH.

The average derivatization efficiency of Method 1 is 2.75-fold greater than the efficiency of Method 2 when maximum molar amounts and 150 μL of BF_3/MeOH were used to accomplish the derivatization. Average derivatization efficiencies of Method 1 vs Method 2 were 2.81-fold, 1.93-fold, and 2.29-fold greater for mono-functional compounds with –COOH moieties, and multi-functional compounds with C=O and -COOH, and -COOH and -OH moieties, respectively. Outliers included mono-functional compounds with -OH moieties that were ineffectively derivatized in Step 3 of Method 2 (Fig. 7) and benzene tricarboxylic acid, which had a derivatization efficiency with TMSD in the presence of MeOH that was 25-fold greater than the efficiency when

BF$_3$/MeOH was used to accomplish the derivatization. The MS responses for BF$_3$/MeOH derivatives of maleic acid and 4-hydroxybenzoic acid were only 0.97 and 18.20% of the TMSD/MeOH derivatives. Esters of the species are quite volatile and are likely lost during reduction of the Hex/DCM extract to 100 µL in preparation for trimethylsilylation with BSTFA. A mixture of carboxylic acids was derivatized with BF$_3$/MeOH and the volume of the Hex/DCM extract reduced to 300 and 100 µL to evaluate losses. Average losses of dicarboxylic acids with 4-6, 7-9 (and dodecanoic acid), and 10-12 (and 1,2,3,4-cyclobutane tetracarboxylic acid) carbon atoms were about 50, 30, and 15%, respectively exhibiting increasing recoveries with decreasing volatility as predicted.

Comparison of Derivatization with BF$_3$/Methanol and BF$_3$/n-Butanol. Advantages of using BF$_3$/n-BuOH to accomplish esterification included production of butyl esters, which are less volatile than methyl esters, and separation of dibutyl oxalate from the solvent peak. However, mono-carboxylic acids were not converted to butyl esters and were instead trimethylsylylated with BSTFA during Step 3. Kawamura[42] accomplished derivatization of –COOH moieties in poly-functional compounds in a single step procedure by heating to 100°C for 1 hr. In Method 2, methyloxime derivatives of carbonyls are dissolved in ACN (b.p. 81-82°C) in Step 1 and the –COOH functionalities converted to butyl esters in Step 2 by heating to 60°C for 20 min, which might be insufficient to accomplish the derivatization. Also, boric acid, tris(2-methylpropyl) ester (C$_{12}$H$_{27}$BO$_3$) was formed as a byproduct of the derivatization with BF$_3$/n-BuOH and elevated the baseline of the TIC.

4.4. Conclusions

Two 3-step derivatization methods for identification and quantification of substances with C=O, –COOH, and –OH moieties that are typical of SOA were compared in the subject study. Three-step derivatization methods are required for unambiguous identification of –OH and –COOH functionalities. The order of derivatization and Steps 1 and 3 were identical for both methods. Carbonyls were converted to methyloximes in Step 1 by reacting with MHA and alcohols reacted with BSTFA in Step 3 to form TMS ethers. Carboxylic acids were converted to alkyl esters in Step 2 with TMSD/MeOH and BF_3/(MeOH or n-BuOH) in Methods 1 and 2, respectively. Method 1 had distinct advantages over Method 2 and derivatization methods that use PFBHA to derivatize carbonyls. Several sample processing steps are required following derivatization of carbonyls with PFBHA and carboxylic acids with BF_3/(MeOH or n-BuOH) that are avoided by derivatizing with MHA and TMSD/MeOH, respectively. Post-derivatization processing procedures prior to the next step of the derivatization method sequence compounds analytic error as exhibited by lower average standard deviations for Method 1 that used TMSD/MeOH (7.42%) than Method 2 that used BF3/MeOH (14.79%). Derivatization of species with more than 2 –OH moieties with BF_3/(MeOH or n-BuOH) was unsuccessful. Detection limits for Method 1 were 0.09-1.89 ng μL^{-1} when the mixture of model compound derivatives was separated using an oven temperature program with 3 temperature ramps.

4.5. Acknowledgements

Flores was supported through a fellowship from the Mexican Council of Science and Technology (CONACyT).
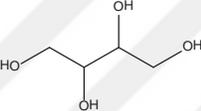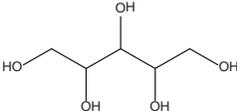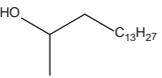
4.6. References

(1) Seinfeld, J. H.; Pandis, S. N. *Atmospheric chemistry and physics: from air pollution to climate change*; John Wiley & Sons, 2012.

(2) Hallquist, M.; Wenger, J.; Baltensperger, U.; Rudich, Y.; Simpson, D.; Claeys, M.; Dommen, J.; Donahue, N.; George, C.; Goldstein, A. *Atmos. Chem. Phys.* **2009**, *9*, 5155-5236.

(3) Liao, H.; Henze, D. K.; Seinfeld, J. H.; Wu, S.; Mickley, L. J. *J. Geophys. Res.* **2007**, *112*, D06201.

(4) Hamilton, J. F. *J. Chromatogr. Sci.* **2010**, *48*, 274-282, 10A-11A.

(5) Kallio, M.; Jussila, M.; Rissanen, T.; Anttila, P.; Hartonen, K.; Reissell, A.; Vreuls, R.; Adahchour, M.; Hyötyläinen, T. *J. Chromatogr., A* **2006**, *1125*, 234-243.

(6) Hamilton, J. F.; Webb, P. J.; Lewis, A. C.; Hopkins, J. R.; Smith, S.; Davy, P. *Atmos. Chem. Phys.* **2004**, *4*, 1279-1290.

(7) Jaoui, M.; Kleindienst, T. E.; Offenberg, J. H.; Lewandowski, M.; Lonneman, W. A. *Atmos. Chem. Phys.* **2012**, *12*, 2173-2188.

(8) Surratt, J. D.; Chan, A. W. H.; Eddingsaas, N. C.; Chan, M.; Loza, C. L.; Kwan, A. J.; Hersey, S. P.; Flagan, R. C.; Wennberg, P. O.; Seinfeld, J. H. *Proceedings of the National Academy of Sciences* **2010**, *107*, 6640-6645.

(9) Szmigielski, R. *J. Mass Spectrom.* **2007**, *42*, 101.

(10) Connelly, B. *The journal of physical chemistry. A* **2012**, *116*, 6180.

(11) Edney, E. O.; Kleindienst, T. E.; Conver, T. S.; McIver, C. D.; Corse, E. W.; Weathers, W. S. *Atmos. Environ.* **2003**, *37*, 3947-3965.

(12) Fu, P.; Kawamura, K.; Chen, J.; Barrie, L. A. *Environ. Sci. Technol.* **2009**, *43*, 4022-4028.

(13) Fu, P. Q.; Kawamura, K.; Pochanart, P.; Tanimoto, H.; Kanaya, Y.; Wang, Z. F. *Atmos. Chem. Phys. Discuss.* **2009**, *9*, 16941-16972.

(14) Kundu, S.; Kawamura, K.; Lee, M. *J. Geophys. Res.* **2010**, *115*, D19307.

(15) Jaoui, M.; Corse, E. W.; Lewandowski, M.; Offenberg, J. H.; Kleindienst, T. E.; Edney, E. O. *Atmos. Environ.* **2010**, *44*, 1798-1805.

(16) Chiappini, L.; Rossignol, S.; Rio, C.; Ustache, A.; Fable, S.; Nicolle, J.; Nicolas, M. *Pollution atmosphérique* **2012**, *99*, 213-214.

(17) Pietrogrande, M.; Bacco, D.; Mercuriali, M. *Anal. Bioanal. Chem.* **2010**, *396*, 877-885.

(18) Hyder, M.; Genberg, J.; Sandahl, M.; Swietlicki, E.; Jönsson, J. Å. *Atmos. Environ.* **2012**, *57*, 197-204.

(19) Kawamura, K.; Matsumoto, K.; Tachibana, E.; Aoki, K. *Atmos. Environ.* **2012**, *62*, 272-280.

(20) Šťávová, J.; Beránek, J.; Nelson, E. P.; Diep, B. A.; Kubátová, A. *Journal of Chromatography B* **2011**, *879*, 1429-1438.

(21) Temime, B.; Healy, R. M.; Wenger, J. C. *Environ. Sci. Technol.* **2007**, *41*, 6514-6520.

(22) Yu, J.; Jeffries, H. E.; Sexton, K. G. *Atmos. Environ.* **1997**, *31*, 2261-2280.

(23) Rossignol, S.; Chiappini, L.; Perraudin, E.; Rio, C.; Fable, S.; Valorso, R.; Doussin, J. F. *Atmos. Meas. Tech. Discuss.* **2012**, *5*, 1153-1231.
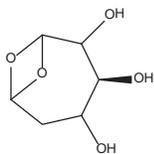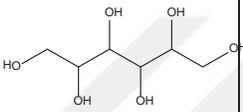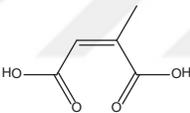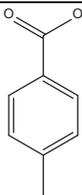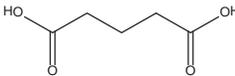
(24) Healy, R. M.; Wenger, J. C.; Metzger, A.; Duplissy, J.; Kalberer, M.; Dommen, J. *Atmos. Chem. Phys.* **2008**, *8*, 3215-3230.

(25) Forester, C. D.; Wells, J. R. *Environ. Sci. Technol.* **2009**, *43*, 3561-3568.

(26) Pashynska, V.; Vermeylen, R.; Vas, G.; Maenhaut, W.; Claeys, M. *J. Mass Spectrom.* **2002**, *37*, 1249-1257.

(27) Wang, W.; Kourtchev, I.; Graham, B.; Cafmeyer, J.; Maenhaut, W.; Claeys, M. *Rapid Commun. Mass Spectrom.* **2005**, *19*, 1343-1351.

(28) Chan, M. N.; Surratt, J. D.; Claeys, M.; Edgerton, E. S.; Tanner, R. L.; Shaw, S. L.; Zheng, M.; Knipping, E. M.; Eddingsaas, N. C.; Wennberg, P. O.; Seinfeld, J. H. *Environ. Sci. Technol.* **2010**, *44*, 4590-4596.

(29) Chiappini, L. *Environ. Chem.* **2006**, *3*, 286.

(30) Pietrogrande, M. C.; Bacco, D. *Anal. Chim. Acta* **2011**, *689*, 257-264.

(31) Kourtchev, I.; Ruuskanen, T.; Maenhaut, W.; Kulmala, M.; Claeys, M.; HAL - CCSD, 2005.

(32) Borras, E. *Int. J. Environ. Anal. Chem.* **2012**, *92*, 110.

(33) Yu, J.; Flagan, R. C.; Seinfeld, J. H. *Environ. Sci. Technol.* **1998**, *32*, 2357-2370.

(34) Lewandowski, M.; Jaoui, M.; Kleindienst, T. E.; Offenberg, J. H.; Edney, E. O. *Atmos. Environ.* **2007**, *41*, 4073-4083.

(35) Cocker Iii, D. R.; Mader, B. T.; Kalberer, M.; Flagan, R. C.; Seinfeld, J. H. *Atmos. Environ.* **2001**, *35*, 6073-6085.

(36) Kubátová, A.; Vermeylen, R.; Claeys, M.; Cafmeyer, J.; Maenhaut, W.; Roberts, G.; Artaxo, P. *Atmos. Environ.* **2000**, *34*, 5037-5051.
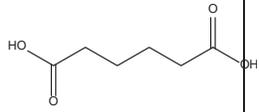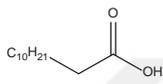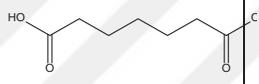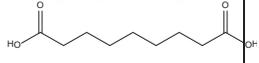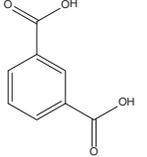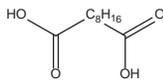
(37) Jaoui, M.; Kleindienst, T. E.; Lewandowski, M.; Edney, E. O. *Anal. Chem.* **2004**, *76*, 4765-4778.

(38) Kowalewski, K.; Gierczak, T. *J. Chromatogr., A* **2011**, *1218*, 7264-7274.

(39) Le Lacheur, R. M.; Sonnenberg, L. B.; Singer, P. C.; Christman, R. F.; Charles, M. J. *Environ. Sci. Technol.* **1993**, *27*, 2745-2753.

(40) Jaoui, M.; Corse, E.; Kleindienst, T. E.; Offenberg, J. H.; Lewandowski, M.; Edney, E. O. *Environ. Sci. Technol.* **2006**, *40*, 3819-3828.

(41) Jaoui, M.; Kleindienst, T. E.; Lewandowski, M.; Offenberg, J. H.; Edney, E. O. *Environ. Sci. Technol.* **2005**, *39*, 5661-5673.

(42) Kawamura, K. *Anal. Chem.* **1993**, *65*, 3505-3511.

(43) Li, Y.-c.; Yu, J. Z. *Environ. Sci. Technol.* **2005**, *39*, 7616-7624.

(44) Hsu, C.-L.; Ding, W.-H. *Talanta* **2009**, *80*, 1025-1028.

(45) Limbeck, A.; Puxbaum, H.; Otter, L.; Scholes, M. C. *Atmos. Environ.* **2001**, *35*, 1853-1862.

(46) Ray, J.; McDow, S. R. *Atmos. Environ.* **2005**, *39*, 7906-7919.

(47) Lewandowski, M.; Jaoui, M.; Offenberg, J. H.; Kleindienst, T. E.; Edney, E. O.; Sheesley, R. J.; Schauer, J. J. *Environ. Sci. Technol.* **2008**, *42*, 3303-3309.

(48) Moretti, F.; Tagliavini, E.; Decesari, S.; Facchini, M. C.; Rinaldi, M.; Fuzzi, S. *Environ. Sci. Technol.* **2008**, *42*, 4844-4849.

(49) Lamoureux, G.; Aguero, C. *Special Issue Reviews and accounts* **2009**, 251–264

(50) Hodnett, N. S. *Synlett* **2003**, *2003*, 2095-2096.

(51) Little, J. L. *J. Chromatogr., A* **1999**, *844*, 1-22.

Table 4.1. Molecular weights of model compounds and derivatives and retention times and most abundant fragment ions of the derivatives.

Compound	Structure	Parent MW	RT (s)	Derivative MW	Fragment ions[1]
Group 1: -OH					
Myrtenol		152.23	418.10	224.33	**73**, 91(82), 103(50), 209(5)
meso-erythritol		122.12	473.06	410.84	**73**, 147(30), 103(25), 321(2)
d-Arabitol		152.15	551.38	513.05	**73**, 103(30), 147(20), 395(1)
2-Hexadecanol		242.44	602.66	314.62	**73**, 43(75), 117(65), 299(10)

[1] Most abundant fragment ions are reported. The base peak (100 % abundance) is represented in bold. Numbers in parenthesis indicate approximate % relative abundance. The least abundant fragment ion is typically a characteristic fragment represented by the molecular ion, M^+ (MW-H) that has lost either a methyl group ($\cdot CH_3$, m/z 15), or a derivatized functional group such as: $\cdot OCH$,(m/z 31), $C_2H_3O_2$ (m/z 59), $\cdot Si(CH_3)_3$ (m/z 73), or $\cdot OSi(CH_3)_3$ (m/z 89).

Compound	Structure	Parent MW	RT (s)	Derivative MW	Fragment ions[1]
Levoglucosan		162.14	620.87	378.68	**73**, 204(18), 217(15), 333(10)
Mannitol		182.17	650.25	615.26	**73**, 103(20), 147(18), 422(1)
Group 2. -COOH					
Citraconic acid		130.10	454.28	158.15	**127**, 59(50), 99(35), 143(5)
P-Toluic acid		136.15	470.21	150.17	**119**, 91(60), 65(25), 150(30)
Pentanedioic acid		132.11	471.69	160.17	**59**, 100(45), 42(30), 129(30)

Compound	Structure	Parent MW	RT (s)	Derivative MW	Fragment ions[1]
Hexanedioic acid		146.14	513.77	174.19	**59**, 55(85), 114(65), 143(38)
Dodecanoic acid		200.32	541.39	214.34	**74**, 87(58), 55(30), 43(55), 183(5)
Heptanedioic acid		160.17	555.34	188.22	**55**, 59(90), 74(82), 157(25)
Azelaic acid		188.22	638.00	216.27	**55**, 74(70), 59(62), 185(25)
Benzene dicarboxylic acid		166.13	638.91	194.06	**163**, 135(40), 76(30), 194(22)
Decanedioic acid		202.25	682.394	230.30	**55**, 74(65), 59(60), 199(20)
Undecanedioic acid		216.27	725.444	244.33	**55**, 74(80), 98(60),
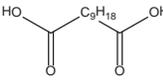
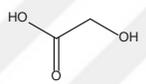| Compound	Structure	Parent MW	RT (s)	Derivative MW	Fragment ions[1]
					213(20)
Dodecanedioic acid		230.30	769.714	258.18	**55**, 74(90), 98(62), 227(15)
1,2,3,4-Cyclobutane tetracarboxylic acid		232.14	841.01	288.25	**59**, 169(75), 111(42), 257(40)
1,2,4,-Benzene tricarboxylic acid		210.14	875.46	252.22	**221**, 75(38), 103(25), 252(5)
Group 3. C=O, -COOH					
cis-Pinonic acid		184.23	553.44	227.15	**58**, 100(85), 42(80), 196(22)
2-Ketoglutaric acid		146.10	545.41	203.19	**59**, 68(35), 140(25), 171(15)
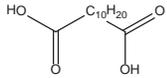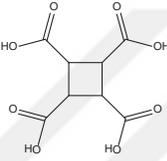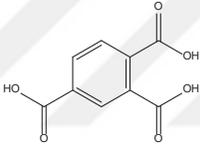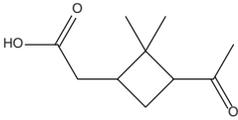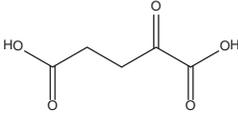
Compound	Structure	Parent MW	RT (s)	Derivative MW	Fragment ions[1]
Ketopinic acid		182.22	632.51	225.14	**67**, 95(98), 41(80), 196(20)
Group 4. –COOH, -OH					
Glycolic acid		76.05	363.08	162.07	Check MS 89, 113(60), 59(50), 145(20), 160(30)
Malic acid		134.09	487.35	234.32	**89**, 73(98), 113(42), 219(20)
3-hydroxy-3-methyl glutaric acid		162.14	509.32	262.37	**43**, 73(62), 117(60), 175(5)
Mandelic acid		152.15	513.77	238.36	**73**, 179(60), 89(50), 223(10)
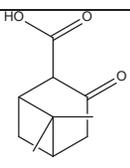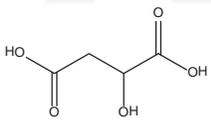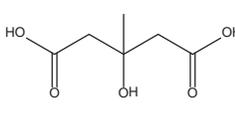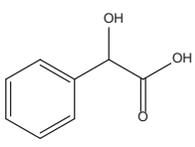
Compound	Structure	Parent MW	RT (s)	Derivative MW	Fragment ions[1]
Salicylic acid		138.12	531.11	224.33	**209**, 59(90), 179(85), 193(20)
L-Tartaric acid		150.09	537.20	322.13	**73**, 89(50), 147(48), 307(10)
4-Hydroxy benzoic acid		138.03	580.52	224.33	**209**, 73(55), 135(55), 224(55)
Gallic acid		170.12	710.63	400.69	**226**, 211(70), 155(70), 195(40)
Group 5. C=O, -OH					
Dihydroxy-acetone		90.08	396.72	263.48	**73**, 147(40), 103(30), 248(10)
Hydroxybenzal dehyde		122.12	511.73	223.34	**73**, 208(95), 89(70),
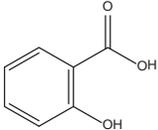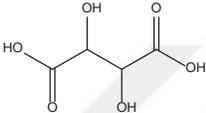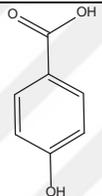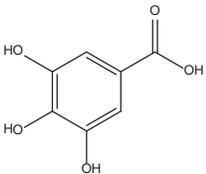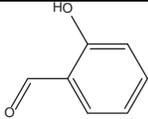
Compound	Structure	Parent MW	RT (s)	Derivative MW	Fragment ions[1]
					223(70)
S-S-2-hydroxy-3-pinanone		168.23	520.61	168.23	**43**, 71(80), 99(50), 125(10)
Nopinone		138.21	490.21	167.25	
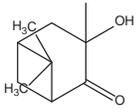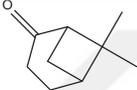
Table 4.2. Standard errors of model compounds derivatized by Methods 1 and 2 and Quant ion and method detection limit (MDL) for Method 1.

| Compound | Method 1 | | | Method 2 |
	Quant ion	Std error (% ±)	MDL (ng µL^{-1})	Std error (±%)
Group 1: -OH				
Myrtenol	91	8.54	0.42	12.92
meso-Erythritol	129	7.73	0.22	ND
d-Arabitol	291	10.08	0.47	ND
2-Hexadecanol	307	5.71	0.20	28.08
Levoglucosan	333	5.14	0.09	ND
Group 2. -COOH				
P-Toluic acid	119	6.84	0.18	13.05
Pentanedioic acid	101	3.17	1.55	5.42
Hexanedioic acid	114	5.94	0.61	2.66
Dodecanoic acid	87	6.31	0.27	12.11
Heptanedioic acid	115	6.16	0.20	4.70
Azelaic acid	152	6.35	0.78	15.48
Benzene dicarboxylic acid	163	6.31	0.44	15.14
Decanedioic acid	98	7.52	0.17	15.08
Undecanedioic acid	74	5.27	0.18	12.40
Dodecanedioic acid	98	8.76	0.25	12.25
1,2,3,4-Cyclobutane tetracarboxylic acid	224	11.91	0.20	9.43
1,2,4,-Benzene tricarboxylic acid	221	11.70	0.29	1.94
Group 3. C=O, -COOH				
cis-Pinonic acid	58	4.53	0.24	8.86

Compound	Method 1			Method 2
	Quant ion	Std error (% ±)	MDL (ng µL^{-1})	Std error (±%)
2-Keto-glutaric acid	112	5.62	0.15	19.30
Keto-pinic acid	165	6.63	0.62	17.09
Group 4. –COOH, -OH				
Mandelic acid	195	5.93	0.46	14.35
Salicylic acid	209	4.45	0.27	20.85
L-Tartaric acid	234	8.71	0.27	35.70
4-Hydroxy benzoic acid	209	3.85	0.24	18.29
Gallic acid	312	7.92	0.20	ND
Group 5. C=O, -OH				
Dihydroxyacetone	84	9.14	0.11	ND
Hydroxybenzaldehyde	209	5.59	1.90	13.60
S-S-2-Hydroxy-3-pinanone	71	10.07	0.34	ND
Nopinone	83	6.88	1.62	ND
Average		**7.42**		**14.75**

ND= not detected

Table 4.3. Mole ratios and amount of derivatization agent used in Method 1.

| MHA | | TMSD | | MeOH | | BSTFA | | Comment* |
Mole ratio	Volume μL	Mole ratio	Volume μL	Mole ratio	Volume μL	Mole ratio	Volume μL	
3.3	20	14	1	171	1	2.3	140	Experimental
3.3	20	90	6	600	3.4	2.4	180	Minum recommended
3.3	20	170	12	1500	8	2.3	245	Maximum recommended

*Adapted from Kowalewski et al. [38]
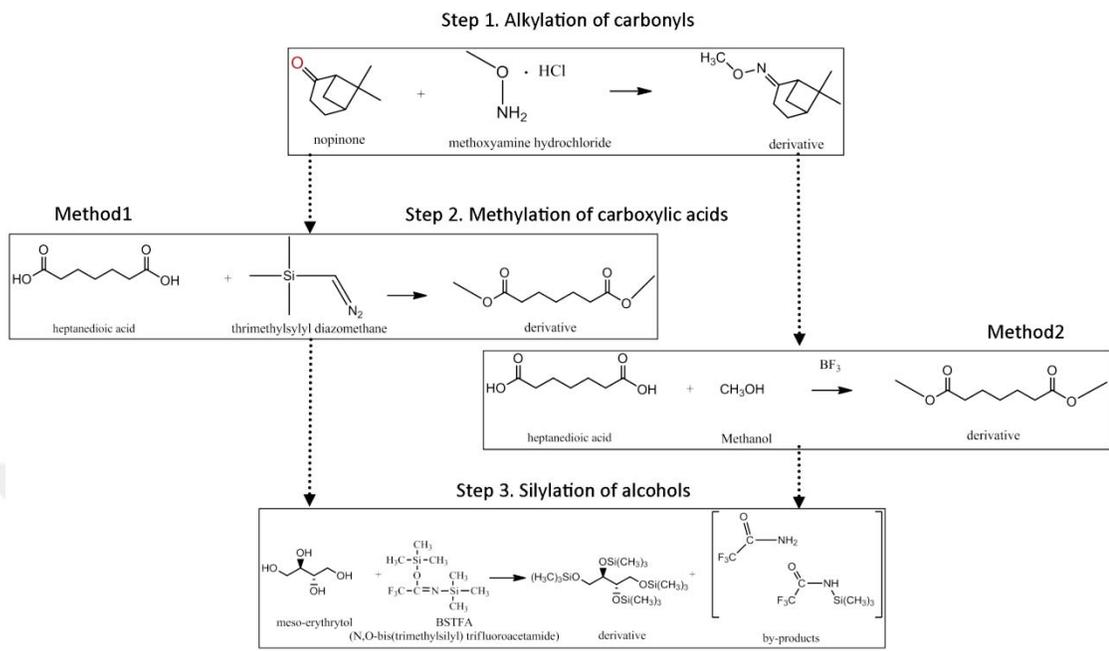
Figure 4.1. Reactions occurring during sequential derivatizations in Methods 1 and 2.
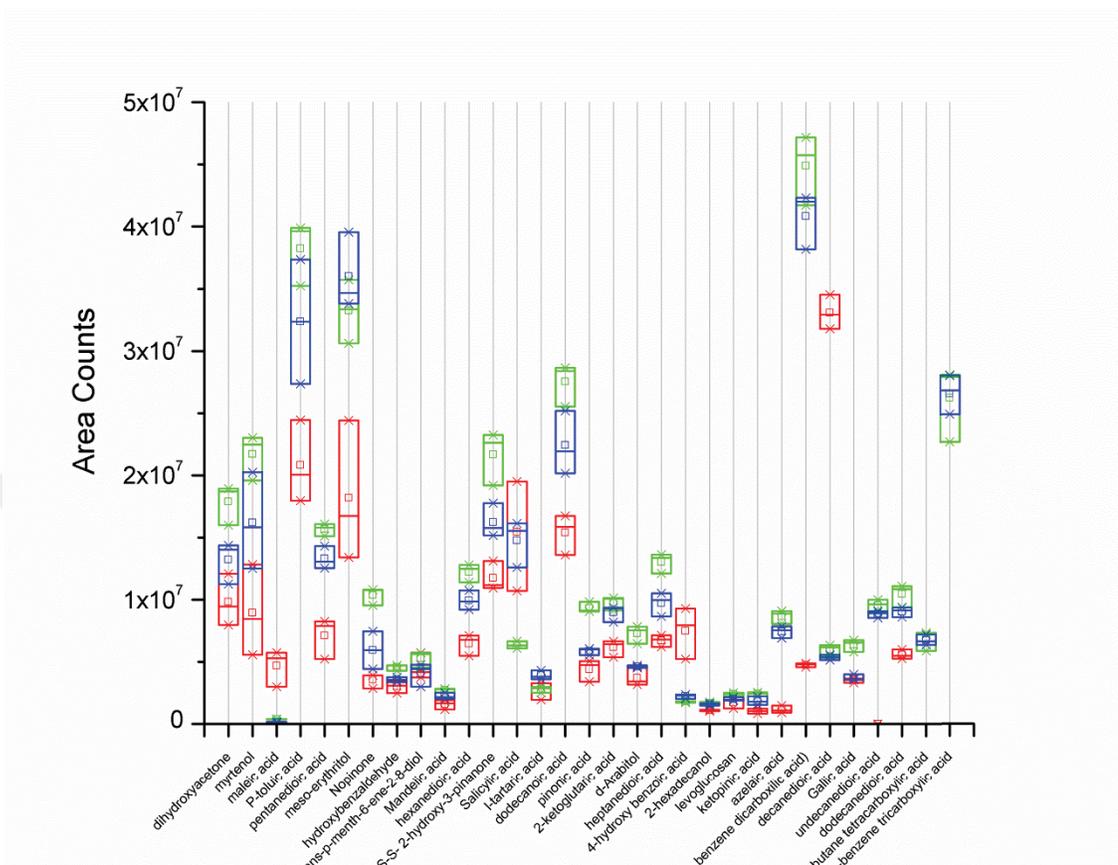
Figure 4.2. Mass spectrometric response for model compounds derivatized in Steps 1, 2, and 3 of Method 1 with (1) 20 µL MHA, (2) 1-12 µL TMSD and 1-8 µL MeOH, and (3) 100-245 µL BSTFA, respectively.
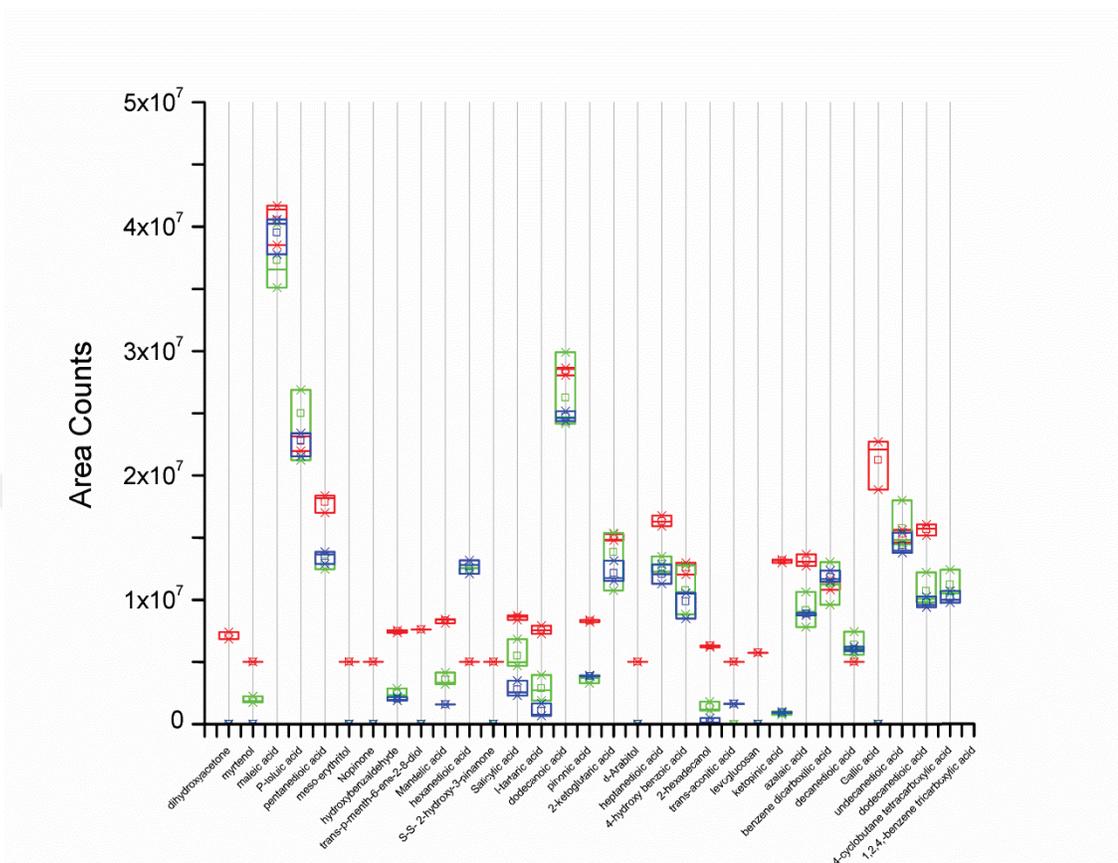
Figure 4.3. Mass spectrometric response for model compounds derivatized in Steps 1, 2, and 3 of Method 2 with (1) 20 μL MHA, (2) 50-150 μL BF$_3$/MeOH, and (3) 180 μL BSTFA.

Chapter 5. Using Multidimensional Gas Chromatography to Define a Carbon Number-Functionality Grid for Characterizing Oxidation of Organic Aerosol

Using Multidimensional Gas Chromatography to Define a Carbon Number-Functionality Grid for Characterizing Oxidation of Organic Aerosol

Rosa M. Flores[1], Judith A. Perlinger[1,2], and Paul V. Doskey[1-3]

[1]Department of Civil and Environmental Engineering, [2]Atmospheric Sciences Program, [3]School of Forest Resources and Environmental Science.

Michigan Technological University, 1400 Townsend Drive, Houghton, MI 49931.

rmflores@mtu.edu, jperl@mtu.edu, pvdoskey@mtu.edu[◊]

[◊] Corresponding author. Phone: +1 906-487-2745.

A B S T R A C T

A carbon number-functionality grid (CNFG) for a complex mixture of secondary organic aerosol (SOA) precursors and oxidation products was developed from the theoretical retention index diagram of a hypothetical, multidimensional gas chromatographic (GC $\times$ 2GC) analysis of a mixture of SOA precursors and derivatized oxidation products. In the GC $\times$ 2GC analysis, comprehensive separation of the complex mixture was achieved by diverting the modulated effluent from a polar primary column into 2 polar secondary columns. Column stationary phases spanned the widest range of selectivity of commercially available GC analytic columns. The polar primary column separated species by the number of carbon atoms in the molecule (a proxy for molecular volume) except for some highly functionalized species and the polar secondary columns provided additional separation according to functionality. An algebraic transformation of the Abraham solvation parameter model was used to estimate linear retention indices of the solutes relative to elution of a homologous series

of diesters on the primary and secondary columns to develop the theoretical GC × 2GC retention diagram. Retention indices of many of the SOA oxidation products were estimated for derivatized forms of the solutes. The GC stationary phases selected for the primary column [(50%-Trifluoropropyl)-methylpolysiloxane] and secondary columns (90% Cyanopropyl Polysilphenylene-siloxane and Polyethylene Glycol in a Sol-Gel matrix) provided a theoretical separation of 33 SOA precursors and 98 derivatized oxidation products into 35 groups by molecular volume and functionality. Quantifying groupings and organic molecular species in a time series of OA sample collections with a CNFG developed through a GC × 2GC analysis is a promising technique for limiting the complexity of organic molecular data in SOA formation models and for modeling the life cycle of OA.

Keywords: Aerosol life cycle; GC × 2GC; Modeling; Multidimensional gas chromatography; Secondary organic aerosol (SOA); Solvation parameter model.

5.1. Introduction

Organic aerosol (OA) is a complex mixture of thousands of organic species directly emitted to the atmosphere and formed through oxidation of primary emissions of gaseous hydrocarbons of anthropogenic and biogenic origin (Hallquist et al., 2009). Molecular structure and functionality of OA species provide information on the origin and oxidation pathways leading to formation and evolution. However, comprehensive separation and identification of OA molecular species by gas- or liquid-chromatographic approaches coupled with various mass spectrometric detection techniques have proven difficult (Hallquist et al., 2009). Instead, approaches that constrain OA composition by relative abundances of carbon (C), hydrogen (H), and

oxygen (O) atoms, and physicochemical properties estimated by, e.g., group contribution methods have been proposed to manage the complexity of OA species, to model secondary OA (SOA) formation, and to visualize evolution of OA. The two-dimensional volatility basis set (2D-VBS) framework constrains OA composition by C:O and the saturation vapor concentration of the oxidized species (Donahue et al., 2011). The saturation vapor concentration is the product of the saturation concentration of a vapor over a pure, sub-cooled liquid and the activity coefficient in the OA mixture, which can be estimated by group contribution methods. The carbon number-polarity grid (CNPG) approach uses the number of C atoms in the molecule (n) and 20 values of total molecular polarity (tmp) of the oxidized species to characterize evolution of OA (Pankow and Barsanti, 2009). The tmp of an oxidized species has been estimated as the difference between the predicted enthalpy of vaporization of the species and the enthalpy of vaporization of the corresponding hydrocarbon (Barsanti et al., 2011).

Multidimensional gas chromatography (GC × 2GC in the work presented here) is a comprehensive separation technique that resolves complex mixtures of organic compounds according to molecular volume and functionality (Seeley et al., 2001). Superior separation compared to one-dimensional GC is achieved by diverting equal volumes of the modulated effluent, typically from a non-polar primary column, which separates organic species through solute interactions with the stationary phase associated with molecular volume, into 2 polar secondary columns with unique selectivities that separate species via interactions of the solute functional groups with the stationary phases (Seeley et al., 2000). Thus, the primary and secondary columns can be selected to separate species primarily by n, which is a proxy for molecular volume, and by functionality, respectively, essentially making a GC × 2GC retention diagram a carbon number-functionality grid (CNFG). A shortcoming of OA analysis by GC techniques is non-quantitative transfer of species like alcohols, aldehydes, ketones, and carboxylic acids through the GC system due to intermolecular interactions of the analytes with surfaces. However, a multistep derivatization technique has been reported,

which converts surface-active moieties of the solutes into unique and identifiable products that are quantitatively transferred through GC systems (Kowalewski and Gierczak, 2011).

Seeley et al. (2009) algebraically transformed the Abraham solvation parameter model to estimate linear retention indices and develop theoretical retention diagrams for GC × GC applications (i.e., multidimensional gas chromatography using one secondary column) involving linear temperature-programmed operation of the GC oven. The Abraham solvation parameter model is an empirical model that accounts for intermolecular interactions during partitioning of molecules between phases in, e.g., a GC column (Abraham, 1993; Abraham et al., 2004). Estimated and measured descriptors that can be used to derive GC retention factors are available for a large number of solutes and GC stationary phases (Abraham, 1993; Abraham et al., 2004; Poole and Poole, 2008a). Good agreement was observed between theoretical and experimental retention diagrams for a complex mixture of volatile monofunctional solutes (Seeley et al., 2009). However, differences were observed between measured linear and isothermal (140ºC) retention indices for cyclic hydrocarbons (Beens et al., 1998; Seeley and Seeley, 2007). Secondary OA (SOA) consists of a complex mixture of linear, branched, and cyclic hydrocarbons and mono- and multifunctional organic species. Comparison of the very few measurements of solute descriptors for bifunctional species with values estimated by assuming additive behavior of functional groups indicates much poorer agreement for diols and diones than diesters (Goss et al., 2009).

Here we use the approach of Seeley and Seeley (2007) and Seeley et al. (2009) to select GC columns for a GC × 2GC system and to separate a hypothetical mixture of SOA precursors and derivatized oxidation products into groups by molecular volume, structure, and functionality. A theoretical retention diagram is developed using an algebraic transformation of the Abraham solvation parameter model (Seeley et al.,

2009). Experimentally observed GC retention times for a suite of multifunctional solutes are compared with model-derived retention indices to evaluate non-additive effects in partitioning behavior of the solutes in a GC column. Errors in retention indices for cyclic species are also estimated.

5.2. Methods

The SOA precursors and oxidation products selected for the hypothetical GC × 2GC analysis are presented in Fig. 1 and Table 1 Suppl. Terpenes (e.g., isoprene, monoterpenes, sesquiterpenes) and n-alkanes, n-alkanols, and diaromatics were chosen as representative precursors to SOA formation (Kroll et al., 2006; Ng et al., 2006; Pye and Seinfeld, 2010). Molecular markers of SOA produced by oxidation of the precursors were identified from chamber studies of SOA production and field samples (Aschmann et al., 1998; Chan et al., 2009; Fu et al., 2009; Griffin et al., 1999; Jang and Kamens, 1999; Jaoui et al., 2004; Kourtchev et al., 2005 and 2008; Kroll et al., 2006; Lewandowski et al., 2007; Lim and Ziemann, 2009; Wang et al., 2010; Wängberg et al., 1997). Volatile SOA precursors like the terpenes, monoaromatics, and light n-alkanes and n-alkanols require different chromatographic conditions than the semivolatiles, and with the exception of the terpenes, C_5 - C_{10} n-alkanes, and C_1 - C_8 n-alkanols, were not included in the analysis. The derivatization technique selected for the study consists of a 3-step process that sequentially converts carbonyls (C=O) to methyloximes, carboxylic acids (-COOH) to methyl esters, and alcohols (-OH) to trimethylsilyl ethers using methyloxyamine, trimethylsilyldiazomethane, and N,O-bis(trimethylsilyl)-trifluoroacetamide, respectively (Kowalewski and Gierczak, 2011). Organonitrates are not derivatized by the method and require injection of a non-derivatized OA extract for analysis.

5.2.1. Estimation of theoretical retention indices

Theoretical retention indices for a hypothetical GC × 2GC separation of 33 SOA precursors and 98 oxidation products with nitrate (-ONO$_2$) and derivatized -COOH, -OH, and C=O functionalities were estimated using an algebraic transformation of the Abraham solvation parameter model (Seeley et al., 2009). The Abraham solvation parameter model for a GC analysis, which does not involve H bond donor or acceptor interactions of the solute with the stationary phase, is represented by the following:

$$\log k = lL + sS + eE + c \qquad (1)$$

where k is defined as a retention factor that is directly related to a partition coefficient (K) by the column phase ratio (β, volume of gas phase/volume of stationary phase). The relationship $K = \beta k$ quantifies the distribution of the solute between the GC carrier gas and stationary phase. Product terms, lL, sS, and eE, represent contributions of intermolecular interactions between the solute and stationary phase related to solute molecular volume, permanent and induced dipoles (i.e., dipolarity), and polarization by lone pairs of electrons, respectively (Poole and Poole, 2008a). The model intercept term, c, includes β and lacks chemical significance. Thus, the sum, $sS + eE$, represents the contribution of intermolecular interactions related to solute functionality and polarity of the stationary phase.

Seeley et al. (2009) calculated retention indices for GC × GC applications involving linear temperature-programmed operation of the GC oven with the following expression:

$$I = \frac{I(Kovats)}{100} = \frac{(\log k - \log k_n)}{(\log k_{n+1} - \log k_n)} + n \qquad (2)$$

where I is the retention index, I (Kovats) is the Kovats index defined for isothermal operation of the GC oven (Kováts, 1965), n is the number of carbon atoms in the largest solute of a homologous series of reference compounds that has a retention factor smaller than k, k_n is the retention factor for the largest solute in the homologous series with n carbon atoms, and k_{n+1} is the retention factor for the solute in the homologous series with $n+1$ carbon atoms. Retention indices for isothermal GC separations are determined with Eq. (2). A linear interpolation of retention factors in Eq. (2) is used to calculate retention indices for linear temperature-programmed operation of the GC oven (van Den Dool and Kratz, 1963). However, when variations in retention indices for compounds under isothermal and linear temperature-programmed operation are similar, application of either the logarithmic or linear interpolation is appropriate to calculate the retention index. Here, we refer to retention indices calculated by Eq. (2) as linear retention indices.

Values of $\log k$, $\log k_n$, and $\log k_{n+1}$ were estimated using Eq. (1) and solute descriptors for alkyl diesters, which were selected as reference compounds. Retention times of n-alkanes can be used to determine retention indices of the species. However, selecting a homologous series of solutes with functionalities that are similar to the target analytes for reference compounds increases separation of reference species and preserves elution order according to n on polar columns (Yabumoto et al., 1977). Homologous series of n-alkanols or n-fatty acid methyl esters have been used in place of n-alkanes (Ramos, 2009). The OA species are transformed during several generations of oxidation producing species with a variety of characteristic multifunctionalities that can be used as molecular markers of the precursor source and oxidation pathway. Selecting a single homologous series to represent the complex mixtures of multifunctional species is not possible. Linear regressions of the solute descriptors against n-values of alkyl diesters

156

with $n = 5 - 12$ (Compounds I27-I34 in Table 1) produced slopes (m) of 0.495, 0.0040, and -0.0023, intercepts (b) of 1.9795, 0.9682, and 0.1379, and R^2 values of 1.0000, 0.9170, and 0.7459 for L, S, and E, respectively.

Equations for $\log k_n$, and $\log k_{n+1}$:

$$\log k_n = l(m_L n + b_L) + s(m_S n + b_S) + e(m_E n + b_E) + c \tag{3}$$

$$\log k_{n+1} = l[m_L(n+1) + b_L] + s[m_S(n+1) + b_S] + e[m_E(n+1) + b_E] + c \tag{4}$$

Substituting Eqs. (3) and (4) into Eq. (2) and simplifying gives the following equation for I,

$$I = \frac{l(L - b_L) + s(S - b_S) + e(E - b_E)}{m_L l + m_S s + m_E e} \tag{5}$$

The GC $\times$ 2GC retention diagram is a 3 dimensional plot of the primary column retention index on the x-axis and $A^{\Delta I}$ on the y- and z-axes for each of the secondary columns, where $A = 10^{0.5l}$ and $\Delta I = I_2 - I_1$ (Seeley and Seeley, 2007). The value of A is specific to the stationary phase and solute elution temperature and is estimated from the linear free energy solvation model (Poole and Poole, 2008a). Solute descriptors were estimated with the Absolv module of ADME Boxes 5.0.7 (Pharma-Algorithms, Toronto, Canada) and descriptors for GC stationary phases were derived from the compilation by Poole and Poole (2008a). The Absolv module estimates solute descriptors by summing contributions of molecular fragments to estimate the solute property of the molecule, and thus, contributions of functional groups to the solute descriptor are assumed to be additive.

5.2.2. Measurement of gas chromatographic retention times for assessment of non-additive effects

A selection of 40 analytes (Table 1) were derivatized according to the procedure of Kowalewski and Gierczak (2011) and analyzed by gas chromatography with time-of-flight mass spectrometric detection (GC-ToF-MS; Leco Pegasus IV, St Joseph, MI). Analytes were injected into a column with a stationary phase composed of 5% Phenyl 95% dimethyl arylene siloxane (DB-5ms; Agilent Technologies, Santa Clara, CA) at 100°C and the column oven was raised to 275°C at 15°C min^{-1}. Descriptors for GC stationary phases vary slightly with solute elution temperature (Poole and Poole, 2008a). Relationships between *l*, *s*, and *e* and the target analyte elution temperatures on the DB-5ms column were developed from data reported by Poole and Poole (2008a) and are presented in Table 2. Values of *L*, *S*, and *E* and retention indices were estimated for each of the 40 analytes with the Absolv module of ADME Boxes 5.0.7 (Pharma-Algorithms) and Eq. (5), respectively.

5.2.3. Error Analysis

Errors were propagated for estimates of the C_3 - C_{12} diester retention factors on the primary and secondary columns and $A^{\Delta I}$ for each of the secondary columns. Retention factors [Eq. (1)] were used to propagate errors rather than retention indices [Eq. (5)]. Errors in retention factors are more indicative of the expected errors in observed retention times than errors in retention indices, which are based on a logarithmic interpolation of retention factors using a homologous series of reference compounds [(Eq. 2)]. Uncertainties in estimates of descriptors for solutes and stationary phases were obtained from Goss et al. (2009) and Poole and Poole (2008a), respectively. The uncertainty in the value of *A*, which is determined empirically from a plot of secondary retention times vs. secondary retention indices (Seeley and Seeley, 2007), was chosen to

be ±0.040 (or approximately ±3.0%). Variances between estimated and experimental retention factors for elution of the diesters on the primary and secondary columns and $A^{\Delta I}$ for the secondary columns were calculated as follows:

$$\sigma^2_{\log k} = \sigma^2_l L^2 + \sigma^2_L l^2 + \sigma^2_s S^2 + \sigma^2_S s^2 + \sigma^2_e E^2 + \sigma^2_E e^2 \qquad (6)$$

Standard errors between linear and isothermal (140ºC) retention indices were estimated for cyclic aliphatic compounds and aromatic species in the target analyte list. Linear and isothermal (140ºC) retention indices for hydrocarbons with 6-membered rings and n-alkyl substitutions (C_7 - C_{16}) reported by Beens et al. (1998) were used to develop relationships between errors and linear retention indices for GC columns with the following stationary phases (listed in order of increasing polarity): poly(50% n-octyl/50% methyl) siloxane (SPB-Octyl; Supelco, Bellefonte, PA), 100% Dimethylpolysiloxane (DB-1; Agilent Technologies), (14%-Cyanopropyl-phenyl)-methylpolysiloxane (DB-1701; Agilent Technologies), and (50% Phenyl-50% dimethyl)-polysiloxane (DB-17; Agilent Technologies). Second-order curve fittings of the standard errors *vs.* retention indices had R^2 values of 0.94-1.00.

5.3. Results and discussion

Poole and Poole (2008b) performed a principal components analysis of the selectivity of GC stationary phases and observed that 32 commercially available stationary phases clustered into 4 groups. The most selective stationary phase groupings were cyanopropyl- and trifluoropropyl-substituted poly(siloxanes), and the poly(ethylene glycols) polymers. The ability of a GC × GC system to separate complex mixtures of solutes exhibiting a wide range of solvation properties related to dipolarity and

159

polarizability is typically optimized when retention factors of solutes in one dimension are not correlated with retention factors in the other dimension (i.e., the GC stationary phases are orthogonal). Orthogonality of stationary phases can be assessed and an angle between column vectors larger than 75° typically represents the orthogonal character required for optimal solute separation (Poole and Poole, 2008b). Orthogonalities of 38 GC stationary phases (Poole and Poole, 2008b) were evaluated and configured in GC × 2GC arrangements to optimize separation of the 33 SOA precursors and 98 oxidation products. The (50%-Trifluoropropyl)-methylpolysiloxane (DB-210)/90% Cyanopropyl Polysilphenylene-siloxane (BPX90)/Polyethylene Glycol (PEG) in a Sol-Gel matrix (SolGel-WAX) arrangement, where DB-210 is the primary column, spanned a selectivity space with individual system constants l = 0.455, 0.427 and 0.548; e = -0.46, 0.027 and 0.197; and s = 1.377, 2.044, and 1.493 for DB-210, BPX90, and SolGel-WAX, respectively. Separation of the SOA precursors and derivatized oxidation products was optimized by the configuration; however, angles for the DB-210/SolGel-Wax and DB-210/BPX-90 arrangements were 51° and 40°, respectively, and thus, less than optimal when orthogonality was used as the column selection criteria. The selected columns represent the most highly functionalized stationary phases in the cyanopropyl- and trifluoropropyl-substituted poly(siloxanes) and poly(ethylene glycols) polymer groupings.

Typical GC × GC systems include non-polar primary and polar secondary columns to optimize orthogonality and to separate complex mixtures of functionalized solutes (Seeley et al., 2009). Less than optimal separation of the SOA solutes was observed for GC × GC arrangements with non-polar GC stationary phases (i.e., SPB-Octyl, DB-1) for the primary column and polar GC stationary phases for the secondary column (Figs. 2a and 3a Suppl.). The best separation was obtained by selecting the most polar columns in the cyanopropyl- and trifluoropropyl-substituted poly(siloxanes) and poly(ethylene glycols) polymer groupings (Figs. 2b and 3b Suppl). The DB-210, BPX90, and SolGel-WAX stationary phases were separated by the largest distances in

the principal components analysis of system constants by Poole and Poole (2008b), and thus, span the widest range of selectivity. The SOA solutes have very large values of L relative to S and E, and thus, separation relative to the reference compounds on the primary column is largely driven by solute molecular volume. Separation on the secondary columns is less dependent of L and is instead determined by differences between s and e of the secondary and primary GC stationary phases. Separation was optimized by selecting the most functionalized of the GC stationary phases for the GC × 2GC arrangement to take advantage of interactions with the stationary phases related to S and E of the SOA solutes.

5.3.1. Estimated retention indices vs. experimental retention times of multifunctional species

Experimentally observed retention times on a DB-5ms column were plotted as a function of the retention indices estimated by the solvation parameter model for 40 derivatized analytes with various multifunctionalities (Table 1). The standard error of the regressions varied from 4.5 to 8% with respect to the various multifunctionalities and was 9.5 % for all 40 analytes (Fig. 2). Seeley et al. (2009) reported a standard error of 1% for the primary column in a GC x GC arrangement for a complex mixture of volatile solutes that included monofunctional species with alcohol, carbonyl, ester, and nitro moieties. Errors for multifunctional species are expected to be greater than errors for monofunctional solutes due to non-additive effects on partitioning of the solute to the GC stationary phase. The effects are related to properties of the solute like proximity of functionalities in the molecule; intramolecular H-bonding; and for p-substituted aromatic molecules, a strong delocalization of π electrons over both functional groups (Goss et al., 2009). Relative errors between measured and hypothetical values of S for methyl diesters, diones, and diols were reported to be 8, 60 and 30%, respectively, when functional groups were on adjacent carbon atoms and were reduced to 6, 16 and 6%, respectively when functional groups were separated by 2

161

carbon atoms (Goss et al., 2009). Non-additive effects related to solute molecular volume of multifunctional species are smaller in comparison to effects related to the proximity of functional groups on the molecule (Goss et al., 2009). Errors in values of L for diesters, diones, and diols were 4, 26, and 10%, respectively, when functional groups were on adjacent carbon atoms, and were reduced to 1, 5, and 6%, respectively, when 2 carbon atoms separated the functional groups. Carboxylic acids, carbonyls, and alcohols were converted to methyl esters, methyloximes, and trimethylsilyl ethers, respectively, for the analysis reported here, which eliminates non-additive behavior due to intramolecular H-bonding and reduces interactions due to dipolarity and polarizability of the molecule.

Values of the descriptors for the solute set indicate that solute molecular volume has the greatest influence on partitioning of multifunctional species with the GC stationary phase, and thus, non-additive behavior related to the proximity of functional groups on the molecule is not likely for the multifunctional species considered in the study. Including solutes H19 and H20 in the regression analysis of the H Group increased the standard error (Fig. 2d). The increase was attributed to poor injection precision, elution in close proximity to the solvent peak, and difficulty in deconvolving fragment ions of the methyloxime derivatives of hydroxyacetone and 3-acetyl-1-propanol. Goss et al. (2009) reported non-additive behavior for nitroaniline and nitrophenol, which are p-substituted aromatic molecules exhibiting strong delocalization of π electrons over both functional groups. The G Group contains p-substituted aromatic molecules with methyl ester and trimethylsilyl ether functionalities (G14-16, G18); however, delocalization of π electrons over both functional groups is not expected to be important. Including only saturated methyl diesters with ester functionalities separated by at least 3 carbon atoms in the regression analysis of the I Group reduced the standard error to 2.9%. Solute I40 has 4 methyl ester functionalities on adjacent carbon atoms and will likely exhibit non-additive behavior when partitioning to a GC stationary phase. Solute descriptors for the derivatized, multifunctional solute set (Table 1, Figure 1) have not been experimentally

162

determined and were estimated with the Absolv module of ADME Boxes 5.0.7 (Pharma-Algorithms). Uncertainties in the estimated values might contribute to the large standard errors reported here for multifunctional species compared to the standard error of 1% reported for monofunctional solutes with measured solute descriptors (Seeley et al., 2009).

5.3.2. GC $\times$ GC and GC $\times$ 2GC retention index diagrams.

In the hypothetical GC $\times$ 2GC analysis, SOA precursors and oxidation products elute (relative to the reference compounds) from the polar DB-210 primary column according to molecular volume (and generally according to *n* with the exception of some highly functionalized solutes). The species are further separated according to functionality on the SolGel-WAX and BPX90 secondary columns. With the exception of the multifunctional organonitrates, the SOA oxidation products are derivatized, which reduces the contribution of interactions related to dipolarity and polarizability, and increases the contribution of interactions due to solute molecular volume to the retention factor. In a GC $\times$ GC separation with a non-polar primary column, solutes in the modulated effluent are sequentially transferred to the secondary column in order of increasing molecular volume. Separation of the derivatized SOA products by the secondary column is determined by solute functionality. The theoretical GC $\times$ GC retention diagram for elution of terpene and naphthalene and alkyl naphthalene oxidation products on the DB-210/SolGel-Wax column combination is shown in Fig. 3a. Due to their aromaticity, naphthalene and alkyl naphthalene oxidation products exhibit larger *E* values than the terpenes. Aromatic species interact more strongly with the SolGel-WAX stationary phase, which lengthens retention times relative to the other solutes.

The various functionalities occupy 35 unique spaces in the CNFG, with molecular markers resolved within the functionality groupings (Fig. 3b). Second-generation

163

products of isoprene oxidation include species having two C=O (G48, G49), C=O and -OH (P101, P102), four -OH (H61, H62), two -OH and -COOH (O99), and an alkene with -OH (I68) and occupy unique spaces in the CNFG (Fig. 3b). First generation products of α- and β-pinene oxidation, which are cyclic compounds having -COOH, -OH and C=O functionalities, are located in a cluster of several groups (cA, cB, cC, cD, cE, cH). Monoterpenes other than α- and β-pinene are transformed during the first generation of oxidation into cyclic compounds containing C=O functionalities and are located in Group G. Aliphatic hydrocarbons oxidized under high concentrations of nitrogen oxides will contain $-ONO_2$ and -OH groups and are resolved in Groups W, X, Y, and Z. Groups that are predicted to co-elute in the DB-210 × SolGel-WAX retention diagram (Fig. 1 Suppl), are predicted to be separated in a GC × 2GC diagram (Fig. 3b) using a BPX-90 column as the third dimension (e.g., K and W; cD and M; and cD and Y).

5.3.3. Error analysis.

Average uncertainties in estimates of retention factors derived by applying Eq. (6) to elution of the C_3 - C_{12} diesters on the primary column (DB-210) and secondary columns (SolGel-WAX and BPX90) were 2.8%, 2.4%, and 3.3%, respectively. The standard error for correlations of estimated and measured retention indices for the diesters on a DB-5ms column was 4.5% (Fig. 2e). Average uncertainties estimated by propagating errors in retention factors are slightly less than the standard error derived from the regression analysis of the diesters. Seeley et al. (2009) reported standard errors of 1% for a correlation of estimated and measured retention indices of volatile, monofunctional species with alcohol, carbonyl, ester, and nitro moieties. Larger standard errors for the multifunctional diesters might indicate non-additive effects in partitioning of the species to the GC stationary phases.

Average uncertainties in estimates of $A^{\Delta I}$ for SolGel-WAX and BPX90 were 0.9% and 13.3%. Values of A at 100ºC for SolGel-WAX and BPX90 are 1.88 and 1.63, respectively, and apparently influence the magnitude of errors propagated on $A^{\Delta I}$ using Eq. (5). To minimize errors associated with the dependence of GC stationary phase descriptors on elution temperature, second-order polynomial equations were developed from the data from Poole and Poole (2008b) to adjust descriptors of the DB-5ms stationary phase to solute elution temperature (Table 2). The value of A is also sensitive to solute elution temperature. Replacing l in the relationship to determine A by the equation that relates l to solute elution temperature (Table 2) is a more rigorous approach to estimate $A^{\Delta I}$.

Differences in retention index units between measured linear and isothermal (140ºC) retention indices for C_7 - C_{16} cyclic hydrocarbons are many times greater than the differences for linear hydrocarbon analogs (Beens et al., 1998). Standard errors decrease with increasing n from about 6 to 1% for C_7 - C_{16} cyclic hydrocarbons and errors related to the polarity of the GC stationary phase are invariable for C_7 cyclic hydrocarbons and increase from 0.1 to 1% for C_{16} species as the polarity increases. Values of n for the 66 cyclic species in the target analyte list (Fig. 1, Table 1 Suppl) are 5 - 17 with an average of 12±3. Cyclic species in the target analyte list contain various functionalities; however, standard errors and trends were similar to those observed by Beens et al. (1998).

5.4. Conclusions

Solute descriptors for 33 SOA precursors and 98 derivatized oxidation products were estimated to derive linear retention indices by an algebraic transformation of the Abraham solvation parameter model. Derivatization facilitates transfer through the GC system; however, partitioning of the solute to the GC stationary phase becomes dominated by interactions related to solute molecular volume as interactions related to

dipolarity and polarizability diminish, which reduces solute separation by interactions related to solute functionality. An analysis of the orthogonality of commercially available GC stationary phases was used as one criteria to select columns in a GC × 2GC arrangement to optimize separation of the complex mixture. However, optimal separation of the relatively non-polar, derivatized SOA oxidation products was estimated for GC stationary phases with descriptors related to dipolarity and polarizability that spanned the widest range of values. Stationary phases of the primary and 2 secondary columns were composed of DB-210, BPX90, and SolGel-WAX, respectively, which represent the most highly functionalized of the trifluoropropyl- and cyanopropyl-substituted poly(siloxanes) and poly(ethylene glycols) polymers of the commercially-available, GC stationary phases.

A theoretical retention index diagram was developed for a hypothetical GC × 2GC analysis of the complex mixture of SOA precursors and derivatized oxidation products. In general, species eluted (relative to the alkyl diester reference compounds) from the primary column (DB-210) in bands according to n and from the secondary columns (BPX90, SolGel-WAX) according to functionality, essentially making the GC × 2GC retention diagram a CNFG. The species clustered into 35 groups by functionality and species within each group exhibited good separation by n. The CNFG is based on measurements of OA composition, which is a distinct advantage over the 2D-VBS and CNPG approaches that use estimates of solute physicochemical properties (i.e., saturation vapor concentration, tmp) as one constraint of OA composition.

A significant fraction of global tropospheric aerosol is attributed to SOA. The SOA precursors and products are transformed in the atmosphere through several generations of oxidation adding various types and numbers of functionalities to the molecule that are characteristic of the precursor oxidation pathway. Molecular structure and functionality regulates absorptive partitioning, aerosol hygroscopicity, and SOA formation (Hemming and Seinfeld, 2001; Pankow, 1994; Pankow and Barsanti, 2009).

166

Approaches to model SOA formation have been developed that use molecular data for SOA precursors and oxidation products [e.g., (Chang and Pankow, 2010)]. Thus, development of CNFGs for a time series of aerosol sample collections is a promising technique (1) to limit complexity of organic molecular data in SOA formation models by grouping species according to molecular structure and functionality, (2) to quantify yields of oxidation products derived from precursors, and (3) to evaluate the life cycle of OA.

A small fraction of species in OA is amenable to analysis by GC. A complex mixture of organosulfates, nitrooxy organosulfates, and imidazoles, which are best analyzed by liquid chromatographic techniques, have been identified in several field studies conducted in areas dominated by terpene emissions (Froyd et al., 2010; Galloway et al., 2009; Gao et al., 2006; Surratt et al., 2006, 2008). Identification and quantification of all molecular species in OA by any single method is likely unachievable; however, quantitation of molecular markers of various SOA precursor oxidation pathways by a combination of analytic approaches will facilitate more accurate forecasting of SOA formation on regional to global scales.

5.5. Acknowledgments

5.6. References

Abraham, M.H., 1993. Scales of solute hydrogen-bonding: Their construction and application to physicochemical and biochemical processes. Chemical Society Reviews 22, 73-83.

Abraham, M.H., Ibrahim, A., Zissimos, A.M., 2004. Determination of sets of solute descriptors from chromatographic measurements. Journal of Chromatography A 1037, 29-47.

Aschmann, S.M., Reisseil, A., Atkinson, R., Arey, J., 1998. Products of the gas phase reactions of the OH radical with α- and β-pinene in the presence of NO. Journal of Geophysical Research 103, 25,553-25,561.

Barsanti, K.C., Smith, J.N., Pankow, J.F., 2011. Application of the np+mP modeling approach for simulating secondary organic particulate matter formation from α-pinene oxidation. Atmospheric Environment 45, 6812-6819.

Beens, J., Tijssen, R., Blomberg, J., 1998. Predictions of comprehensive two-dimensional gas chromatographic separations: A theoretical and practical exercise. Journal of Chromatography A 822, 233-251.

Chan, A.W.H., Kautzman, K.E., Chhabra, P.S., Surratt, J.D., Chan, M.N., Crounse, J.D., Kürten, A., Wennberg, P.O., Flagan, R.C., Seinfeld, J.H., 2009. Secondary organic aerosol formation from photooxidation of naphthalene and alkylnaphthalenes: implication for oxidation of intermediate volatility organic compounds (IVOCs). Atmospheric Chemistry and Physics 9, 3049-3060.

Chang, E.I., Pankow, J.F., 2010. Organic particulate matter formation at varying relative humidity using surrogate secondary and primary organic compounds with activity corrections in the condensed phase obtained using a method based on the Wilson equation. Atmospheric Chemistry and Physics 10, 5475-5490.

van Den Dool, H., Kratz, P.D., A generalization of the retention index system including linear temperature programmed gas—liquid partition chromatography. Journal of Chromatography A 11, 463-471, 1963.

Donahue, N.M., Epstein, S.A., Pandis, S.N., Robinson, A.L., 2011. A two-dimensional volatility basis set: 1. organic-aerosol mixing thermodynamics. Atmospheric Chemistry and Physics 11, 3303-3318.

Froyd, K.D., Murphy, S.M., Murphy, D.M., de Gouw, J.A., Eddingsaas, N.C., Wennberg, P.O., 2010. Contribution of isoprene-derived organosulfates to free tropospheric aerosol mass. Proceedings of the National Academy of Sciences 107, 21,360-21,365.

Fu, T.-M., Jacob, D.J., Heald, C.L., 2009. Aqueous-phase reactive uptake of dicarbonyls as a source of organic aerosol over eastern North America. Atmospheric Environment 43, 1814-1822.

Galloway, M.M., Chhabra, P.S., Chan, A.W.H., Suratt, J.D., Flagan, R.C., Seinfeld, J.H., Keutsch, F.N., 2009. Glyoxal uptake on ammonium sulphate seed aerosol: reaction products and reversibility of uptake under dark and irradiated conditions. Atmospheric Chemistry and Physics 9, 3331-3345.

Gao, S., Surratt, J.D., Knipping, E.M., Edgerton, E.S., Shahgholi, M., Seinfeld, J.H., 2006. Characterization of polar organic components in fine aerosols in the southeastern United States: Identity, origin, and evolution. Journal of Geophysical Research 111, D14314, doi:10.1029/2005JD006601.

Goss, K.-U., Arp, H.P.H, Bronner, G., Niederer, C., 2009. Nonadditive effects in the partitioning behavior of various aliphatic and aromatic molecules. Environmental Toxicology & Chemistry 28, 52-60.

Griffin, R.J., Cocker III, D.R., Flagan, R.C., Seinfeld, J.H., 1999. Organic aerosol formation from the oxidation of biogenic hydrocarbons. Journal of Geophysical Research 104, 3555-3567.

Hallquist, M., Wenger, J.C., Baltensperger, U., Rudich, Y., Simpson, D., Claeys, M., Dommen, J., Donahue, N.M., George, C., Goldstein, A.H., Hamilton, J.F., Hermann,

H., Hoffmann, T., Iinuma, Y., Jang, M., Jenkin, M., Jimenez, J.L., Kiendler-Scharr, A., Maenhaut, W., McFiggans, G., Mentel, T.F., Monod, A., Prévôt, A.S.H., Seinfeld, J.H., Surratt, J.D., Szmigielski, R., Wildt, J., 2009. The formation, properties and impact of secondary organic aerosol: current and emerging issues. Atmospheric Chemistry and Physics 9, 5155-5236.

Hemming, B.L., Seinfeld, J.H., 2001. On the hygroscopic behavior of atmospheric organic aerosols. Industrial & Engineering Chemistry Research 40, 4162-4171.

Jang, M., Kamens, R.M., 1999. Newly characterized products and composition of secondary aerosols from the reaction of α-pinene with ozone. Atmospheric Environment 33, 459-474.

Jaoui, M., Kleindienst, T.E., Lewandowski, M., Edney, E.O., 2004. Identification and quantification of aerosol polar oxygenated compounds bearing carboxylic or hydroxyl groups. 1. Method Development. Analytical Chemistry 76, 4765-4778.

Kourtchev, I., Ruuskanen, T.M., Maenhaut, W., Kulmala , M., Claeys, M., 2005. Observations of 2-methyltetrols and related photo-oxidation products of isoprene in boreal forest aerosols from Hyytiälä, Finland. Atmospheric Chemistry and Physics 5, 2761-2770.

Kourtchev, I., Ruuskanen, T., Keronen, P., Sogacheva, L., Dal Maso, M., Reissell, A., Chi, X., Vermeylen, R., Kulmala, M., Maenhaut, W., Claeys, M., 2008. Determination

of isoprene and α-/β-pinene oxidation products in boreal forest aerosols from Hyytiälä, Finland: diel variations and possible link with particle formation events. Plant Biology 10, 138-149.

Kováts, E., 1965. *Advances in Chromatography*, Vol. 1, p. 229, Marcel Dekker, New York.

Kowalewski, K., Gierczak, T., 2011. Multistep derivatization method for the determination of multifunctional oxidation products from the reaction of α-pinene with ozone. Journal of Chromatography A 1218, 7264-7274.

Kroll, J.H., Ng, N.L., Murphy, S.M., Flagan, R.C., Seinfeld, J.H., 2006. Secondary organic aerosol formation from isoprene photooxidation. Environmental Science & Technology 40, 1869-1877.

Lewandowski, M., Jaoui, M., Kleindienst, T.E., Offenberg, J.H., Edney, E.O., 2007. Composition of PM2.5 during the summer of 2003 in Research Triangle Park, North Carolina. Atmospheric Environment 41, 4073-4083.

Lim, Y.B., Ziemann, P.J., 2009. Effects of molecular structure on aerosol yield from OH radical-initiated reactions of linear, branched, and cyclic alkanes in the presence of NOx. Environmental Science & Technology 43, 2328-2334.

Ng, N.L., Kroll, J.H., Keywood, M.D., Bahreini, R., Varutbangkul, V., Flagan, R.C., Seinfeld, J.H., Lee, A., Goldstein, A.H., 2006. Contribution of first- versus second-generation products to secondary organic aerosols formed in the oxidation of biogenic hydrocarbons. Environmental Science & Technology 40, 2283-2297.

Pankow, J.F., 1994. An absorption model of the gas/aerosol partitioning involved in the formation of secondary organic aerosol. Atmospheric Environment 28, 189-193.

Pankow, J.F., Barsanti, K.C., 2009. The carbon number-polarity grid: A means to manage the complexity of the mix of organic compounds when modeling atmospheric organic particulate matter. Atmospheric Environment 43, 2829-2835.

Poole, C.F., Poole, S.K., 2008a. Separation characteristics of wall-coated open-tubular columns for gas chromatography. Journal of Chromatography A 1184, 254-280.

Poole, C.F., Poole, S.K., 2011. Ionic liquid stationary phases for gas chromatography. Journal of Separation Science 34, 888-900.

Poole, S.K., Poole, C.F., 2008b. The orthogonal character of stationary phases for gas chromatography. Journal of Separation Science 31, 1118-1123.

Pye, H.O.T., Seinfeld, J.H., 2010. A global perspective on aerosol from low-volatility organic compounds. Atmospheric Chemistry and Physics 10, 4377-4401.

Ramos, L., 2009. Comprehensive two dimensional gas chromatography, in: Barcelo D. (Ed.), Comprehensive Analytical Chemistry, Elsevier, Amsterdam, pp. 55-57.

Seeley, J.V., Kramp, F., Hicks, C.J., 2000. Comprehensive two-dimensional gas chromatography via differential flow modulation. Analytical Chemistry 72, 4346-4352.

Seeley, J.V., Kramp, F.J., Sharpe, K.S., 2001. A dual-secondary column comprehensive two-dimensional gas chromatograph for the analysis of volatile organic compound mixtures. Journal of Separation Science 24, 444-450.

Seeley, J.V., Libby, E.M., Edwards, K.A.H., Seeley, S.K., 2009. Solvation parameter model of comprehensive two-dimensional gas chromatography separations. Journal of Chromatography A 1216, 1650-1657.

Seeley, J.V., Seeley, S.K., 2007. Model for predicting comprehensive two-dimensional gas chromatography retention times. Journal of Chromatography A 1172, 72-83.

Seeley, J.V., Seeley, S.K., Libby, E.K., McCurry, J.D., 2007. Analysis of biodiesel/petroleum diesel blends with comprehensive two-dimensional gas chromatography. Journal of Chromatographic Science 45, 650-656.

Surratt, J.D., Gómez-González, Y., Chan, A.W.H., Vermeylen, R., Shahgholi, M., Kleindienst, T.E., Edney, E.O., Offenberg, J.H., Lewandowski, M., Maenhaut, W., Claeys, M., Flagan, R.C., Seinfeld, J.H., 2008. Organosulfate formation in biogenic secondary organic aerosol. Journal of Physical Chemistry A 112, 8345-8378.

Surratt, J.D., Kroll, J.H., Kleindienst, T.E., Edney, E.O., Claeys, M., Sorooshian, A., Ng, N.L., Offenberg, J.H. Lewandowski, M., Jaoui, M., Flagan, R.C., Seinfeld, J.H., 2006. Evidence for organosulfates in secondary organic aerosol. Environmental Science & Technology, 41, 517-527.

Wang, L., Atkinson, R., Arey, J., 2010. Comparison of alkylnitronaphthalenes formed in NO3 and OH radical-initiated chamber reactions with those observed in ambient air. Environmental Science & Technology, 44, 2981-2987.

Wängberg, I., Barnes, I., Becker, K.H., 1997. Product and mechanistic study of the reaction of NO3 radicals with α-pinene. Environmental Science & Technology 31, 2130-2135.

Yabumoto, K., Jennings, W.G., Yamaguchi, M., 1977. Gas chromatographic retentions as identification criteria, Analytical Biochemistry 78, 244-251.

Table 5.1. Estimates of solute descriptors for 40 derivatized analytes for assessment of non-additive effects.

ID[a]	Solute	L[b]	S[b]	E[b]
-OH Derivatives				
F1	Glycolaldehyde Dimer	5.68	0.71	0.04
F2	Verbenol	6.03	0.39	0.39
F3	Myrtenol	6.15	0.41	0.38
F4	*trans-p*-Mehth-6-ene-2-8-diol	7.43	0.40	0.01
F5	Meso-Erythritol	7.79	0.47	0.69
F6	Galactosan	8.19	0.84	0.02
F7	Mannosan	8.19	0.84	0.02
F8	Levoglucosan	8.19	0.84	0.02
F9	2-Hexadecanol	9.13	0.30	0.19
F10	*D*-Arabitol	9.73	0.54	0.85
F11	Mannitol	11.68	0.61	1.02
-COOH, -OH Derivatives				
G12	Glycolic Acid	3.43	0.65	0.11
G13	Malic Acid	5.41	1.05	0.04
G14	Salicylic Acid	6.08	1.05	0.49
G15	4-Hydroxy Benzoic Acid	6.08	1.05	0.49
G16	Mandelic Acid	6.49	1.10	0.47
G17	*L*-Tartaric Acid	6.87	1.11	0.21
G18	Gallic Acid	9.26	1.08	0.14
-C=O, -COOH, -OH Derivatives				
H19	Hydroxyacetone	3.65	0.29	0.04
H20	3-Acetyl-1-Propanol	4.64	0.30	0.03
H21	Dihydroxyacetone	5.22	0.37	0.14

H22	2-Keto-Glutaric Acid	5.28	1.02	0.33
H23	Hydroxybenzaldehyde	5.94	0.74	0.66
H24	Pinonic Acid	6.37	0.63	0.48
H25	Keto-Pinic Acid	6.55	0.70	0.70
-COOH Derivatives				
I26	Maleic Acid	3.95	1.08	0.28
I27	Pentanedioic (Glutaric) Acid	4.45	0.99	0.13
I28	Hexanedioic (Adipic) Acid	4.95	0.99	0.12
I29	Heptanedioic Acid	5.44	1.00	0.12
I30	Octanedioic Acid	5.94	1.00	0.12
I31	Azelaic Acid	6.43	1.00	0.12
I32	Sebacic Acid	6.92	1.01	0.12
I33	Undecanedioic Acid	7.42	1.01	0.11
I34	Dodecanedioic Acid	7.91	1.02	0.11
I35	Citraconic Acid	4.31	1.03	0.26
I36	*trans*-Aconitic Acid	5.91	1.43	0.32
I37	*iso*-Phthalic Acid	6.12	1.38	0.73
I38	1,2,4-Benzene Tricarboxylic Acid	7.70	1.72	0.82
I39	*p*-Toluic Acid	5.01	0.98	0.67
I40	1,2,3,4-Cyclobutane Tetracarboxylic Acid	7.98	1.82	0.49

[a]Identification number on GC retention diagram.

[b]Solute descriptor.

Table 5.2. Equations for deriving stationary phase descriptors as a function of solute elution temperature (T, °C) for DB-5ms (data from Poole and Poole, 2008b).

Descriptor	Second Order Polynomial Equation[a]	R^2
l	$l = 1.00 \times 10^{-5} T^2 - 4.80 \times 10^{-3} T + 9.79 \times 10^{-1}$	0.9997
s	$s = 9.00 \times 10^{-6} T^2 - 3.60 \times 10^{-3} T + 6.17 \times 10^{-1}$	0.9980
e	$e = -8.00 \times 10^{-6} T^2 + 3.30 \times 10^{-3} T - 2.73 \times 10^{-1}$	0.9990

[a]Based on values of the descriptors at 5 temperatures.

Figure 5.1. Structures of the SOA precursors and non-derivatized oxidation products.
(Compound identifications correspond to designations in Table 1 Suppl).

179
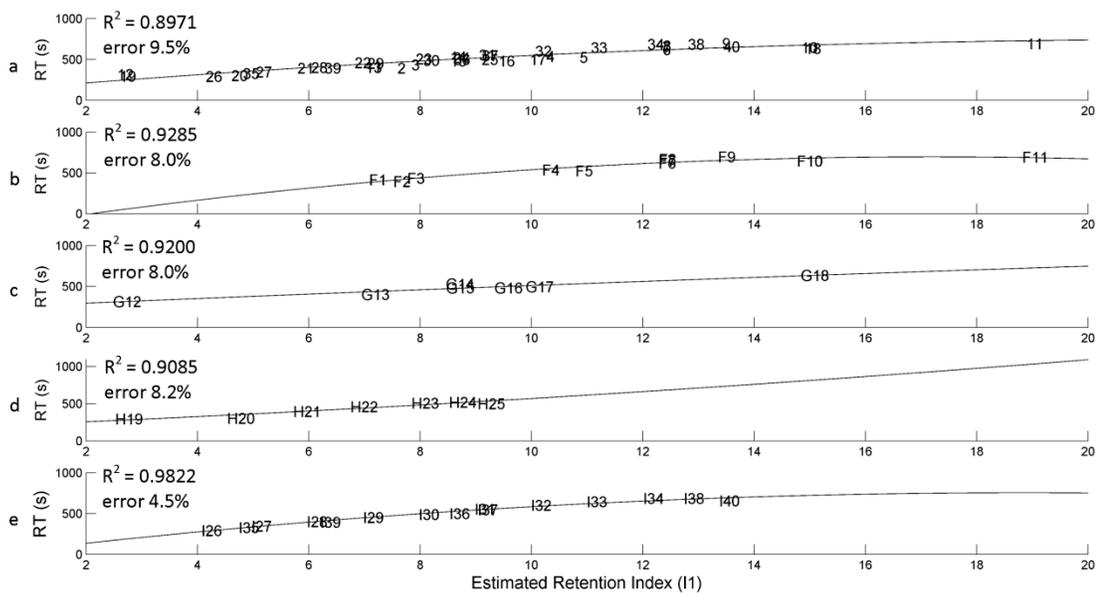
Figure 5.2. Experimentally observed retention times of the solutes in Table 1 for the DB-5ms column plotted as a function of the retention index predicted by Eq. (5).

Fig. 5.3a
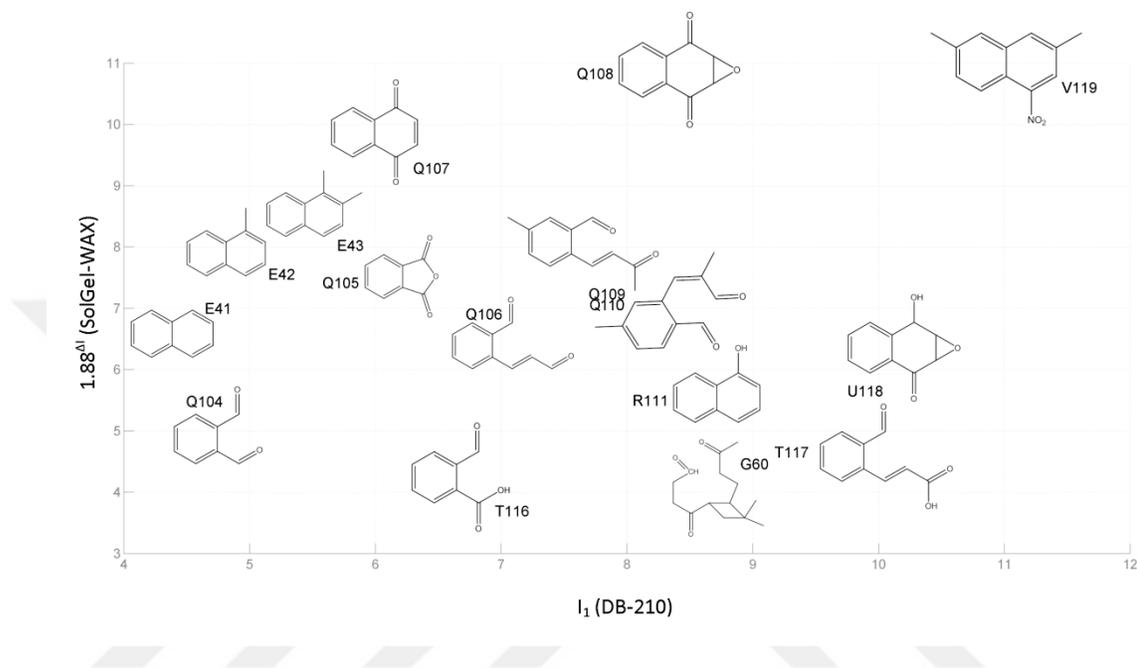
Figure 5.3. Theoretical retention index diagrams of (a) naphthalene oxidation products for the DB-210/SolGel-WAX column combination and (b) of all the other analytes on the DB-210/SolGel-WAX/BPX90 column combination. (Compound identifications correspond to designations in Table 1 Suppl. with the exception of the *n*-alkanes and *n*-alkanols.)

Fig. 5.3b
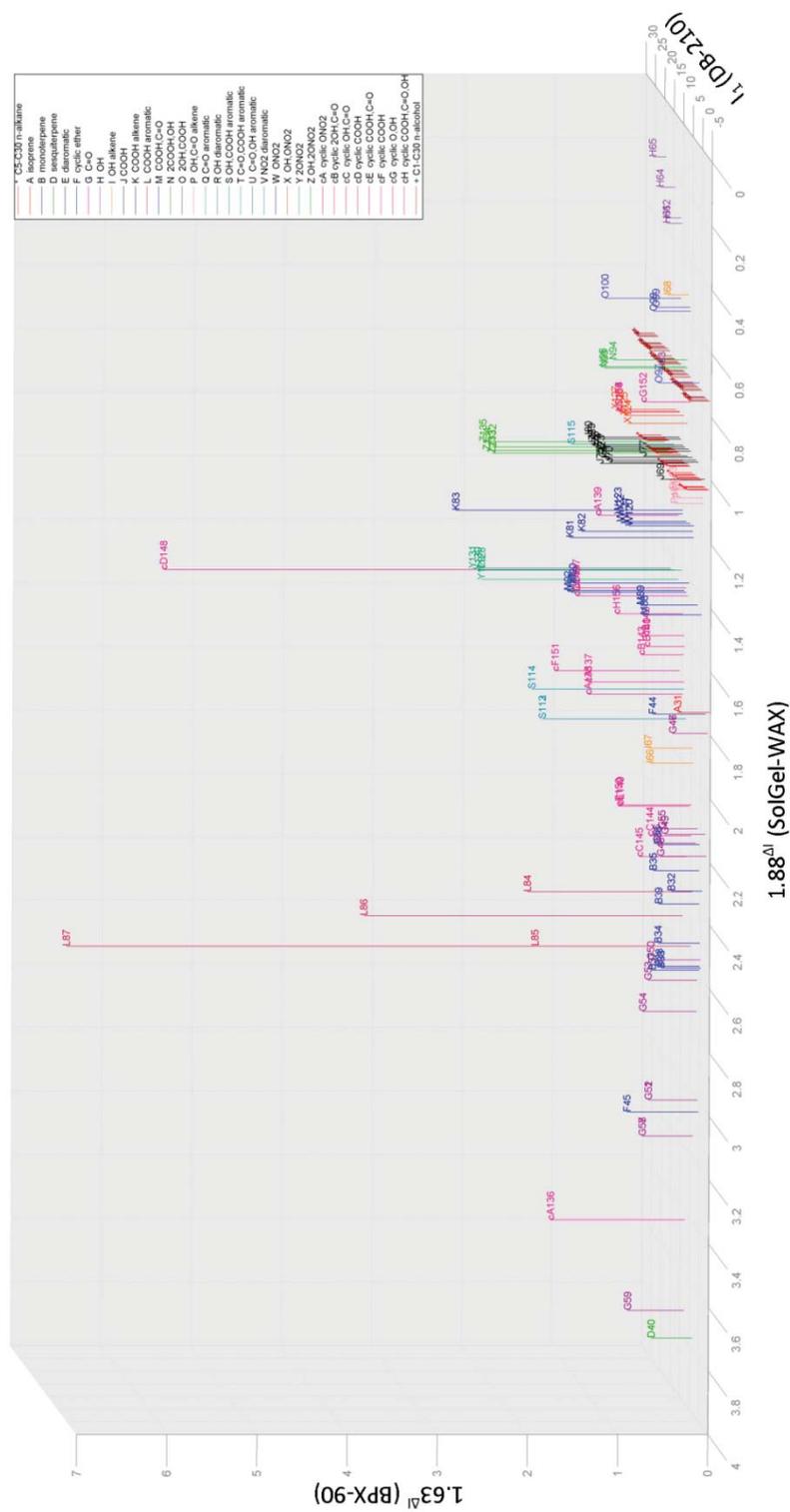
5.7. Supplementary Material

Table S5.1. Solvation parameters for solutes in Figs. 5.3a and 5.3b estimated using Absolv module of ADME Boxes 5.0.7.

Group	ID	Compound Name	L	S	E
	HC5	*n*-Pentane	2.24	0.19	0.00
	HC6	*n*-Hexane	2.73	0.19	0.00
	HC7	*n*-Heptane	3.22	0.20	0.00
	HC8	*n*-Octane	3.72	0.20	0.00
	HC9	*n*-Nonane	4.21	0.20	-0.01
	HC10	*n*-Decane	4.71	0.21	-0.01
	HC11	*n*-Undecane	5.20	0.21	-0.01
HC	HC12	*n*-Dodecane	5.70	0.22	-0.01
	HC13	*n*-Tridecane	6.19	0.22	-0.01
	HC14	*n*-Tetradecane	6.69	0.23	-0.01
	HC15	*n*-Pentadecane	7.18	0.23	-0.02
	HC16	*n*-Hexadecane	7.67	0.23	-0.02
	HC17	*n*-Heptadecane	8.17	0.24	-0.02
	HC18	*n*-Octadecane	8.66	0.24	-0.02
	HC19	*n*-Nonadecane	9.16	0.25	-0.02

Group	ID	Compound Name	L	S	E
	HC20	*n*-Eicosane	9.65	0.25	-0.03
	HC21	*n*-Heneicosane	10.15	0.26	-0.03
	HC22	*n*-Docosane	10.64	0.26	-0.03
	HC23	*n*-Tricosane	11.14	0.27	-0.03
	HC24	*n*-Tetracosane	11.63	0.27	-0.03
	HC25	*n*-Pentacosane	12.12	0.27	-0.03
	HC26	*n*-Hexacosane	12.62	0.28	-0.04
	HC27	*n*-Heptacosane	13.11	0.28	-0.04
	HC28	*n*-Octacosane	13.61	0.29	-0.04
	HC29	*n*-Nonacosane	14.10	0.29	-0.04
	HC30	*n*-Triacontane	14.60	0.30	-0.04
Hemiterpene	A31	Isoprene	2.10	0.23	0.31
	B32	α-Pinene	4.31	0.14	0.45
	B33	β-Pinene	4.39	0.24	0.53
	B34	Sabinene	4.53	0.28	0.52
Monoterpenes	B35	β-Phellandrene	4.56	0.36	0.48
	B36	Terpinolene	4.57	0.32	0.45
	B37	3-Carene	4.58	0.33	0.55

Group	ID	Compound Name	L	S	E
	B38	Terpinene	4.72	0.25	0.53
	B39	Limonene	4.73	0.28	0.49
Sesquiterpene	D40	Caryophyllene	6.87	0.15	0.72
Diaromatic	E41	Naphthalene	5.33	1.02	1.27
	E42	1-Methylnaphthalene	5.80	0.96	1.30
	E43	1,2-Dimethylnaphthalene	6.28	0.90	1.32
Cyclic Epoxide/Ether	F44	3-Methylfuran	2.51	0.50	0.37
	F45	Pinane Epoxide	4.28	0.50	0.68
C=O[a]	G46	Methacrolein	2.51	0.27	0.34
	G47	Methyl Vinyl Ketone	2.51	0.27	0.34
	G48	Glyoxal	2.69	0.35	0.47
	G49	Methyl Glyoxal	3.05	0.30	0.44
	G50	4-Methyl-3-Cyclohexenone	4.20	0.36	0.55
	G51	Nopinone	5.06	0.31	0.63
	G52	Sabinaketone	5.06	0.31	0.63
	G53	Limonaketone	5.08	0.35	0.56
	G54	Phellandra Ketone	5.10	0.39	0.59
	G55	6-Methyl-Hepta-2,5-Dione	5.27	0.25	0.42

Group	ID	Compound Name	L	S	E
	G56	Limonon Aldehyde	5.66	0.29	0.44
	G57	Pinonaldehyde	6.23	0.32	0.65
	G58	3-Caronaldehyde	6.23	0.32	0.65
	G59	Caryophyllon Aldehyde	8.51	0.34	0.74
	G60	Keto-β-Caryophyllonaldehyde	9.04	0.37	0.85
	H61	2-Methylerythritol	8.17	0.46	-0.68
	H62	2-Methylthreitol	8.56	0.43	-0.71
OH Alkane[a]	H63	2-Hexadecanol	9.13	0.30	-0.19
	H64	D-Arabitol	9.73	0.54	-0.85
	H65	Mannitol	11.68	0.61	-1.02
	I66	Verbenol	6.03	0.39	0.39
OH Alkene[a]	I67	Myrtenol	6.15	0.41	0.38
	I68	2-Methyl-1,3,4-Trihydroxy-1-Butene	6.68	0.45	-0.39
	J69	Propionic acid	2.35	0.58	0.07
	J70	Oxalic acid	2.97	0.97	0.13
COOH[a]	J71	Propanedioic acid	3.46	0.98	0.13
	J72	Pentanedioic acid	4.45	0.99	0.13
	J73	Hexanedioic acid	4.95	0.99	0.12

Group	ID	Compound Name	L	S	E
	J74	Heptanedioic acid	5.44	1.00	0.12
	J75	3-Isopropylpentanedioic acid	5.71	0.97	0.14
	J76	Azelaic acid	6.43	1.00	0.12
	J77	Lauric acid	6.81	0.62	0.05
	J78	Sebacic acid	6.92	1.01	0.12
	J79	Undecanedioic acid	7.42	1.01	0.11
	J80	Dodecanedioic acid	7.91	1.02	0.11
COOH Alkene[a]	K81	Maleic acid	3.95	1.08	0.28
	K82	Citraconic acid	4.31	1.03	0.26
	K83	*trans*-Aconitic acid	5.91	1.43	0.32
COOH Aromatic[a]	L84	Benzoic acid	4.54	1.03	0.64
	L85	*p*-Toluic acid	5.01	0.98	0.67
	L86	*i*-Phthalic acid	6.12	1.38	0.73
	L87	1,2,4,-Benzene Tricarboxylic acid	7.70	1.72	0.82
COOH, C=O[a]	M88	Pyruvic acid	3.19	0.61	0.28
	M89	Levulinic acid	4.18	0.62	0.27
	M90	2-Ketoglutaric acid	5.28	1.02	0.33
	M91	3-Acetyl Pentanedioic acid	6.16	1.01	0.34

Group	ID	Compound Name	L	S	E
	M92	3-Acetyl Hexanedioic acid	6.65	1.02	0.34
2COOH, OH[a]	N93	Malic acid	5.41	1.05	-0.04
	N94	Citramalic acid	5.69	1.00	-0.07
	N95	3-Hydroxyglutaric acid	5.91	1.05	-0.04
	N96	α-Hydroxyglutaric acid	5.91	1.05	-0.04
2OH, COOH[a]	O97	Glycolic acid	3.43	0.65	-0.11
	O98	Glyceric acid	5.38	0.72	-0.28
	O99	2-Methylglyceric acid	5.65	0.68	-0.30
	O100	*L*-Tartaric acid	6.87	1.11	-0.21
OH, C=O Alkane[a]	P101	Glycolaldehyde	3.29	0.34	0.06
	P102	Hydroxyacetone	3.65	0.29	0.04
	P103	3-Acetyl-1-Propanol	4.64	0.30	0.03
C=O Aromatic[a]	Q104	Phthaldialdehyde	5.84	0.76	1.07
	Q105	Phthalic Anhydride	6.23	0.88	1.27
	Q106	2-Formyl-Cinnamaldehyde	6.82	0.86	1.22
	Q107	1,4-Naphthoquinone	6.84	0.84	1.39
	Q108	2,3-Epoxy-1-4-Quinone	7.28	0.95	1.50
	Q109	Ketoaldehyde	7.65	0.75	1.22

Group	ID	Compound Name	L	S	E
	Q110	Dialdehyde	7.65	0.75	1.22
OH Aromatic[a]	R111	Naphthol	6.88	1.03	1.12
OH, COOH Aromatic[a]	S112	Salicylic acid	6.08	1.05	0.49
	S113	4-Hydroxy Benzoic acid	6.08	1.05	0.49
	S114	Mandelic acid	6.49	1.10	0.47
	S115	Gallic acid	9.26	1.08	0.14
C=O, COOH Aromatic[a]	T116	Formylbenzoic acid	5.98	1.07	0.90
	T117	Formylcinnamic acid	6.96	1.17	1.05
OH, C=O Aromatic[a]	U118	7-Hydroxy-7,7a-Dihydronaptho[2,3]oxiren-2(1aH)-one	7.90	0.98	1.12
Nitroaromatic	V119	3,6-Dimethyl-Nitronaphthalene	7.76	1.47	1.59
ONO2	W120	3-Heptanylnitrate	4.81	0.75	0.19
	W121	4-Nonanylnitrate	5.80	0.76	0.19
	W122	5-Undecanylnitrate	6.79	0.77	0.19
	W123	6-Tridecanylnitrate	7.77	0.77	0.18
OH, ONO2	X124	5-Hydroxyheptan-2-yl Nitrate	6.26	0.81	0.03

Group	ID	Compound Name	L	S	E
	X125	6-Hydroxynonan-3-yl Nitrate	7.25	0.82	0.02
	X126	7-Hydroxyundecan-4-yl Nitrate	8.24	0.83	0.02
	X127	8-Hydroxytridecan-5-yl Nitrate	9.23	0.84	0.02
2ONO2	Y128	Heptane-1,3-diyl Dinitrate	6.51	1.32	0.38
	Y129	Nonane-2,4-diyl Dinitrate	7.38	1.31	0.39
	Y130	Undecane-3,5-diyl Dinitrate	8.37	1.32	0.38
	Y131	Tridecane-4,6-diyl Dinitrate	9.36	1.33	0.38
OH, 2ONO2	Z132	3-Hydroxyheptane-1,6-diyl Dinitrate	7.96	1.38	0.21
	Z133	4-Hydroxynonane-2,7-diyl Dinitrate	8.83	1.37	0.22
	Z134	5-Hydroxyundecane-3,8-diyl Dinitrate	9.82	1.38	0.22
	Z135	6-Hydroxytridecane-4,9-diyl Dinitrate	10.81	1.39	0.21
ONO2 Cycloalkane	cA136	3-Oxopinan-2-Nitrate	6.92	0.82	0.80
	cA137	1-Hydroxypinan-1-Nitrate	7.16	0.86	0.41
	cA138	2-Hydroxypinan-3-Nitrate	7.54	0.85	0.42
	cA139	1,1-Dihydroxypinan-5-Nitrate	8.51	0.89	0.21
2OH, Keto-	cB140	1,2 Dihydroxy 5-Keto-	8.24	0.40	0.27

Group	ID	Compound Name	L	S	E
Cycloalkane [a]		Cyclohexane			
	cB141	1,5 Dihydroxy, 2-Keto-Cyclohexane	8.24	0.40	0.27
	cB142	1,1 Dihydroxy, 5-Keto-Cyclohexane	8.36	0.41	0.26
	cB143	1,5 Dihydroxy, 1-Keto-Cyclohexane	8.38	0.45	0.29
OH, C=O Cycloalkane [a]	cC144	R-R- 2-Hydroxy-3-Pinanone	6.79	0.33	0.44
	cC145	Hydroxy-Pinonaldehyde	7.80	0.40	0.47
COOH Cycloalkane [a]	cD146	Norpinic acid	5.66	0.99	0.34
	cD147	Pinic acid	6.16	0.99	0.33
	cD148	1,2,3,4-Cyclobutane Tetracarboxylic acid	7.98	1.82	0.49
COOH, C=O Cycloalkane [a]	cE149	Norpinonic acid	5.88	0.63	0.48
	cE150	Pinonic acid	6.37	0.63	0.48
COOH Cycloalkene [a]	cF151	β-Caryophylinic acid	7.94	1.01	0.43
O, OH	cG152	Glycolaldehyde Dimer	5.68	0.71	-0.04

Group	ID	Compound Name	L	S	E
Cycloalkane [a]	cG153	Levoglucosan	8.19	0.84	0.02
	cG154	Mannosan	8.19	0.84	0.02
	cG155	Galactosan	8.19	0.84	0.02
COOH, C=O, OH Cycloalkane [a]	cH156	Hydroxy-Pinonic acid	7.94	0.71	0.30
	OH157	Methanol	1.83	0.25	-0.17
	OH158	Ethanol	2.32	0.25	-0.17
	OH159	Propanol	2.82	0.26	-0.17
	OH160	*n*-Butanol	3.31	0.26	-0.17
	OH161	*n*-Pentanol	3.80	0.27	-0.18
	OH162	*n*-Hexanol	4.30	0.27	-0.18
OH	OH163	*n*-Heptanol	4.79	0.28	-0.18
	OH164	*n*-Octanol	5.29	0.28	-0.18
	OH165	*n*-Nonanol	5.78	0.28	-0.18
	OH166	*n*-Decanol	6.28	0.29	-0.18
	OH167	*n*-Undecanol	6.77	0.29	-0.19
	OH168	*n*-Dodecanol	7.27	0.30	-0.19

Group	ID	Compound Name	L	S	E
	OH169	*n*-Tridecanol	7.76	0.30	-0.19
	OH170	*n*-Tetradecanol	8.25	0.31	-0.19
	OH171	*n*-Pentadecanol	8.75	0.31	-0.19
	OH172	*n*-Hexadecanol	9.24	0.32	-0.20
	OH173	*n*-Heptadecanol	9.74	0.32	-0.20
	OH174	*n*-Octadecanol	10.23	0.32	-0.20
	OH175	*n*-Nonadecanol	10.73	0.33	-0.20
	OH176	*n*-Eicosanol	11.22	0.33	-0.20
	OH177	*n*-Henicosanol	11.72	0.34	-0.20
	OH178	*n*-Docosanol	12.21	0.34	-0.21
	OH179	*n*-Tricosanol	12.70	0.35	-0.21
	OH180	*n*-Tetracosanol	13.20	0.35	-0.21
	OH181	*n*-Pentacosanol	13.69	0.35	-0.21
	OH182	*n*-Hexacosanol	14.19	0.36	-0.21
	OH183	*n*-Heptacosanol	14.68	0.36	-0.21
	OH184	*n*-Octacosanol	15.18	0.37	-0.22
	OH185	*n*-Nonacosanol	15.67	0.37	-0.22
	OH186	*n*-Triacontanol	16.17	0.38	-0.22

[a]Solvation parameters are for derivatized solutes.

Figure S5.1. Drawing of theoretical retention index diagram for DB-210 × SolGel-WAX column combination. (Compound identifications correspond to designations in Table 1 Suppl.)
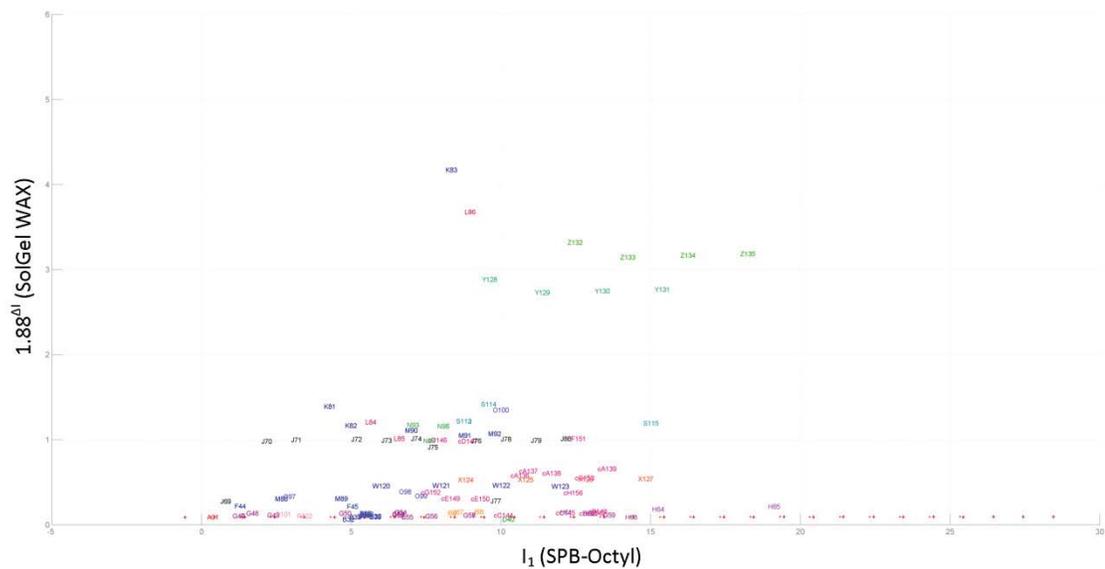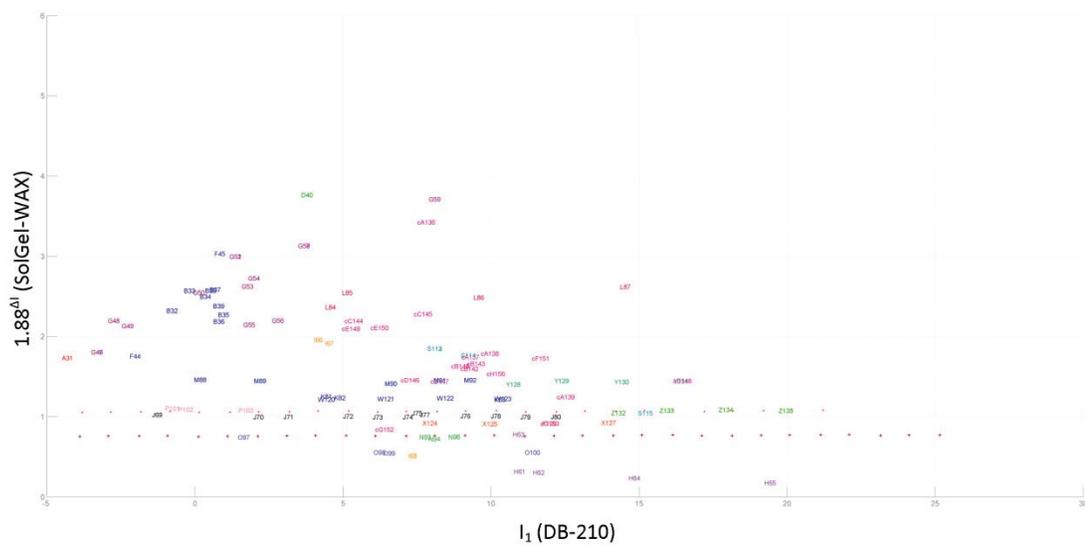
Fig. S5.2a

Fig. S5.2b

Figure S5.2 Suppl. Comparison of retention index diagrams for (a) SPB-Octyl ×
SolGel-WAX and (b) DB-210 × SolGel-WAX column combinations. (Compound
identifications correspond to designations in Table 1 Suppl.)

Fig. S5.3a

Fig. 5.3b

Figure S5.3. Comparison of retention index diagrams for (a) SPB-Octyl × BPX-90 and
(b) DB-210 × BPX-90 column combinations. (Compound identifications correspond to
designations in Table 1 Suppl.)

Chapter 6. Vapor- and Aerosol-Phase Atmospheric Organic Matter in the Midwestern United States: Methods and Measurements

Rosa M. Flores[†] and Paul V. Doskey[*,†,‡,§]

[†]Department of Civil and Environmental Engineering, Michigan Technological University, Houghton, Michigan 49931, United States
[‡]School of Forest Resources and Environmental Science, Michigan Technological University, Houghton, Michigan 49931, United States
[§]Atmospheric Sciences Program, Michigan Technological University, Houghton, Michigan 49931, United States

ABSTRACT

The high-volume (hi-vol) sampling method with XAD-2 resin was implemented, and sample processing and analytic methods were developed to evaluate temporal and diurnal trends in semivolatile aliphatic and aromatic hydrocarbons (HSVOCs) and functionalized organic aerosol (OA) species in St. Louis, Missouri. The regional atmospheric burden of secondary aerosol is large and principal sources of secondary OA (SOA) precursors and OA include the Ozark Forest and vehicle emissions. The OA and HSVOCs were collected on a quartz fiber filter and XAD-2 resin, respectively, in a hi-vol sampler operating at 200 L min^{-1}. Average recoveries of n-alkanes and polyaromatic hydrocarbons (PAHs) by Soxhlet extraction of XAD-2 resin with dichloromethane were 80.1 ± 16.1 and $76.1 \pm 17.5\%$, respectively. Low recoveries were observed for C_{10}-C_{20} n-alkanes PAHs with 2 aromatic rings (i.e., naphthalene, fluorene, acenaphthene) that were attributed to losses during rotary evaporation of extracts. Silanization of glassware was necessary for quantitative recovery of functionalized OA species. Average recoveries by Soxhlet extraction with an equal mixture of dichloromethane and methanol were $74.5 \pm 21.8\%$ for model compounds grouped according to the following: (1) –OH, (2) –COOH, (3) C=O and –COOH, (4) C=O and –OH, and (5) –COOH and –OH. Samples were analyzed by GC × GC with time-of-flight mass spectrometric (ToF-MS) detection. Method detection limits for HSVOCs and functionalized OA species were 0.012 and 0.013 ng m^{-3}, respectively, for a 35 m^3 ambient air sample. Vehicle emissions were the common source for HSVOCs [i.e., resolved alkanes, the unresolved complex mixture (UCM), alkylbenzenes, and 2- and 3-ring PAHs]. Ratios of average concentrations at 1000-1400 and 0600-1000 for alkylbenzenes, resolved n-alkanes, and the UCM were 0.26, 0.50, and 0.79 and appeared to correlate with OH reactivity. Average concentrations of monoterpenes and their oxidation products (i.e., monoterpenoids) were correlated on 2 of the 5 sampling days when emissions from the Ozark Forest were likely transported to the St. Louis metropolitan area. Diurnal trends indicated a balance between emissions and photochemical oxidation during the day. An absence of monoterpenes at 0600-1000 and

high concentrations of monoterpenoids during the same period was indicative of substantial losses of monoterpenes overnight and the early morning hours. Post-collection, comprehensive organic molecular characterization of SOA precursors and products by GC × GC-ToF-MS in ambient air collected with ~2 hr resolution is a promising method for determining biogenic and anthropogenic SOA yields that can be used to evaluate SOA formation models.

KEYWORDS

Semivolatile organic compounds, secondary organic aerosol, St. Louis-Midwest Supersite, Biogenic emissions, Vehicle emissions.

6.1. Introduction

Approximately 90% of fine aerosol ($PM_{2.5}$) in major urban areas of the Upper Midwest has a regional component with a sizable fraction attributed to secondary production. A source attribution of $PM_{2.5}$ in St Louis indicated 51-60% was contributed by regional sources of secondary sulfate (SO_4^{-2}) and nitrate and biomass burning, 17-26% by gasoline- and diesel-powered vehicles, 16-18% by local industrial plants including zinc/lead smelting, copper production and steel processing, and 3% by airborne soil with Saharan dust influences. The secondary SO_4^{-2} factor was characterized by high concentrations of SO_4^{-2}, ammonium, and organic carbon (OC), particularly in summer during elevated photochemical activity. The contribution of SOA to particle OC (POC) was 20-70% from July to November with the highest contribution occurring during July when isoprene was responsible for 70% of the SOA.

Precursors of secondary organic aerosol (SOA) are generated by biogenic and anthropogenic sources. The Ozark Forest is an important source of biogenic SOA precursors like isoprene (> 150 mg m^{-2} d^{-1}), monoterpenes (10-40 mg m^{-2}d^{-1}), and sesquiterpenes (10-40 mg m^{-2}d^{-1}) *(3)*. Vehicle emissions are the principal source of fine-mode primary OA (POA), volatile organic compounds (VOCs) like monoaromatic hydrocarbons, and a complex mixture of $C_{11} - C_{31}$ normal, branched, cyclic, and aromatic hydrocarbons that are considered vapor-phase, semivolatile OCs (SVOCs). The POA of biogenic and anthropogenic origin (BPOA and APOA, respectively) is a complex mixture of *n*-alkanes, *n*-alkanols, *n*-fatty acids, sugars, and polyaromatic hydrocarbons (PAHs) that are characteristic of the source. Biogenic and anthropogenic VOCs (BVOCs and AVOCs, respectively) and hydrocarbon-like SVOCs (HSVOCs) react rapidly with hydroxyl (OH) and nitrate (NO_3) radicals and ozone (O_3) producing a complex mixture of SOA species with nitrate ($-ONO_2$), carboxylic acid (-COOH), alcohol (-OH), and carbonyl (C=O) functionalities and multi-functionalities.

Considerable uncertainty exists in predicting SOA formation on regional scales and is related to the following: (1) an incomplete understanding of the atmospheric transformation of biogenic-derived organic matter by anthropogenic emissions of oxidants and gas- and aerosol-phase substances, (2) an incomplete characterization of biogenic and anthropogenic sources of SOA precursors, and (3) uncertainties in the seasonal and diurnal variability of SOA precursors and oxidation products. Chamber experiments have been useful in developing reaction mechanisms for SOA formed through oxidation of biogenic and anthropogenic precursors and in identifying oxidation products and deriving yields. To reduce model complexity and evaluate SOA models, SOA species are typically grouped by volatility and chamber-derived yields of the groupings are compared with non-specific, ambient measurements of the mass of oxygenated species in OA (e.g., *(6-8)*). Discrepancies are large between SOA yields predicted using modeling approaches that are based on chamber experiments and yields derived through non-specific, ambient measurement of OA species. Models that use molecular data for SOA precursors and oxidation products show promise in reducing uncertainties in predicting SOA formation *(9)*. However, comprehensive measurement of organic molecular composition of SOA precursors and oxidation products under a variety of environmental conditions with sufficient temporal resolution to determine ambient yields are few.

The short lifetime and wide range of physicochemical properties (particularly vapor pressure) exhibited by the complex mixture of POA and SOA precursors and oxidation products complicate sampling, processing, and analysis of OA. Rapid sampling techniques and sensitive analytic methods that resolve, identify, and quantify the complex mixture of precursors and oxidation products are required to understand SOA formation pathways and to determine OA yields. Rapidly reacting BVOCs like isoprene and α-pinene, which are present in urban atmospheres near biogenic sources at levels in the 10's of pptv, have OH rate constants of 100×10^{-12} and 54×10^{-12} cm^3 molecule^{-1} s^{-1}, respectively, lifetimes of about 22-41 min, and are typically collected in Summa$^{®}$

passivated canisters in sampling periods that are about 5 min in duration. Vapor-phase C_{11}-C_{21} n-alkanes and 2- and 3-ring PAHs, which are estimated to be present at 20-200 pptv in urban air, have OH rate constants of 20 x 10^{-12} and 40×10^{-12} cm^3 molecule^{-1} s^{-1}, respectively, lifetimes of about 1-2 hr, and (due to vapor pressures that are much lower than the VOCs) are typically collected on a solid sorbent downstream of a glass fiber filter that collects aerosol. Sampling periods for VOCs and HSVOCs must be similar to time scales of chemical reactivity for unambiguous observation of atmospheric dynamics. The high-volume (hi-vol) sampling technique that uses 35 g of XAD-2 resin to collect vapor-phase SVOCs has a breakthrough volume of about 25,000 m^3 for n-C_{11}. Changes in temperature, relative humidity, and HSVOC mixing ratios during hi-vol sampling alter vapor-particle partitioning of the collected aerosol and are minimized when sampling periods are short in duration.

Soxhlet extraction using various solvents is a proven technique for extracting SVOCs from aerosols on glass fiber filters and vapors adsorbed to XAD-2 resin. The solvent is typically reduced by rotary evaporation, the analytes derivatized to facilitate transfer through the gas chromatographic (GC) system and to reduce ambiguities in compound identification by mass spectrometry (MS), and the complex mixture resolved by high-resolution GC with MS detection. However, multidimensional GC, due to the ability to resolve complex mixtures of organic compounds according to molecular volume and functionality, is now becoming the GC method of choice for organic molecular characterization of atmospheric organic matter.

Here we report implementation of the hi-vol sampling technique with XAD-2 resin and development of an analytical method for comprehensive organic molecular characterization of HSVOCs and OA. Samples were collected over 4- or 5-hr intervals during the day and in 11-hr intervals overnight over a 5-day period during August 2011 at the St. Louis – Midwest Supersite (East St. Louis, MO). Post-collection analysis was by Soxhlet extraction with derivatization of functionalized species prior to

comprehensive separation and identification by GC × GC with time-of-flight MS (ToF-MS). Details of the sampling and analytic method are given and extraction efficiencies, reproducibilities, and method detection limits are presented. Temporal and diurnal trends in concentrations of HSVOCs and functionalized OA species are presented and discussed.

6.2. Experimental Methods

6.2.1. Chemicals and solvents.

Standards of the highest purity were purchased from Sigma-Aldrich Chemical Co. (St. Louis, MO), with exception of dicarbonyls dihydroxyacetone, pyruvic acid, and hydroxybenzaldehyde, which were purchased from MP Biomedicals (Santa Ana, CA) and Wako Chemicals (Richmond, VA). All solvents were specified for GC analysis and were purchased from Burdick and Jackson (Muskegon, MI). The glassware silanizing agent (1-5% 1,7-Dichloro-1,1,3,3,5,5,7,7-octamethyltetrasiloxane in heptane; SIGMACOTE®) and derivatizing reagents, methoxyamine hydrochloride (MHA), (Trimethylsilyl)diazomethane (TMSD), and 1% (trimethylchlorosilane) TMCS in N,O-bis(trimethylsilyl)-trifluoroacetamide (BSTFA) (v/v), were also obtained from Sigma-Aldrich. Ultrahigh purity gases 99.999 % were obtained from Superior Water & Welding (Chassell, MI).

6.2.2. Sample Collection.

The St. Louis – Midwest Supersite (East St. Louis, MO) is located 3 km east of St. Louis near interstate highways and approximately 15 km to the northeast of the Ozark Mountain region. Ambient air samples were collected over 4- or 5-hr intervals during the day (0600-1900) and overnight (1900-0600) from Monday, August 22 to Friday, August 25, 2011. Aerosol- and vapor-phase organic matter were collected on 20.3 × 25.4 cm^2 quartz fiber filters (Tisch Environmental, Cleves, OH) and 35 g of Amberlite

XAD-2 polymeric adsorbent (Sigma-Aldrich) with a Tisch PNY1123 hi-vol at 0.1 - 0.2 m^3 min^{-1} Sample volumes averaged 35 m^3 during the day and 99 m^3 overnight. The sampler was located on the roof of a trailer about 10 m above the surface. A high-pressure system with light, variable winds from the N, NE, S, and SE dominated the meteorology during the sampling period. Temperatures ranged from 16.6 to 36.6°C with daily average relative humidities of 42 to 64%. A light precipitation event of 2.03 mm was observed on Monday at 0800.

6.2.3. Glassware Preparation.

Glassware that contacted concentrated extracts (i.e., centrifuge tubes and round-bottomed and pear-shaped flasks for rotary evaporation) was carefully cleaned and silanized. The glassware was washed with soap in preparation for silanization, rinsed with deionized water, dried overnight (70°C), rinsed with a 1:1 solution of hydrochloric acid and methanol (MeOH) for 30 min, rinsed with deionized water, and dried overnight (70°C). The chlorinated organopolysiloxane, silanizing agent was applied by liquid deposition, dried (100°C) for 60 min, rinsed with deionized water, and dried (70°C) overnight.

6.2.4. Sample processing.

The HSVOCs were isolated from XAD-2 by Soxhlet extraction with dichloromethane (DCM). Volumes of extracts in round-bottomed flasks were reduced to approximately 30 mL by rotary evaporation (35°C, 750 mm Hg), transferred to pear-shaped flasks, and further reduced to 2 mL. The 2 mL extracts were transferred to 5 ml centrifuge tubes, filtered and dried through sodium sulfate powder (activated at 500°C and stored in a dessicator) in a Pasteur pipette, and slowly reduced to 500 μL with ultrahigh purity nitrogen, and stored at 4°C.

Whole quartz fiber filters were cut into strips with a scalpel, placed in glass thimbles, and Soxhlet extracted for 24 hr with 300 ml of 1:1 (v/v) DCM/MeOH or DCM/acetonitrile (ACN). Volumes of filter extracts in round-bottom flasks were reduced to 30 mL by rotary evaporation($35°C$, 735 mm Hg), the extract transferred to pear-shaped flasks and further reduced to 2 mL($35°C$, 400 mm Hg), transferred to centrifuge tubes, slowly evaporated to dryness with a gentle stream of ultrapure nitrogen, and stored at $4°C$ until derivatization. The 3-step derivatization technique is reported elsewhere *(12)*. Briefly, C=O functionalities were converted to methyl oximes with 20 µL of MHA in ACN and reacted at $70°C$ for 60 min. In step 2, -COOH moieties were converted to methyl esters with 6 µL of TMSD and 3.4 µL of MeOH and the reaction assisted by ultrasonication for 20 min. The –OH functionalities are converted to TMS ethers in step 3 with 180 µL of BSTFA and reacted at $70°C$ for 60 min.

6.2.5. GC-MS analysis.

Aerosol and XAD-2 extracts were analyzed on a Leco Pegasus 4D GC × GC-ToF-MS (St Joseph, MI). Analyses were performed on a 30 m × 0.25 mm ID (primary) column coated with a 0.25-µm-film thickness of (50%-Trifluoropropyl)-methylpolysiloxane (DB-210; Agilent Technologies, Santa Clara, CA) connected in series with a 10 m × 0.10 mm ID (secondary) column coated with 0.10-µm-film thickness of Polyethylene Glycol in a Sol-Gel matrix (SolGel-WAX; SGE Analytical Science, Austin, TX) (Chapter 5). Flow of He through the column was 1.0 ml min^{-1}. Mass spectra were collected from 25-500 amu at 200 Hz.

Aliquots of XAD-2 extracts (1 µL) were injected into the deactivated glass inlet liner of a programmable temperature vaporization inlet (PTV; Gerstel, Linthicum, MD) packed with silanized glass wool. The extract was injected into the PTV in the solvent vent mode with helium flowing through the vent at 3 mL min^{-1} for 12 s. The purge valve was opened after 72 s and the inlet was purged at 80 ml min^{-1}. The PTV was operated at 152

kPa and held at 50°C for 0.2 min after injection and the temperature rapidly increased to 240°C at 12°C s^{-1} to transfer analytes to the DB-210 column. Temperature of the GC oven was held at 50°C for 1 min, increased to 240°C at 12°C min^{-1}, and the temperature held for 14 min. Temperatures of the secondary column oven and modulator were offset at 10 and 5°C, respectively, with respect to the temperature of the primary and secondary ovens, respectively. Modulation times were 0 and 6 s for GC- and GC×GC-ToF-MS analyses, respectively.

Aliquots of derivatized aerosol extracts (2.8 μL) were injected in the solvent vent mode into the deactivated glass inlet liner of the PTV packed with silanized glasswool and a 20-mm-thick bed of 10% Carbowax 20M on Chromosorb W-AW (Ohio Valley Specialty, Marietta, OH). Solvent and purge vent flows were 50 and 80 mL min^{-1}, respectively. Duration of the solvent vent mode was 12 s and the purge valve was opened 72 s after injection. The PTV was operated at 72.4 kPa and held at 60°C for 0.2 min after injection and increased in temperature to 230°C at 12°C s^{-1} to transfer the analytes to the primary column. Temperature of the GC oven was held at 60°C for 1 min after injection, increased to 230°C at 5.5°C min^{-1}, and the temperature held for 3 min. Temperatures of the secondary column oven and modulator were offset at 5°C and 3°C, respectively, relative to the temperature of the primary and secondary ovens, respectively. Modulation times were 0 and 6 s for GC- and GC×GC-ToF-MS analyses, respectively.

6.2.6. Method Detection Limits and Quantification.

Method linearity and sensitivity were investigated with 5-point calibrations using standard solutions of *n*-alkanes and PAHs at concentrations of 0.2-24.0 ng μL^{-1}, equivalent to 0.057-0.685 ng m^{-3} assuming 35 m^3 of air were sampled per measurement period. Each point of the calibration curve expressed as peak area is the average of six replicate analyses. Regression parameters were calculated by the least squares method

using a second-order polynomial fit of the calibration curves. Detection limits (X_{LOD}) were calculated as $3y_b \, m^{-1}$, where y_b is the standard deviation of 6 replicate analyses of the lowest point of the calibration curve (i.e., the response for an injection of 2 ng of analyte), and m is the slope of the calibration curve.

Quantification of analytes was performed by using calibration curves of compounds with similar functionalities and retention times, as follows: (1) n-alkanes, alkyl hydrocarbons, and alkylbenzenes with n-alkanes, (2) the unresolved complex mixture (UCM) with n-octadecane, (3) PAH with fluorene, (4) monoterpenes ($C_{10}H_{16}$) with limonene, (5) monoterpenoids ($C_9H_{14}O$ and $C_{10}H_{16}O$) with nopinone. Solutes identified in aerosol were separated into seven groups according to type and number of functionalities and were quantified as follows: (1) n-alkanoic acids with dodecanoic acid, (2) n-alkadioic acids with C_5-C_{10} dicarboxylic acids, (3) straight chain hydrocarbons with -COOH and C=O functionalities with ketoglutaric acid, (4) straight chain hydrocarbons with 4-5 –OH moieties, with meso-erythritol, (5) cyclic hydrocarbons with 3 –OH and C=O functionalities with levoglucosan, (6) aromatic hydrocarbons with –COOH substitutions with p-toluic acid, and (7) aromatic hydrocarbons with –OH and –COOH moieties with 4-hydroxybenzoic acid.

6.3. Results and Discussion

6.3.1. Extraction Efficiencies and Method Detection Limits for *n*-Alkanes and PAH.

Reproducibility and extraction efficiency were evaluated by analyzing 5 replicates of 800 ng of n-alkanes (C_{10} - C_{31}) and 800 ng of 2- and 3-ring PAHs (naphthalene, acenaphthene, fluorene, phenanthrene, anthracene, fluoranthene, and pyrene) (Table 1) and 600 ng of oxygenated analytes characteristic of OA, respectively, applied to quartz fiber filters (Fig. 1). Method reproducibility was determined as the relative standard deviation (RSTD %) of 5 replicate analyses. Extraction efficiencies were evaluated by

comparing analyte responses (i.e., peak areas) to responses of the analyte in a standard mixture analyzed in triplicate. Average recoveries of n-alkanes and PAH were 80.1±16.1 and 76.1±17.5%, respectively, and varied with compound vapor pressure. The $C_{10} - C_{12}$ and a fraction of the C_{13} - C_{20} n-alkanes were not resolved from the solvent front and were lost out the purge vent, respectively, which is related to the PTV injection technique. Thus, extraction efficiencies were corrected for injection losses. Exchanging the extract solvent with i-octane and splitless injection at 30°C below the boiling point (70°C) to concentrate analytes at the head of the primary column would improve resolution. Low recoveries of C_{10}-C_{20} n-alkanes, naphthalene, fluorene, and acenaphthene, which are the most volatile of the n-alkanes and PAHs, are likely due to losses during solvent reduction by rotary evaporation. Solvent reduction with a Kuderna-Danish concentrator has proven to be an effective method for quantitative recovery of the species. The PAHs with 4-rings or more (e.g., chrysene; boiling point 448°C) were not recovered since the maximum temperature of the SolGel-WAX column is 240°C. Method detection limits of n-alkanes and 2- and 3-ring PAHs were 0.08 - 0.83 ng μL^{-1} (0.002 - 0.023 ng m^{-3}) and 0.08 - 0.96 ng μL^{-1} (0.002 - 0.027 ng m^{-3}), respectively (Table 1). Correlation coefficients for calibration curves had R^2 values > 0.99.

Recoveries of OA species were determined for extraction and solvent reduction steps for samples processed in untreated glassware. Model compounds are separated into groups by functionalities according to the following: (1) –OH, (2) –COOH, (3) C=O and –COOH, (4) C=O and –OH, and (5) –COOH and –OH. The 3-step derivitization procedure reported by Flores (12) was used in the experiments. Recoveries were determined for the entire procedure using a 1:1 (v/v) mixture of MeOH/DCM, rotary evaporation, and solvent reduction to dryness with nitrogen. Results of the experiments (performed in triplicate) are shown in Fig. 1. About 20.0% of the model compounds were lost during solvent reduction to dryness with nitrogen. Recoveries from rotary evaporation and the entire procedure were approximately 30, and 13%, respectively,

and indicated the bulk of the losses were attributed to the rotary evaporation step. Compounds containing 2 or more –COOH functionalities (i.e., dodecanedioic acid, cyclobutane tetracarboxylic acid, benzene tricarboxylic acid, 2-ketoglutaric acid, gallic acid, and tartaric acid) exhibit recoveries < 5.0% from rotary evaporation.

Recoveries were determined for the entire procedure using DCM and a mixture of 1:1 (v/v) DCM/ACN as extraction solvents and untreated and silanized glassware. The average recovery from untreated glassware was 42.1% for all compounds when DCM/ACN was used as the extraction solvent (Fig. 2). Replacing MeOH with ACN improved average recoveries of compounds containing –COOH from 18.3 to 35.7%, which is likely attributed to higher solubility in ACN. However, carboxylic acids containing 7 or more carbons atoms and 2 or more –COOH moieties were not recovered. Hydroxybenzaldehyde and dihydroxyacetone were completely recovered when DCM/ACN was the extraction solvent. The average recovery of carboxylic acids increased from 35.7 to 39.1% when silanized glassware was used and DCM/ACN was the solvent mixture; however the average recovery of all compounds was fairly similar for silanized and untreated glassware (Fig. 2). Compounds with C=O functionalities, which are the most volatile substances in the model compound mixture exhibited lower recoveries when silanized glass was used. Loses likely occur during rotary evaporation or solvent reduction to dryness using nitrogen. The average recovery improved to 74.5 ± 21.8% by replacing ACN with MeOH and using silanized glass.

6.3.2. Temporal Trends in HSVOCs, Monoterpenes, and Monoterpenoids.

Diurnal trends in average concentrations of the UCM and resolved alkanes were similar (with the exception of Tuesday) and diminished throughout the day (starting with the 0600 sampling period) and continued overnight (Fig. 3a). Highest average concentrations of resolved alkanes (i.e., those eluting above the UCM) were observed at 0600-1000 on Wednesday (0.516 ng m^{-3}) and Friday (0.432 ng m^{-3}) when winds were 8.7 m s^{-1} and variable from the south to west at 4.6 m s^{-1} and from the northeast,

respectively. Lowest levels of resolved alkanes were observed on Monday at 1000-1400 (0.097 ng m^{-3}) during a peak in radiation intensity and also on Tuesday at 0600-1000 (0.102 ng m^{-3}) when winds were prevalent from the south (frequency = 60%) and from the south/southeast (frequency = 35%) at a maximum of 8.7 m s^{-1}. Highest concentrations of the UCM were found at 0600-1000 on Wednesday (4.60 ng m^{-3}) and Thursday (4.68 ng m^{-3}) and lowest levels at 1900-0600 on Monday (1.22) and Wednesday (1.49 ng m^{-3}). The UCM is a complex mixture of branched and cyclic aliphatic hydrocarbons *(19,20)* that cannot be resolved by high-resolution GC techniques. Both the UCM and resolved alkanes also have origins in vehicle emissions and petroleum residues released by refineries; however, the resolved alkane/UCM ratio is lower in vehicle emissions. The correlation coefficient between the UCM and the alkanes was 0.820 and might indicate a fraction of the emissions has a refinery origin. The diurnal trend is attributed to vehicular emissions during the morning rush hour and losses due to photochemical oxidation throughout the day by OH and during the night by NO_3.

Similar to diurnal trends in average concentrations of the UCM and resolved alkanes, average concentrations of alkylbenzenes diminished throughout the day (starting with the 0600 sampling period) and continued overnight (Fig. 3a). Like the UCM and resolved alkanes, lack of a diurnal trend on Tuesday was also observed for alkylbenzenes. Highest concentrations of alkylbenzenes were observed on at 0600-1000 on Monday (0.187 ng m^{-3}) and Thursday (0.225 ng m^{-3}). Diurnal trends in PAHs were similar to the other HSVOCs; however, highest concentrations were observed at 0600-1000 on Thursday (0.225 ng m^{-3}, respectively) and Friday (0.213 ng m^{-3}). Alkylbenzenes and PAHs are emitted by vehicles *(20)* and followed the same trend as resolved alkanes. However, lifetimes of alkylbenzenes with respect to reaction with OH are much shorter than the resolved n-alkanes and PAHs without alkyl substitutions *(21)*. The unsubstituted PAHs like benzene are susceptible to oxidation by O_3 *(21)*, and thus, levels of alkylbenzenes decreased more rapidly at 1000-1400. Ratios of average

concentrations observed at 1000-1400 to levels at 0600-1000 for the alkylbenzenes, resolved alkanes, and UCM were 0.26, 0.50, and 0.79, and appear to correlate with OH reactivity; however, the bulk of species in the UCM might be more resistant to oxidation and have a greater atmospheric lifetime. The common source for the HSVOCs is vehicle emissions; however, PAHs are low in abundance in emissions from petroleum refineries. Diurnal trends in the UCM and PAHs on Tuesday were dissimilar and might indicate a contribution of petroleum refinery emissions to UCM concentrations.

Monoterpenes were sporadically observed during the entire week of sampling (Fig. 3b). Average concentrations diminished slightly on Tuesday when they were observed starting with the 1000-1400 sampling period. They were observed more frequently on Tuesday and Wednesday when winds were predominantly from the south and southwest, which might transport terpene emissions from the region of the Ozark Forest. Average concentrations of the Σ monoterpenoids ($C_9H_{16}O + C_{10}H_{16}O$) were highest starting at 1000-1400 on Tuesday. A balance between monoterpene production in the Ozark Forest and transport to St. Louis was likely responsible for measurable levels of the monoterpenes during the day on Tuesday and Wednesday. Monoterpene emissions from specialized storage sites in conifers are largely dependent on temperature, and thus, transport overnight to the St. Louis metropolitan was likely. Reaction with NO_3 overnight might have diminished levels to below detection by 0600-1000 on Wednesday. Winds continued from the southeast on Wednesday and levels of monoterpenes increased during the 1000-1400 sampling period and diminished thereafter. Reaction of monoterpenes with NO_3 is much more rapid than reaction with OH. The highest concentration of monoterpenes was observed overnight on Friday (10.5 ng m^{-3}); however, monoterpenes were not observed during the day. Local emissions into a diminished overnight boundary layer might be responsible for elevated levels during the night.

6.3.3. Temporal Trends in Functionalized OA Species

Temporal and diurnal variations of average concentrations of functionalized OA species are presented in Fig. 4. Monoterpenoids that are products of monoterpene oxidation were correlated on Tuesday and Wednesday (Fig. 3b). The *n*-alkanoic acids are present in vehicle emissions and plant waxes sloughed from vegetation and can also be formed in the atmosphere through photochemical oxidation. Trends were somewhat similar to the resolved alkanes (Fig. 3a) on Monday and Wednesday, which might indicate a common vehicle emission source on those days. Correlations of other functionalized OA species with HSVOCs (Fig. 3a), which are the suspected precursors, were not obvious. The functionalized OA species might be products of several generations of oxidation of VOCs, and thus, a lack of correlation with the HSVOCs might be expected.

6.3.4. GC × GC-ToF-MS Capabilities.

To demonstrate the superior capabilities of comprehensive, multidimensional GC, XAD-2 and aerosol extracts were analyzed for HSVOCs and functionalized OA species, respectively, by GC and GC × GC with ToF-MS. The maximum UCM concentration was observed at 1400-1900 on Tuesday. As observed by others, a typical high-resolution GC analysis was unable to resolve the bulk of species in the UCM (Fig. 5). However, about 258 HSVOCs were observed in the total ion GC × GC chromatogram of the UCM (Fig. 5) and tentative identification of 99 compounds was possible with the NIST Mass Spectral Library using a similarity point of 70 % as the criteria for identification. In addition to branched aliphatics, the UCM was also composed of homologous series of alkyl PAH, alkyl benzenes, and branched cyclic aliphatics, which is in agreement with observations by others *(19,20)*. Functionalized HSVOCs (i.e., oxygen- and nitrogen- containing species) were also observed (Fig. 5), which has implications for estimating chemical reactivity of the UCM. When analysis by GC × GC-ToF-MS is unavailable, the deconvolution capability of other MS analyzers allows focusing on single compounds based on characteristic fragment ions; however, in some

cases, analytes are not resolved using the technique and GC × GC-ToF-MS is necessary. For example, C_5-C_{10} *n*-alkanoic acids (m/z 60) are resolved using GC × GC and unresolved by conventional GC (Fig. 6). Post-collection, comprehensive organic molecular characterization of SOA precursors and products by GC × GC-ToF-MS in ambient air collected with ~2 hr resolution is a promising method for determining biogenic and anthropogenic SOA yields that can be used to evaluate SOA formation models.

6.4. Acknowledgments

6.5. References

(1)   Seinfeld, J. H.; Pankow, J. F. Organic Atmospheric Particulate Material. *Annu. Rev. Phys. Chem.* **2003**, *54*, 121.

(2)   Pankow, J. F.; Luo, W.; Melnychenko, A. N.; Barsanti, K. C.; Isabelle, L. M.; Chen, C.; Guenther, A. B.; Rosenstiel, T. N. Volatilizable biogenic organic compounds (VBOCs) with two dimensional gas chromatography-time of flight mass spectrometry (GC × GC-TOFMS): sampling methods, VBOC complexity, and chromatographic retention data. *Atmos. Meas. Tech. Discuss.* **2011**, *4*, 3647-3684.

(3)   Guenther, A.; Karl, T.; Harley, P.; Wiedinmyer, C.; Palmer, P. I.; Geron, C. Estimates of global terrestrial isoprene emissions using MEGAN (Model of Emissions of Gases and Aerosols from Nature). *Atmos. Chem. Phys.* **2006**, *6*, 3181-3210.

(4)   Tani, A.; Hayward, S.; Hansel, A.; Hewitt, C. N. Effect of water vapour pressure on monoterpene measurements using proton transfer reaction-mass spectrometry (PTR-MS). *Int. J. Mass Spectrom.* **2004**, *239*, 161-169.

(5)   Calogirou, A.; Larsen, B. R.; Kotzias, D. Gas-phase terpene oxidation products: a review. *Atmos. Environ.* **1999**, *33*, 1423-1439.

(6)   Liao, H.; Henze, D. K.; Seinfeld, J. H.; Wu, S.; Mickley, L. J. Biogenic secondary organic aerosol over the United States: Comparison of climatological simulations with observations. *J. Geophys. Res.* **2007**, *112*, D06201.

(7)   Chung, S. H.; Seinfeld, J. H. Global distribution and climate forcing of carbonaceous aerosols. *J. Geophys. Res.* **2002**, *107*.

(8)   Donahue, N. M.; Robinson, A. L.; Stanier, C. O.; Pandis, S. N. Coupled Partitioning, Dilution, and Chemical Aging of Semivolatile Organics. *Environ. Sci. Technol.* **2006**, *40*, 2635-2643.

(9)   Chang, E. I.; Pankow, J. F. Organic particulate matter formation at varying relative humidity using surrogate secondary and primary organic compounds

with activity corrections in the condensed phase obtained using a method based on the Wilson equation. *Atmos. Chem. Phys.* **2010**, *10*, 5475-5490.

(10)   Jaoui, M.; Kleindienst, T. E.; Lewandowski, M.; Offenberg, J. H.; Edney, E. O. Identification and Quantification of Aerosol Polar Oxygenated Compounds Bearing Carboxylic or Hydroxyl Groups. 2. Organic Tracer Compounds from Monoterpenes. *Environ. Sci. Technol.* **2005**, *39*, 5661-5673.

(11)   Kowalewski, K.; Gierczak, T. Multistep derivatization method for the determination of multifunctional oxidation products from the reaction of α-pinene with ozone. *J. Chromatogr., A.* **2011**, *1218*, 7264-7274.

(12)   Flores, R. M.; Doskey, P. V. Comparison of Multistep Derivatization Methods for Identification and Quantification of Oxygenated Species in Organic Aerosol. **In review**.

(13)   Beyer, M.; Felgenhauer, T.; Ralf Bischoff, F.; Breitling, F.; Stadler, V. A novel glass slide-based peptide array support with high functionality resisting non-specific protein adsorption. *Biomaterials.* **2006**, *27*, 3505-3514.

(14)   Seed, B. In *Current Protocols in Immunology*; John Wiley & Sons, Inc., 2001.

(15)   Labit, H.; Goldar, A.; Guilbaud, G.; Douarche, C.; Hyrien, O.; Marheineke, K. A simple and optimized method of producing silanized surfaces for FISH and replication mapping on combed DNA fibers. *BioTechniques.* **2008**, *45*, 649-652.

(16)   Cras, J.; Rowe-Taitt, C.; Nivens, D.; Ligler, F. Comparison of chemical cleaning methods of glass in preparation for silanization. *Biosensors and bioelectronics.* **1999**, *14*, 683-688.

(18)   Lewandowski, M.; Jaoui, M.; Offenberg, J. H.; Kleindienst, T. E.; Edney, E. O.; Sheesley, R. J.; Schauer, J. J. Primary and Secondary Contributions to Ambient PM in the Midwestern United States. *Environ. Sci. Technol.* **2008**, *42*, 3303-3309.

(19)   Schauer, J. J.; Kleeman, M. J.; Cass, G. R.; Simoneit, B. R. Measurement of emissions from air pollution sources. 2. C1 through C30 organic compounds from medium duty diesel trucks. *Environ. Sci. Technol.* **1999**, *33*, 1578-1587.

(20)   Schauer, J. J.; Kleeman, M. J.; Cass, G. R.; Simoneit, B. R. T. Measurement of Emissions from Air Pollution Sources. 5. C1−C32 Organic Compounds from Gasoline-Powered Motor Vehicles. *Environ. Sci. Technol.* **2002**, *36*, 1169-1180.

(21)   Seinfeld, J. H.; Pandis, S. N. *Atmospheric Chemistry and Physics. From Air Pollution to Climate Change*; 2nd ed.; Wiley and Sons: Hoboken, New Jersey, 2006.

Table 6.1. Detection limits and Soxhlet extraction efficiencies of *n*-alkanes and polyaromatic hydrocarbons. [Limits of detection (LOD) are for a 35 m^3 air sample.]

Compound	Retention Time (s)	Formula	Molecular Weight	LOD (ng m^{-3})	Recovery (%)	STD (%)
n-Decane	324.34	C$_{10}$H$_{22}$	142.28	0.023	Not resolved	-
n-Undecane	486.65	C$_{11}$H$_{24}$	156.30	0.014	Not resolved	-
n-Dodecane	531.97	C$_{12}$H$_{26}$	170.33	0.007	Not resolved	-
n-Tridecane	583.48	C$_{13}$H$_{28}$	184.36	0.006	21.77	25.92
n-Tetradecane	625.98	C$_{14}$H$_{30}$	198.38	0.009	16.79	13.54
Naphthalene	642.19	C$_{10}$H$_8$	128.17	0.005	1.78	71.07
n-Pentadecane	680.03	C$_{15}$H$_{32}$	212.41	0.016	12.19	25.14
n-Hexadecane	720.05	C$_{16}$H$_{34}$	226.44	0.006	47.15	17.11
n-Heptadecane	762.85	C$_{17}$H$_{36}$	240.46	0.005	73.53	16.00
Acenaphthene	784.55	C$_{12}$H$_{10}$	154.20	0.002	56.23	14.14
n-Octadecane	808.06	C$_{18}$H$_{38}$	254.49	0.004	77.48	16.81
n-Nonadecane	851.73	C$_{19}$H$_{40}$	268.52	0.003	77.96	15.49
Fluorene	869.48	C$_{13}$H$_{10}$	166.21	0.023	53.18	9.67
n-Eicosane	890.81	C$_{20}$H$_{42}$	282.54	0.002	82.39	14.90
n-Heneicosane	931.72	C$_{21}$H$_{44}$	296.57	0.007	93.28	15.33
n-Docosane	968.19	C$_{22}$H$_{46}$	310.60	0.014	93.77	13.32
Phenanthrene	984.44	C$_{14}$H$_{10}$	178.22	0.003	103.15	14.12
Anthracene	994.62	C$_{14}$H$_{10}$	178.22	0.009	80.78	9.36
n-Tricosane	1003.47	C$_{23}$H$_{48}$	324.62	0.007	93.79	14.20
n-Tetracosane	1039.28	C$_{24}$H$_{50}$	338.65	0.013	94.68	15.14

Compound	Retention Time (s)	Formula	Molecular Weight	LOD (ng m^{-3})	Recovery (%)	STD (%)
n-Pentacosane	1077.23	$C_{25}H_{52}$	352.68	0.015	94.26	14.65
n-Hexacosane	1118.54	$C_{26}H_{54}$	366.70	0.017	89.40	14.73
Fluoranthene	1143.03	$C_{16}H_{10}$	202.25	0.012	95.76	9.57
n-Heptacosane	1164.45	$C_{27}H_{56}$	380.73	0.015	88.26	14.34
Pyrene	1170.43	$C_{16}H_{10}$	202.25	0.027	102.59	7.63
n-Octacosane	1217.39	$C_{28}H_{58}$	394.76	0.009	92.71	14.14
n-Nonacosane	1257.63	$C_{29}H_{60}$	408.78	0.022	110.66	14.37
n-Triacontane	1356.59	$C_{30}H_{62}$	422.81	0.019	115.71	16.41
n-Hentriacontane	1453.35	$C_{31}H_{64}$	436.83	0.024	145.11	14.31
Average				**0.012**	**77.475**	**16.977**

Table 6.2. Detection limits and Soxhlet extraction efficiencies of functionalized organic aerosol species. [Limits of detection (LOD) are for a 35 m^3 air sample.]

Compound	Extraction Yield	STD %	MDL (ng m^{-3})	MDL (ng)
Group 1: -OH				
Myrtenol	14.422	45.373	0.012	0.420
meso-Erythritol	85.812	27.346	0.006	0.220
d-Arabitol	139.000	26.437	0.013	0.470
2-Hexadecanol	106.490	13.370	0.006	0.200
Levoglucosan	102.360	21.745	0.003	0.090
Group 2. -COOH				
Citraconic acid	106.284	18.804	NI	NI
P-Toluic acid	73.461	11.523	0.005	0.180
Pentanedioic acid	76.847	21.913	0.044	1.550
Hexanedioic acid	93.956	7.692	0.017	0.595
Dodecanoic acid	86.198	33.044	0.008	0.270
Heptanedioic acid	101.186	18.237	0.006	0.200
Azelaic acid	90.600	18.115	0.022	0.770
Benzene dicarboxylic acid	114.716	24.929	0.013	0.440
Decanedioic acid	97.125	6.076	0.005	0.170
Undecanedioic acid	91.941	12.179	0.005	0.180
Dodecanedioic acid	96.642	42.172	0.007	0.250
1,2,3,4-Cyclobutane tetracarboxylic acid	5.140	11.380	0.006	0.200
1,2,4,-Benzene tricarboxylic acid	83.019	59.853	0.008	0.290
Group 3. C=O, -COOH				
cis-Pinonic acid	71.416	21.043	0.007	0.240
2-Keto-glutaric acid	68.892	22.660	0.004	0.150

Compound	Extraction Yield	STD %	MDL (ng m^{-3})	MDL (ng)
Keto-pinic acid	97.561	8.633	0.018	0.620
Group 4. –COOH, -OH				
Mandelic acid	96.959	12.441	0.013	0.460
Salicylic acid	58.785	26.393	0.008	0.270
L-Tartaric acid	4.554	36.451	0.008	0.270
4-Hydroxy benzoic acid	48.327	3.203	0.007	0.240
Gallic acid	2.011	12.880	0.006	0.200
Group 5. C=O, -OH				
Dihydroxyacetone	50.770	22.272	0.003	0.110
Hydroxybenzaldehyde	73.342	15.970	0.054	1.900
S-S-2-Hydroxy-3-pinanone	7.770	13.460	0.010	0.340
Nopinone	8.611	1.240	0.046	1.617
Average	**71.807**	**20.561**	**0.013**	**0.445**
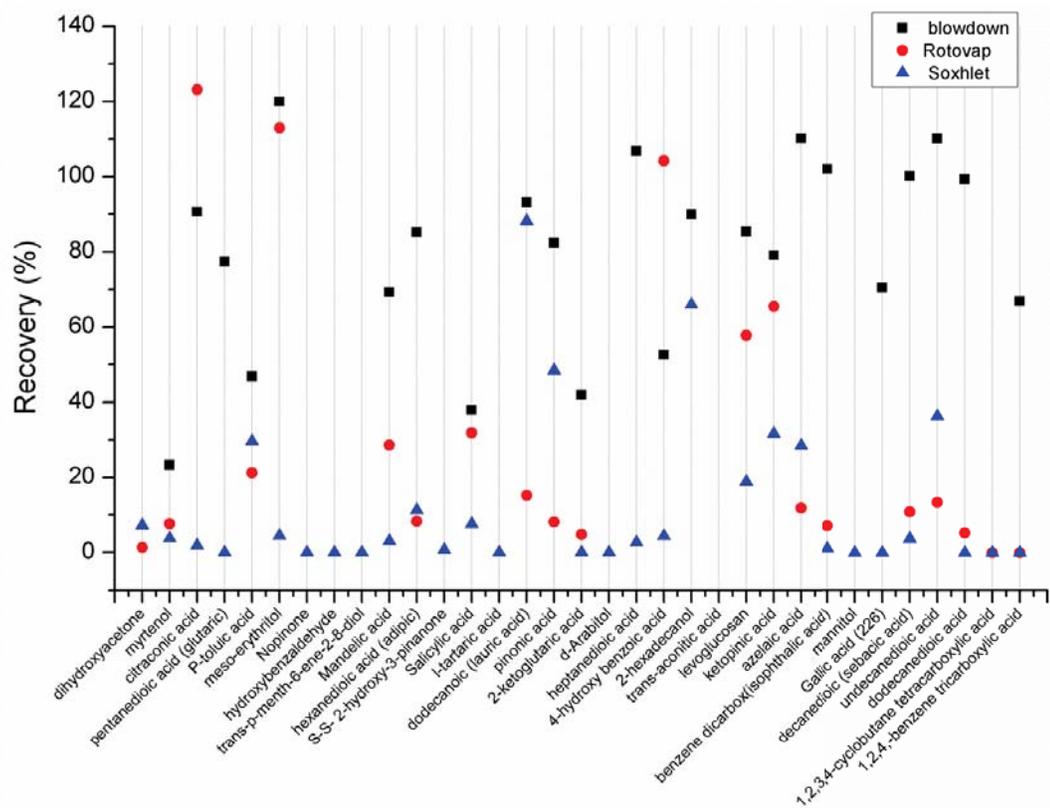
Fig 6.1. Recoveries of SOA model compounds from (1) nitrogen blowdown and (2) rotary evaporation + nitrogen blowdown steps, and (3) the entire method using 1:1 (v/v) dichloromethane and methanol as the Soxhlet extraction solvent. Glassware was untreated.
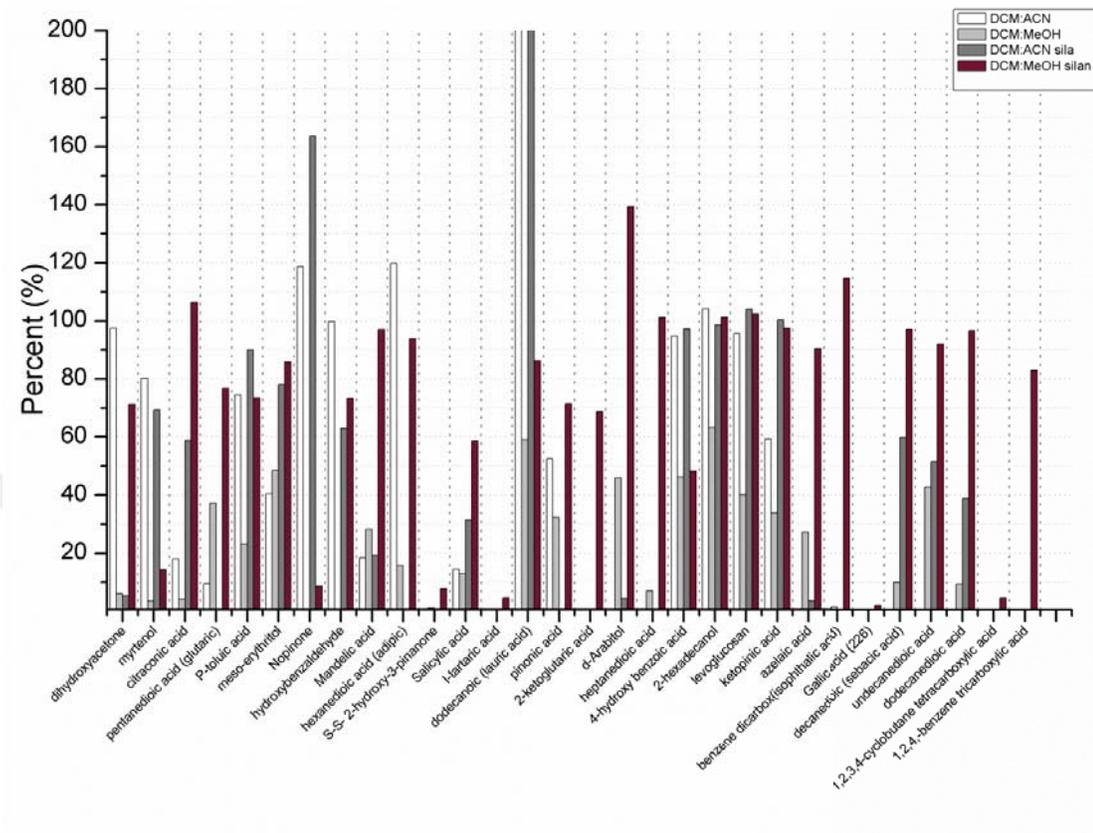
Fig.6.2. Recoveries of SOA model compounds using Soxhlet extraction with 1:1 (v/v) mixtures of dichloromethane and acetonitrile or methanol in untreated and silanized glassware.
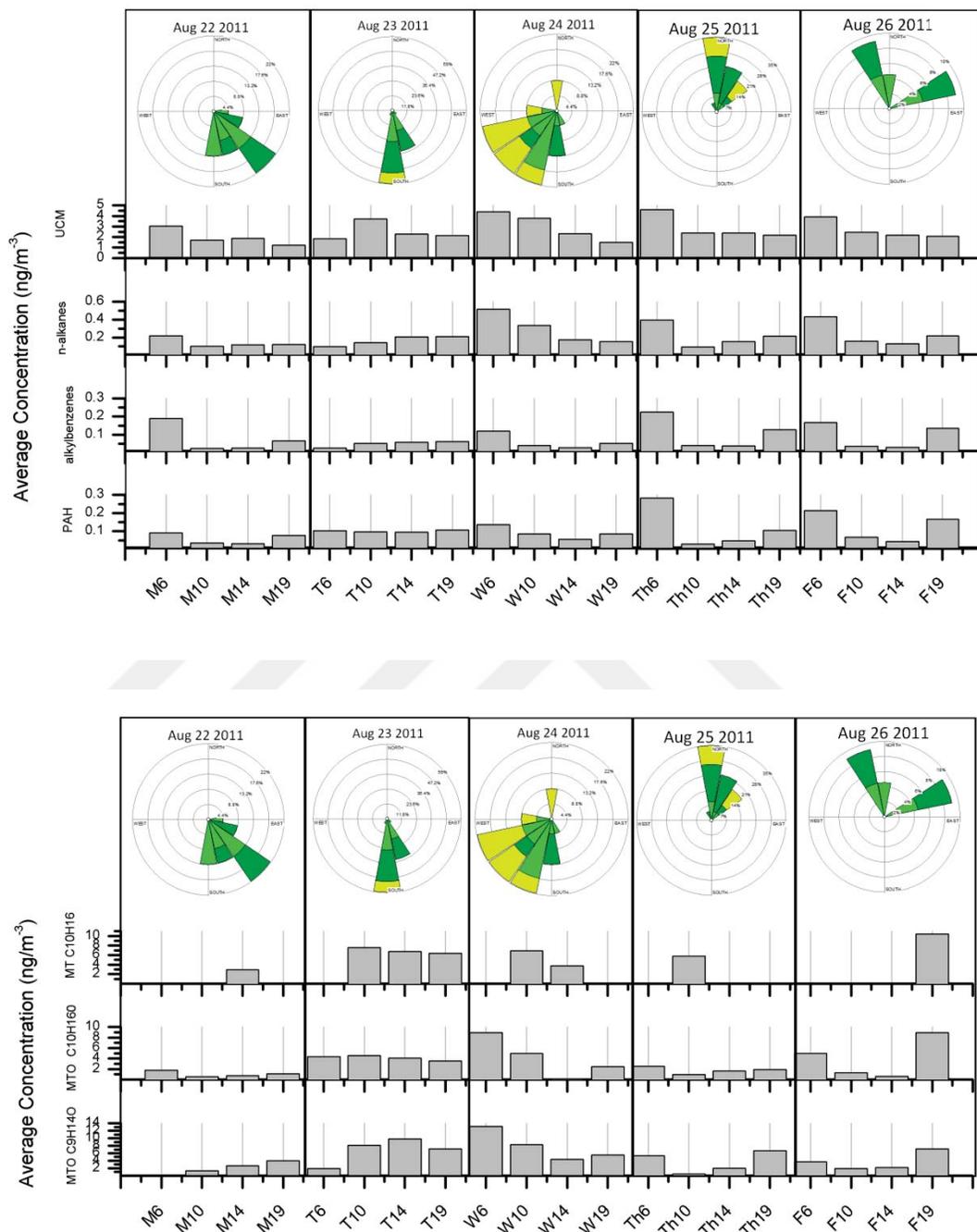
Figure 6.3. Temporal and diurnal trends in concentrations (ng m^{-3}) of (a) gas-phase, semivolatile aliphatic and aromatic hydrocarbons and (b) monoterpenes and monoterpenoids ($C_{10}H_{16}O$, $C_9H_{14}O$).
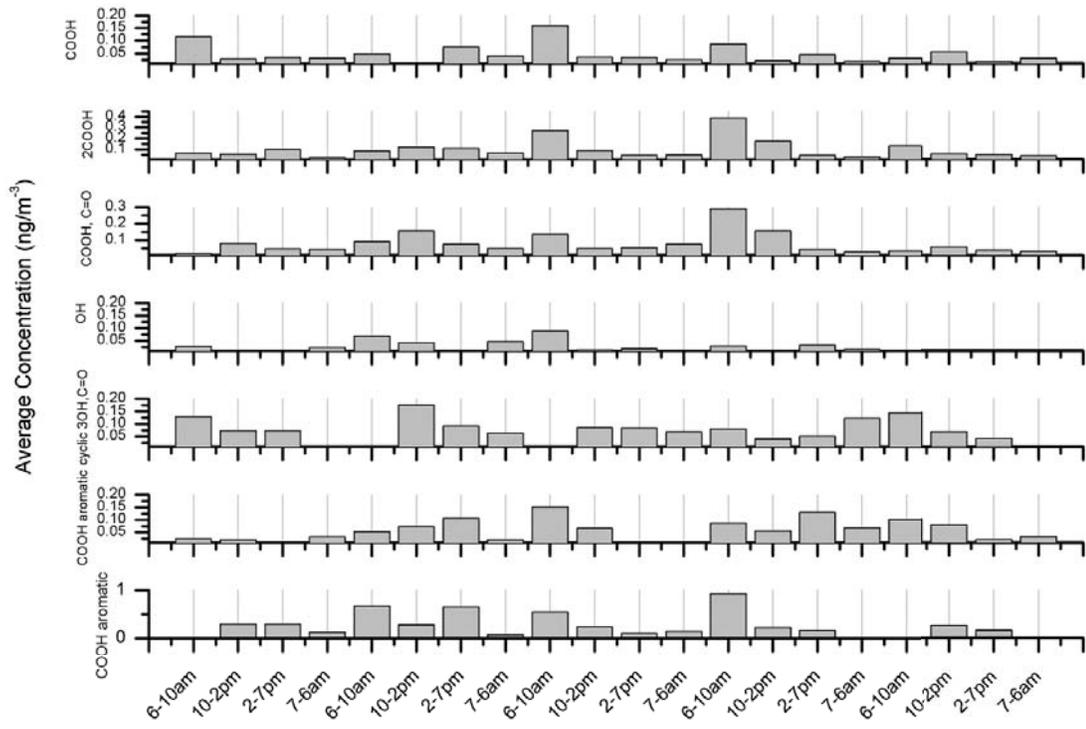
Fig 6.4. Concentrations (ng m^{-3}) of functionalized organic aerosol species.
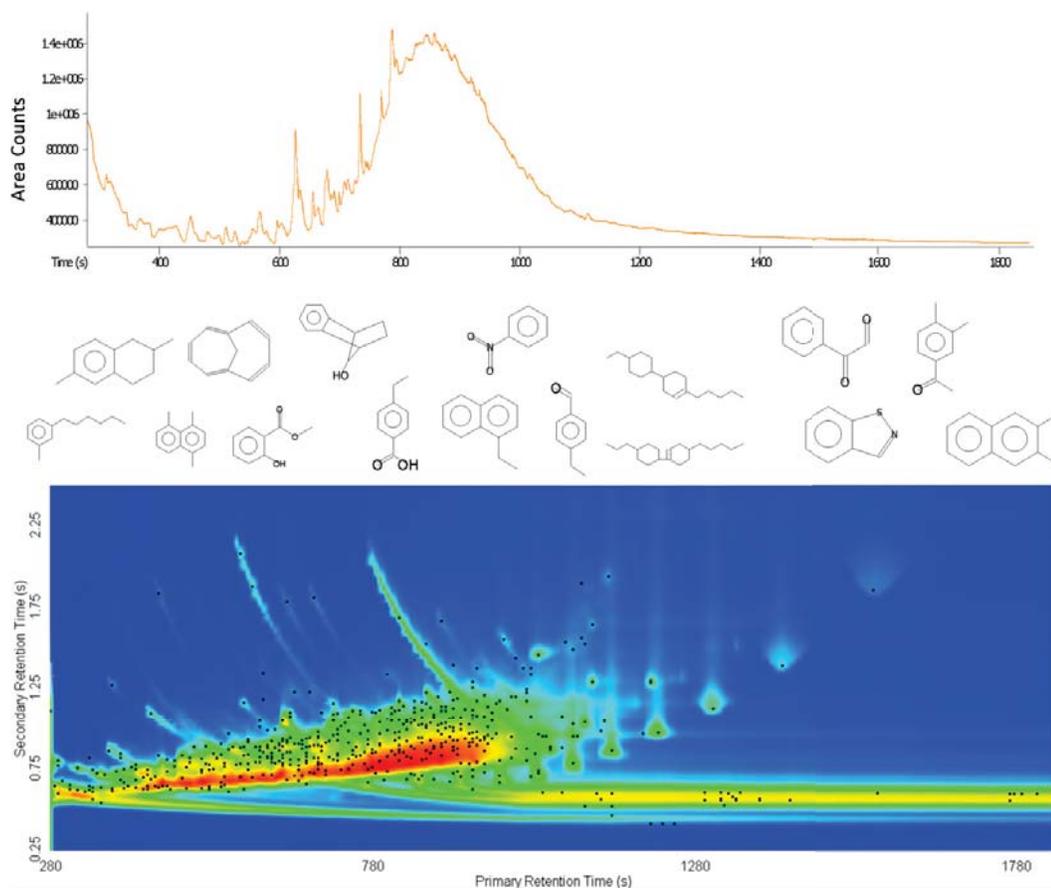
Figure 6.5. Response of the unresolved complex mixture (UCM) by gas chromatography with time-of-flight mass spectrometry (GC-ToF-MS; upper panel) and by GC × GC-ToF-MS (lower panel). Structures of selected compounds identified in the UCM are shown in between the upper and lower panels.
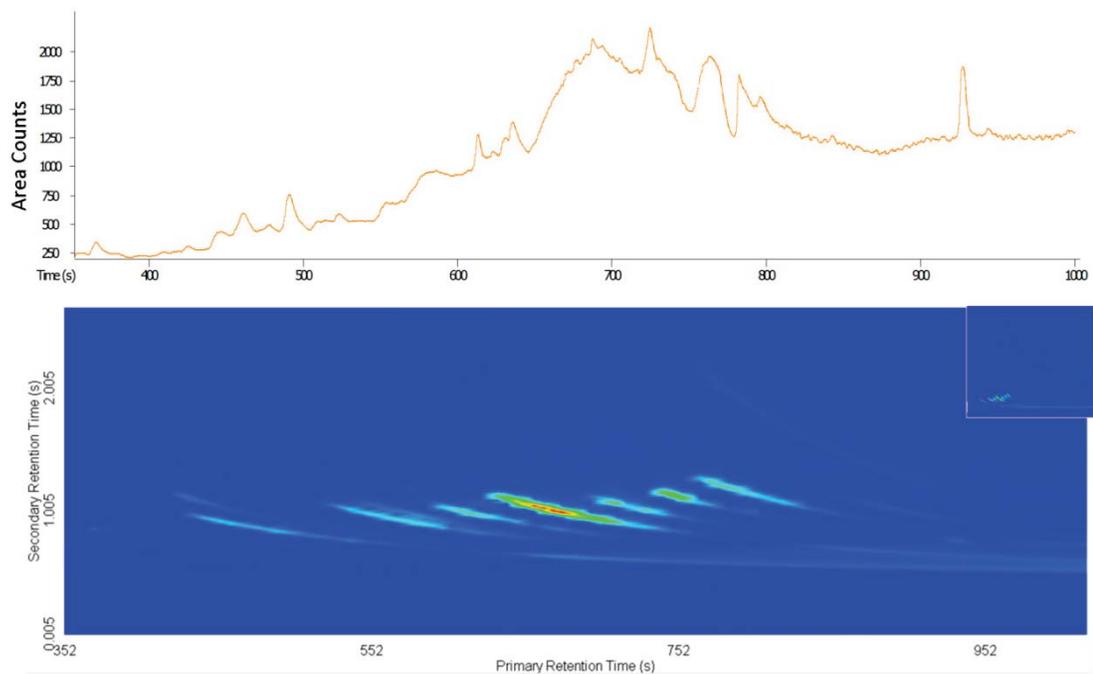
Fig 6.6. Response of the C_5-C_9 n-alkanoic acids by gas chromatography with time-of-flight mass spectrometry (GC-ToF-MS) using selected ion monitoring (m/z 60) (upper panel) and by GC × GC-ToF-MS (bottom panel).

Chapter 7. Conclusions

Predicting SOA formation on regional scales is complicated by uncertainties in biogenic emission inventories, comprehensive organic molecular characterization of SOA, and quantification of SOA yields. A bottom-up approach to develop terpene and terpenoid emission inventories was presented that is based on comprehensive, organic molecular characterization of conifer oleoresin, which is composed of oil and the less volatile resin acids. Commercially available essential oils of *Pinus sylvestris*, *Picea mariana*, and *Thuja occidentalis*, were analyzed by comprehensive, two-dimensional gas chromatography with time-of-flight mass spectrometric detection (GC × GC-ToF-MS). Many more chemical species were identified and quantified by GC × GC-ToF-MS than analyses by the much lower resolution, GC-MS technique reported by others. A review of the literature indicated distinctive features of the molecular signatures of the *Pinaceae* and *Cupressaceae* families at the subfamily, genera, subgenera, and species levels. Variability in molecular signatures was also observed and related to phenology and age, biotic and abiotic stressors, and isolation and analytic techniques. Comprehensive investigation of variations in oleoresin composition related to phenology and age and measurement of molar composition using exhaustive extraction techniques like SFE with quantitation by GC × GC-ToF-MS would greatly improve the accuracy of emission inventories developed by bottom-up approaches.

Emission signatures of terpenes and terpenoids from conifer oleoresin composition were estimated via an emission model that considered 2 pathways of emission from conifers, (1) exhalation from foliar stomata and (2) evaporation from resin blisters or traumatic resin ducts on the bole of the tree. Estimated partial pressures of terpenes and terpenoids above cortical oleoresin eluted from the bole were greater than estimates of partial pressures in the substomatal cavity. Lower partial pressures of terpene alcohols than the terpenes were predicted for the substomatal cavity and above cortical oleoresin with a high resin content due a propensity of hydrogen bonding of the terpene alcohols with

mesophyll immersed in apoplastic fluid and resin acids of cortical oleoresin. Terpenes exerted lower partial pressures above cortical oleoresin rich in monoterpenes than the terpene alcohols due to van der Waals interactions of the terpenes with the monoterpenes in oleoresin. Molar composition of foliar oleoresin was similar to the signature of emissions from *Pinus strobus*; however, β-phellandrene, terpinolene, myrcene, and α-terpineol did not follow the same trends as species with similar values of K_{AO}. Emission potentials of the foliar and bole release pathways are dissimilar and should be considered for conifer species that develop resin blisters or are infested with herbivores or pathogens.

Analytic methods were developed to improve organic molecular characterization of SOA precursors and oxidation products. Derivatization of oxidation products is necessary to minimize losses in GC analytic systems and to reduce ambiguity in identification by MS. Two, 3-step derivatization methods that differed in the reaction to derivatize carboxylic acids were compared. In Step 2 of Methods 1 and 2 derivatization of –COOH moieties is accomplished with TMSD/MeOH and 10% (v/v) boron trifluoride (BF_3) in MeOH or *n*-butanol (*n*-BuOH), respectively. The BF_3/(MeOH or *n*-BuOH) was ineffective at converting species with more than 2 –OH moieties. Average standard deviations for derivatization of 36 model compounds by the 3-step methods using TMSD/MeOH and BF_3/(MeOH) were 7.42 and 14.75%, respectively. Average derivatization efficiencies for Methods 1 and 2 were 87.9 and 114%, respectively. Despite the lower average derivatization efficiency of Method 1, distinct advantages included a greater certainty of derivatization yield for the entire suite of multi- and poly-functional species and fewer processing steps for sequential derivatization. Detection limits for Method 1 using GC × GC- ToF-MS were 0.09-1.89 ng μL^{-1}.

A carbon number-functionality grid (CNFG) for a complex mixture of secondary organic aerosol (SOA) precursors and oxidation products was developed from the theoretical retention index diagram of a hypothetical, multidimensional gas

chromatographic (GC × 2GC) analysis of a mixture of SOA precursors and derivatized oxidation products. In general, species eluted (relative to the alkyl diester reference compounds) from the primary column (DB-210) in bands according to the number of carbon atoms (n) in the diester and from the secondary columns (BPX90, SolGel-WAX) according to functionality, essentially making the GC × 2GC retention diagram a CNFG. Selecting a homologous series of solutes with functionalities that are similar to the target analytes for reference compounds increases separation of reference species and preserves elution order according to n on polar columns like DB-210, BPX90 and SolGel-WAX. The GC stationary phases provided a theoretical separation of 33 SOA precursors and 98 derivatized oxidation products into 35 groups by molecular volume and functionality. Quantifying groupings and organic molecular species in a time series of OA sample collections with a CNFG developed through a GC × 2GC analysis is a promising technique for limiting the complexity of organic molecular data in SOA formation models.

The high-volume (hi-vol) sampling method with XAD-2 resin was implemented, and sample processing and analytic methods were developed to evaluate temporal and diurnal trends in semivolatile aliphatic and aromatic hydrocarbons (HSVOCs) and functionalized OA species in St. Louis, Missouri. The OA and HSVOCs were collected on a quartz fiber filter and XAD-2 resin, respectively, in a hi-vol sampler operating at 200 L min^{-1}. Average recoveries of n-alkanes and polyaromatic hydrocarbons (PAHs) by Soxhlet extraction of XAD-2 resin with dichloromethane were 80.1 ± 16.1 and 76.1 ± 17.5%, respectively. Silanization of glassware was necessary for quantitative recovery of functionalized OA species. Average recoveries by Soxhlet extraction with an equal mixture of dichloromethane and methanol were 74.5 ± 21.8%. Diurnal trends indicated a balance between emissions and photochemical oxidation during the day. An absence of monoterpenes at 0600-1000 and high concentrations of monoterpenoids during the same period was indicative of substantial losses of monoterpenes overnight and the early morning hours. Post-collection, comprehensive organic molecular characterization

of SOA precursors and products by GC × GC-ToF-MS in ambient air collected with ~2 hr resolution is a promising method for determining biogenic and anthropogenic SOA yields that can be used to evaluate SOA formation models.